

2-P

FLUID PHYSICS BRANCH  
RESEARCH DIVISION  
OFFICE OF ADVANCED RESEARCH AND TECHNOLOGY

# FIFTH INTERCENTER AND CONTRACTORS CONFERENCE ON PLASMA PHYSICS

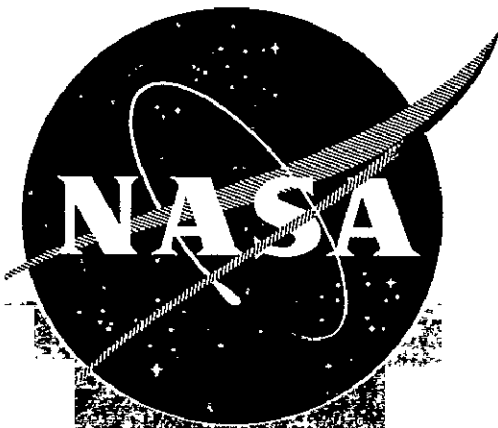
## Part V Plasma Physics Research under NASA Program Offices Contracts:

OART – RRP

OART – RRE

OART – RNT

OSSA – SG



Reproduced by  
NATIONAL TECHNICAL  
INFORMATION SERVICE  
Springfield, Va. 22151

WASHINGTON, D. C.

MAY 24 – 26, 1966

FACILITY FORM 602	N71-19806	
	(ACCESSION NUMBER)	(THRU)
	132	63
	(PAGES)	(CODE)
TMX-66952	25	
(NASA CR OR TMX OR AD NUMBER)	(CATEGORY)	

FIFTH NASA INTERCENTER AND CONTRACTORS  
CONFERENCE ON PLASMA PHYSICS

Part V: Plasma Physics Research  
under  
RRP, RRE, RNT and SG  
Programs

Washington, D. C.  
May 24-26, 1966

Table of Contents

A. Plasma Physics Research under RRP Programs	Page
Stability of Plane Magnetohydrodynamic Channel Flow with Parallel Magnetic Field P. Nachtsheim, NASA Lewis Research Center, and E. Reshotko, Case Institute of Technology	1
Magnetohydrodynamic Boundary Layers Involving Non-Equilibrium Ionization A. Sherman, General Electric, King of Prussia, and E. Reshotko, Case Institute of Technology	2
Plasma Boundaries J. Fay, Massachusetts Institute of Technology	3
✓ Electrode Effects in Accelerators S. Aisenberg, P. Hu, V. Rohatgi and S. Ziering, Space Science Inc.	5
✓ Magneto aerodynamic Drag and Shock Stand-Off Distance C. Chang, R. Nowak, S. Kranc, R. Porter, G. Trezek, M. Yuen, T. Anderson, and A. Cambel, Northwestern University	11
Properties of a Magnetically Suspended Arc in Supersonic Flow A. Kuethe, University of Michigan	18
A Critical Mass Flow Model for the MPD Arc Jet H. Hassan, North Carolina State University	20
✓ Analysis of Instabilities in a Linear Hall Current Accelerator G. W. Garrison, Jr., and H. A. Hassan, North Carolina State University	24
Experimental Investigations of Strong Shock Waves Moving Through an Ionized Gas G. L. Spencer, Case Institute of Technology	29

	Page
Harmonic Generation in a Microwave Plasma F. J. Mayer and O. K. Mawardi, Case Institute of Technology	30
A Wide-Band Dicke Type Radiometer A. T. Alper and O. K. Mawardi Case Institute of Technology	31
Experimental Study of the Interaction of Energetic Electron and a Plasma W. B. Johnson and M. R. Smith, Case Institute of Technology	32
A Beat Frequency Interferometer For Plasma Diagnostics W. B. Johnson, A. B. Larsen, and T. P. Sosnowski, Case Institute of Technology	33
Turbulence in a Rarefied Plasma C. Tchen, National Bureau of Standards, Washington	35
Plasma Vortices and their Motion in Inhomogeneous Magnetic Fields W. Bostick, Stevens Institute of Technology	36
Experimental Investigations of the Fundamental Modes of a Collisionless Plasma J. Malmberg, General Atomic	40
Plasma Radiation and the Detection of Non-Maxwellian Velocity Distributions J. Noon, P. Blaszkuk and E. Holt, Rensselaer Institute of Technology	42
Modes of the Kadomtsev Instability D. Huchital and E. Holt, Rensselaer Inst. of Tech.	44
Stability of Plasmas Subject to Convective Instabilities E. Holt and D. Hutchital, Rensselaer Inst. of Tech.	46
Plasma Measurements from 3 to 120 Kilobars of Pressure J. Robinson, University of Michigan	48

	Page
Investigations on the Mechanism of the Material Release in the High Vacuum Breakdown R. Schneider, University of Florida	51
✓ Synthesis and Characterization of Magneto Fluids R. Rosensweig, Avco RAD	53
B. Plasma Physics Research under RRE Programs	
✓ Propagation and Dispersion of Hydromagnetic and Ion Cyclotron Waves in Plasmas Immersed in Magnetic Fields A. A. Dougal, The University of Texas	60
A - C Power Generation Through Wave-Type Interactions G. L. Wilson, MIT	65
✓ Anode Oscillations in Cesium Plasmas H. S. Robertson, University of Miami	66
Transverse Stream Instabilities in Plasmas W. Bennet, North Carolina State University	72
C. Plasma Research under RNT Programs	
✓ Pulsed Plasma Propulsion R. G. Jahn and W. von Jaskowsky, Princeton Univ.	75
✓ Pulsed Plasma Accelerator P. Gloersen, B. Gorowitz, and T. W. Karras GE Space Sciences Lab.	83
Coaxial Plasma Gun A. V. Larson, L. Liebing, A. R. Miller, and R. Dethlefsen Space Science Lab., General Dynamics Convair	99

Diagnostics of Accelerating Plasma 102  
 C. C. Chang, T. N. Lie and A. W. Ali,  
 The Catholic University of America

MPD Arc Jet Thrustor Research 103  
 R. R. John and S. Bennet  
 Avco, Space Systems Division

Permanent Magnets For MPD Arc Thrusters 106  
 A. C. Eckert and D. B. Miller  
 G. E. Space Sciences Lab., King of Prussia, Pa.

Electron Cyclotron Resonance Plasma 107  
 Thruster Development  
 D. B. Miller, A. C. Eckert and C. S. Cook  
 G. E. Space Sciences Lab., King of Prussia, Pa.

Hall Current ACCELERATOR 109  
 G. L. Cann, P. F. Jacobs  
 Electro Optical Systems, Inc.

D. Plasma Research under OSSA Physics and  
 Astronomy Programs

Plasma Aspects of Space Physics 117  
 A. G. Opp, NASA Headquarters, OSSA

Experimental and Theoretical Investigation 119  
 on Selected Aspects of Plasma Turbulence  
 I. B. Bernstein, Yale Univ., New Haven, Conn.

E. Supplement

Investigation of Plasma Resonance Phenomena 121  
 S. J. Tetenbaum, Lockheed Research Labs,  
 Palo Alto, California

A - C Travelling Wave-Plasma Stream 125  
 Interactions  
 M. Lessen, The Univ. of Rochester, N. Y.

STABILITY OF PLANE MAGNETOHYDRODYNAMIC CHANNEL FLOW  
WITH PARALLEL MAGNETIC FIELD

P. R. Nachtsheim,\* NASA-Lewis Research Center  
and

E. Reshotko, Case Institute of Technology  
Cleveland, Ohio

An approximate solution to the title problem was given in a paper by J. T. Stuart<sup>1</sup> where a reduced fourth-order disturbance differential equation proposed for small magnetic Reynolds number was solved using asymptotic methods. The problem has been reexamined through exact numerical integration of the pertinent sixth-order system of disturbance equations throughout an extended range of magnetic Reynolds numbers<sup>2</sup>. For comparison, exact numerical results were also obtained to Stuart's fourth-order equation. The results indicate that Stuart's simplifying assumption is justified only for magnetic Reynolds numbers small compared to one. For magnetic Reynolds numbers of order one or greater, there are significant changes in the stability characteristics reflecting the increased importance of magnetic effects. This is also borne out in a calculation of the various viscous and magnetic contributions to the rate of change of disturbance energy. It is shown that the resistivity enters this problem in two ways: (1) it sets up a time-independent Maxwell stress that augments the disturbance energy when it is of the same sign as the vorticity of the basic flow, and (2), through joule dissipation the disturbance energy is decreased. For small resistivity ( $Re_m \gg 1$ ) the former dominates, leading to a net augmentation of the disturbance energy, while for large resistivity ( $Re_m \ll 1$ ) the dissipative effect is dominant.

---

\*Now at NASA-Ames Research Center

<sup>1</sup>Stuart, J.T.: Proc. Roy Soc A221 189 (1954)

<sup>2</sup>Nachtsheim, P.R. and Reshotko, E.: NASA TN D-3144 December, 1965

MAGNETOHYDRODYNAMIC BOUNDARY LAYERS  
INVOLVING NON-EQUILIBRIUM IONIZATION

A. Sherman

General Electric Space Sciences Laboratory, Valley Forge, Pa.

and

E. Reshotko

Case Institute of Technology, Division of Engineering, Cleveland, O.  
(Consultant, General Electric Space Sciences Laboratory)

In the study of practical magnetohydrodynamic devices such as generators and accelerators recent experimental and theoretical research has shown the importance of non-equilibrium ionization for their successful operation. At the same time, these experimental results have demonstrated the existence of large voltage drops at the electrodes, thereby preventing full utilization of the non-equilibrium ionization. These voltage drops occur not only in the thin sheath at the base of the channel boundary layer, but also partially in the boundary layer itself. Presently available theoretical analyses of the magnetohydrodynamic boundary layer take into account non-equilibrium ionization in only an approximate manner, and neglect the sheath as well. They have not been able to predict the large voltage drops observed experimentally.

The present paper will formulate the magnetohydrodynamic boundary layer problem when non-equilibrium ionization exists. In particular it will be shown that when non-equilibrium ionization is taken into account properly, that the characteristics of the sheath at the base of the continuum boundary layer are essential to the correct solution of the problem. In addition, since non-equilibrium ionization occurs more readily when segmented electrodes prevent Hall currents, it is important to be able to analyze the boundary layer over an electrode wall with alternate finite electrode and insulator segments. For this reason solution of the equations will be carried out by a finite difference technique.



PROBLEMS IN  $J \times B$  PLASMA ACCELERATION

James A. Fay, Marvin Goldstein and Peter Sockol  
Department of Mechanical Engineering  
Massachusetts Institute of Technology

This research is concerned with problems encountered in accelerating collision-dominated plasmas by an externally applied magnetic field interacting with currents also supplied from an external source. A principle focus of the research is the interaction of the current-carrying plasma with solid boundaries. Summarized briefly below are accounts of progress on four related problems.

(a) Experimental measurement of heat transfer to the walls of a Faraday shock tunnel is being investigated. Heat transfer is measured by monitoring the temperature rise of "thin" and "thick" film heat transfer gages with an infrared detector. Two types of gages are being developed. The first is a heat capacity gage with 0.1 microsecond response time for measuring rapidly varying heat transfer. The gage consists of carbon and aluminum coatings applied to thallium bromide or arsenic trisulfide windows, the temperature being monitored by a mercury doped germanium detector at liquid helium temperature. The second gage which is being developed to measure heat transfer to an emitting electrode, consists of a thicker metallic coating for which the response time is about 10 microseconds but which is sufficiently thick to conduct the emitted current without being heated by Joule losses in the electrode surface of which the gage is an integral part. At the present time problems of gage coating, infrared transmission, calibration, etc. are being studied. Also, a test section for use with the gages is being tested.

(b) A new formulation for transport effects in multi-component boundary layers has been devised which shows promise of simplifying the numerical solution of plasma boundary layer problems. This new method involves direct use of certain moments of the linearized Boltzmann equation from which the gradients of conserved properties are linearly related to the fluxes of these same quantities, and bears some resemblance to the transport limit of the Grad moment method. In combination with the conservation laws relating the divergence of the fluxes with convective derivatives and source terms, a set of first order differential equations is obtained (total differentials in the case of similarity-type boundary layers) in which the usual multi-component transport coefficients, such as the total thermal conductivity, do not appear explicitly. An additional advantage of this method is that different temperatures of electrons and heavy species and different levels of approximation in the Sonine polynomial expansion of the perturbation to the distribution function may be used for different species, which is important for plasma boundary layers. A report is being written for distribution.

(c) A theoretical study of Hartmann boundary layers in a homopolar device has yielded preliminary results which are in approximate agreement with experimental measurements. The theory takes into account two energy equations, (one for the electrons and a second for the heavy particles), a diffusion equation for the electron-ion pairs and a momentum equation for

the heavy species. Approximate solutions, which use average values of the transport coefficients, show that the flow velocity in the homopolar device is an appreciable fraction of the "ionization velocity," i.e., the velocity of an atom whose kinetic energy equals its ionization energy, and that appreciable variation in the degree of ionization can result from small changes in the total current, at least for the small degrees of ionization for which the present approximate solutions are valid.

(d) A zero-order theory for the stabilization by a magnetic field of an arc transverse to a flowing stream has been devised. It is based on a model in which the hot arc column is motionless, but is in static equilibrium with the dynamic pressure of the "cold" stream in which it is immersed, and to which heat is conducted from the hot column. In this zero-order theory, the cross-sectional shape of the arc column is determined from the momentum equation and the temperature distribution within the column is determined from the energy equation. The solution of these equations leads to relationships between the stabilizing magnetic field strength and the flow velocity, between the electric field and the width of the column, and also between the arc power and the average temperature. The first two relationships are in approximate agreement with the measurements of Myers .

---

\* Meyers, T. W., "Experimental Investigation of the Balancing Mechanism and Electrical Properties of an Argon Arc in Crossed Convective and Magnetic Fields," 7th Symposium on Engineering Aspects of MHD. (1966)

## ELECTRODE EFFECTS IN ACCELERATORS

By

S. Aisenberg  
P. Hu  
V. Rohatgi  
S. Ziering

SPACE SCIENCES, INC.  
301 Bear Hill Road  
Waltham, Massachusetts

### 1. Experiments and Analysis

A number of problems are investigated experimentally and analytically in order to give a better understanding of some of the important physical processes involved in plasma surface interactions. The features studied include: the tangential drag on electrodes in  $J \times B$  accelerations; the arc construction processes; and a theory proposed to explain electron emission from cold cathodes by an ion microfield emission process.

The tangential electrode drag forces are measured for an arc in a transverse magnetic field, and it is shown that the cathode and the anode tangential forces are an appreciable fraction of the  $J \times B$  force driving the plasma. The presence of tangential electrode (and boundary) friction forces is expected for a hot plasma flowing in a channel when one considers that some of the tangential momentum is transferred each time an ion, electron, or gas atom collides with the surface.

The basic features of the electrode structure used in this experiment are shown in Figure 1. The force measurements are made for the central electrode which is operated as the cathode or alternatively as the anode. This central electrode is supported on a torsion spring structure so that the tangential force (or torque) can be determined from the angle of rotation.

Some results are illustrated in Figure 2 where the measured tangential force is shown as a function of magnetic field for a 77 amp dc arc in 24 Torr of argon, and where the central electrode is operated as a cathode as well as an anode. The cathode force due to ion current drag is deduced by assuming that the neutral gas component at the cathode is the same as the anode drag. (This assumption should be examined further because the boundary layers at the anode and cathode may be very different). The measurements show that:

- 1) There is a pronounced threshold in the cathode and anode force as a function of magnetic field and of arc current.
- 2) If it can be assumed that the momentum transfer to the anode is predominately due to the neutral gas atoms, there appears to be a threshold in the electrode drag by the neutral gas components.
- 3) The cathode drag appears to show a saturation.
- 4) The cathode force is as large as 24% of the input force driving the plasma, and the anode force is as large as 13%.
- 5) The deduced ion current component is larger than the neutral gas component, and in the range measured, is about 16% of the plasma driving force.

The tangential force on an electrode is proportional to the tangential velocity, to the perpendicular particle current flow, and to the tangential momentum accommodation coefficient. The observation that the tangential force at the cathode was larger than the anode force indicates that the positive ion current flow to the cathode is capable of transferring an appreciable tangential force to the cathode. The direct measurements of the electrode drag forces show that the effect is serious enough to be considered further and at the same time gives interesting data that should be considered by any proposed models.

An analysis was made of the arc constriction processes because the constriction influences the plasma surface interaction. The constriction mechanisms considered involve the balance between the input power to the plasma and the following modes of power loss: 1) diffusion loss for low pressure plasmas, 2) radiation loss for high density, high temperature plasmas, 3) thermal energy loss for higher pressure plasmas, 4) convective energy loss due to the flow of cooler gas. The available data and the theory both show that for the diffusion and for the thermal conductivity mode loss, the product of the current density  $T$  and the arc current should be constant.

## 2. Theory

In order to clarify plasma electrode interactions and facilitate a clearer understanding of the physical parameters governing sheath phenomena, the existing collisionless theory of a plasma sheath near an infinite planar electrode is examined in detail. Ranges of validity, as well as difficulties with the existing sheath models are investigated. The assumption of monoenergetic particle distributions, as used for instance in "Bohm's Sheath Criterion" restricts the usual analysis. To remove this difficulty Maxwellian particle distribution functions are

assumed. In addition, microscopic boundary conditions are assumed to incorporate the respective electrode and plasma parameters. A new sheath model is then developed without imposing the usual sheath criterion for the conditions specified at the sheath edge. Explicit results for the current-voltage relation and for the sheath thickness are obtained for the improved sheath model proposed in this study. Other important physical quantities are expressed in terms of the electrostatic potential, which can be calculated by a quadrature subject to the physical parameters to be specified. The general solution reduces to a simple analytic form for the special case where the temperature of the electrons, ions and the electrode are identical.

Based on the above work, the next logical step in a systematic analysis necessitates consideration of ionization processes in the domain of the pre-sheath as well as the sheath itself. Towards this end it was found necessary to construct kinetic equations which incorporate ionization processes. Ionization processes are usually introduced into the equations of magnetohydrodynamics as gross parameters to be determined by experiment. The mathematical accessibility of model kinetic equations in neutral and ionized gases, motivates the formulation of kinetic equations for a three-component plasma which incorporate the ionization process in this study. As a first attempt, only the ionization processes resulting from electron-neutral collisions are considered. The resulting mathematical formalism yields a set of model equations which are mathematically not more complicated than those for plasmas without consideration of ionization. The possible application of the present model equations to various problems is discussed, such as the ionization growth in a gas, the cathode sheath, and the structure of an ionizing shock wave.

### Reports and Publications

The following publications have been generated as a result of the research performed under this contract:

- 1) Aisenberg, S. and Rohatgi, V;  
"Measured Tangential Electrode Forces for an Arc in a Transverse Magnetic Field". App. Phy. Letters, 8, 194 (1966)
- 2) Aisenberg, S. and Rohatgi, V. ;  
"A Study of Arc Constriction Processes ", Presented at the 7th Symposium on Engineering Aspects of Magnetohydrodynamics in Princeton, N.J., March, 1966

- 3) Aisenberg, S. and Rohatgi, V. ;  
"A Metallic Insulator for Arc Electrodes", (to be submitted for publication)
- 4) Hu, P.N., and Ziering, S., "Collisionless Theory of a Plasma Sheath Near an Electrode" (submitted for publication)
- 5) Hu, P.N. and Ziering, S., "Kinetic Model for Three-Component Plasmas With Ionization", (submitted for publication)

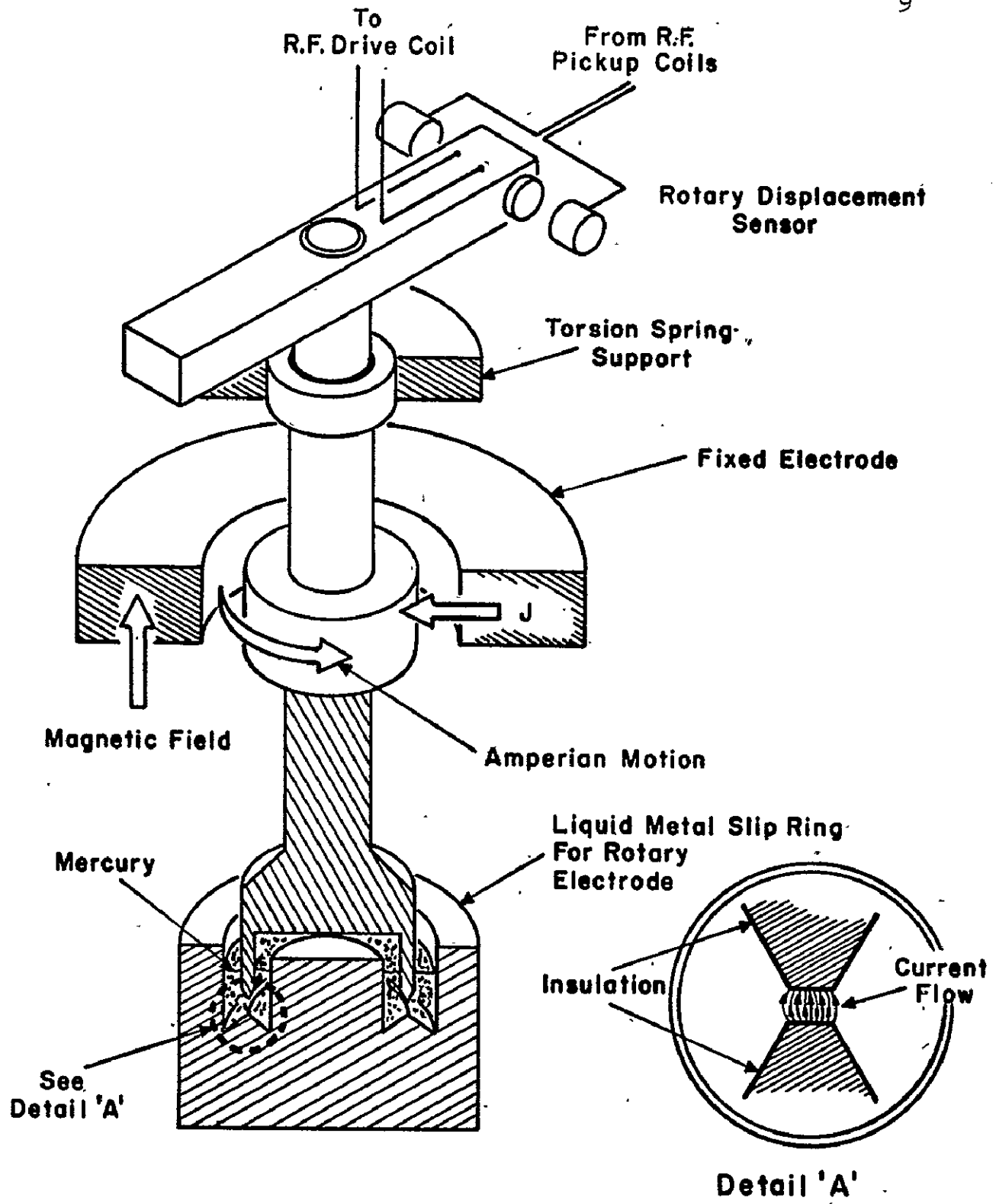


FIGURE 1.  
SCHEMATIC OF ROTARY ELECTRODE STRUCTURE FOR THE  
MEASUREMENT OF TANGENTIAL ELECTRODE FORCES.

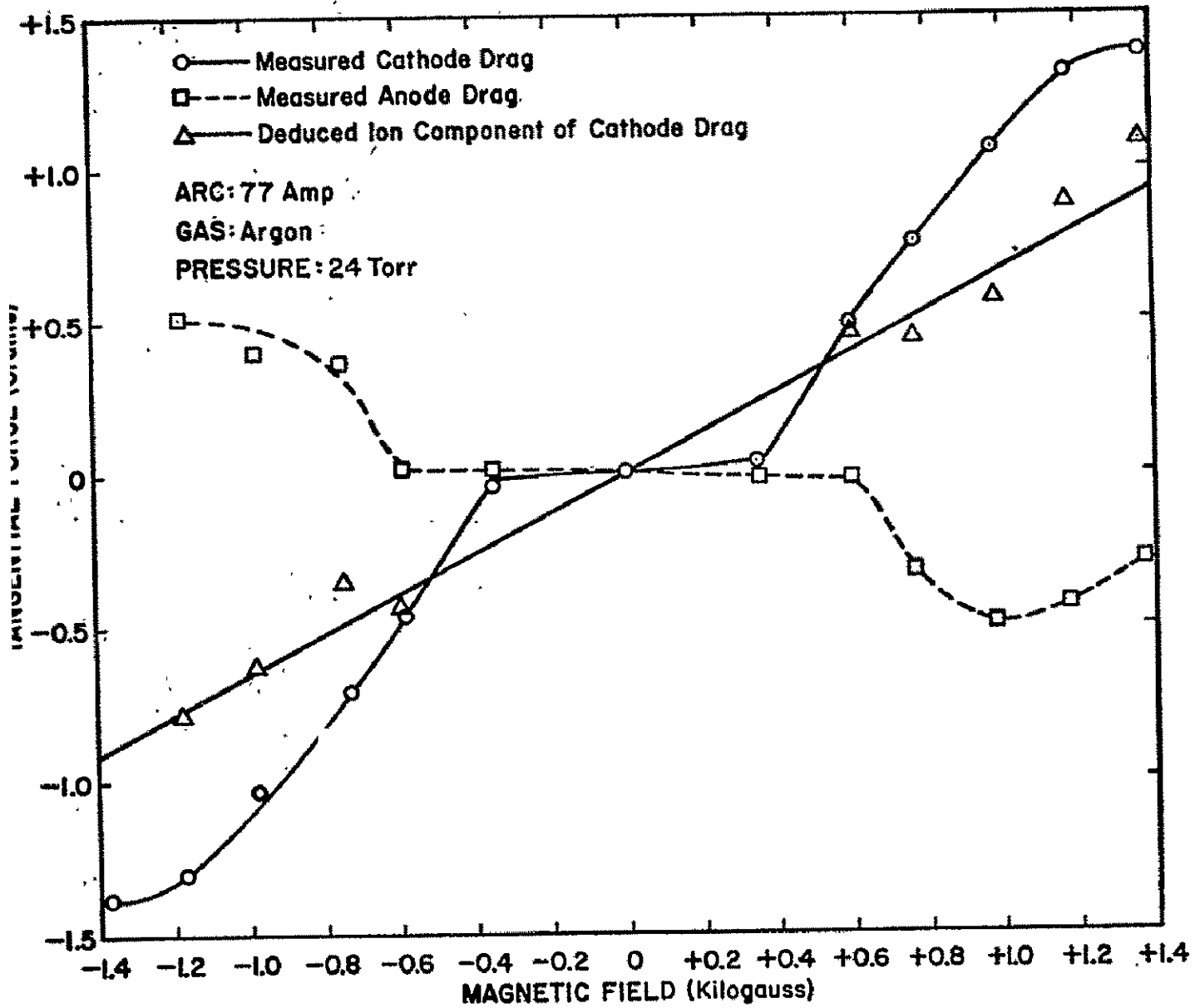


FIGURE 2. DRAG FORCE ON ELECTRODES OF A JXB ARC.



MAGNETOAERODYNAMIC DRAG AND  
SHOCK STAND-OFF DISTANCE

C. F. Chang,<sup>(1)</sup> R. J. Nowak,<sup>(1)</sup> S. Kranc,<sup>(1)</sup> R. Porter<sup>(1)</sup>  
G. Trezek,<sup>(2)</sup> M. C. Yuen,<sup>(2)</sup> T. P. Anderson,<sup>(2)</sup> and A. B. Cambel<sup>(3)</sup>

Gas Dynamics Laboratory  
Northwestern University

It has been shown that the incorporation of magnetic field coils in space vehicles offers interesting possibilities in alleviating some of the problems of space flight. For example, the coupling of the flow field with a magnetic field has the salutary effect of increasing the drag experienced by an entry vehicle. Other promising applications of external magnetogas-dynamics are: the opening of communications windows, enhanced flexibility of maneuvers by virtue of flight control, active shielding against radiation, the reduction of convective heat transfer and the elimination of the non-reusable heat shield. So far, such schemes have not been exploited due to hardware design limitations and due to the fact that current design philosophy has been successful in current programs. However, continuing progress in superconducting magnets and the demands of advanced space programs lend practical significance to equipping space vehicles with powerful electromagnets. The purpose of this program is to investigate this problem systematically from both analytical and experimental viewpoints.

A theoretical study was initiated in order to study and compare the factors important in blunt body, flight magnetohydrodynamics and laboratory simulation in the thermal arc plasma facility.

Consideration of the flow regimes indicates that assumptions of continuum flow, a Hugoniot shock, and sub-layers of viscous and sheath effects are valid for entry flight below 250 kilofeet. The assumptions of a Hugoniot shock and thin boundary layer are considerably less valid for the laboratory conditions owing to the low Reynolds numbers. Therefore, a viscous shock layer was included in some of the analyses discussed below. Theoretical

(1) Graduate Students

(2) Faculty

(3) Chairman and Walter P. Murphy Professor of Mechanical Engineering and Astronautical Sciences.

difficulties prevented including the shock structure, however.

The effects of viscosity, deformation of the magnetic field and the Hall effect on the magnetic interaction were studied by the local similarity method for the stagnation region of aerodynamic - like flow. The flow observables were found for a range of dimensionless parameters appropriate for the flight and laboratory conditions.

It was found that the effect of low Reynolds number (laboratory flow) is very important for low magnetic interaction parameter but that a boundary layer develops at high interaction. Thus, the outer flow becomes essentially inviscid for large Hartmann number similar to MHD Poiseuille flow. The effect of the deformation of the magnetic Reynolds number was negligible for magnetic Reynolds numbers up to an order of magnitude greater than that for unseeded, equilibrium plasma. However, an increase of an additional order of magnitude resulted in the field being considerably distorted with a wrapping of flux lines about the body. The stand-off was decreased and the drag increased for increasing magnetic Reynolds number. The analysis showed that it is incorrect to assume that a dipole source looks like a dipole at the body surface when there is distortion but that the assumption of a (reduced) dipole strength at the shock is valid. The Hall effect is very important for flight and laboratory conditions with kilogauss field strengths at the stagnation point. The magnetic interaction is reduced more so for an insulated body than a conducting one but the effect is important for both. A rolling moment is introduced because of azimuthal flow generated by the Hall effect. All of the special effects tend to increase the critical interaction parameter associated with magnetic support where the attached shock layer theory fails.

Experimental investigations of magnetoaerodynamic drag have shown substantial (~15%) increase in drag with magnetic field. Tests have been run under a variety of flow conditions with both 1-1/2" and 3" bodies. In general the experimental aerodynamic drag component agrees reasonably with theoretical predictions. The measurements of drag with field for the 3" body do not agree with prediction nearly so well as do those tests for the 1-1/2" body. The main reason is the non-uniformity in free stream conditions which affect the 3" body more than the 1-1/2" body.

Experimental values of drag increase are compared to theory for a regime where the viscous and Hall effects are important. No theory exists for the combined effects. The magnetic interaction parameter is obtained from experimentally measured quantities except for the electrical conductivity which is estimated from equilibrium calculations. We have found that while drag appears to be greater under conditions where the Hall and viscous effects are lessened, the various data may be brought closer by plotting against the product of the interaction parameter and the shock density ratio. The remaining differences may be attributed to the Hall effect. Future work will include the measurements of different drag components.

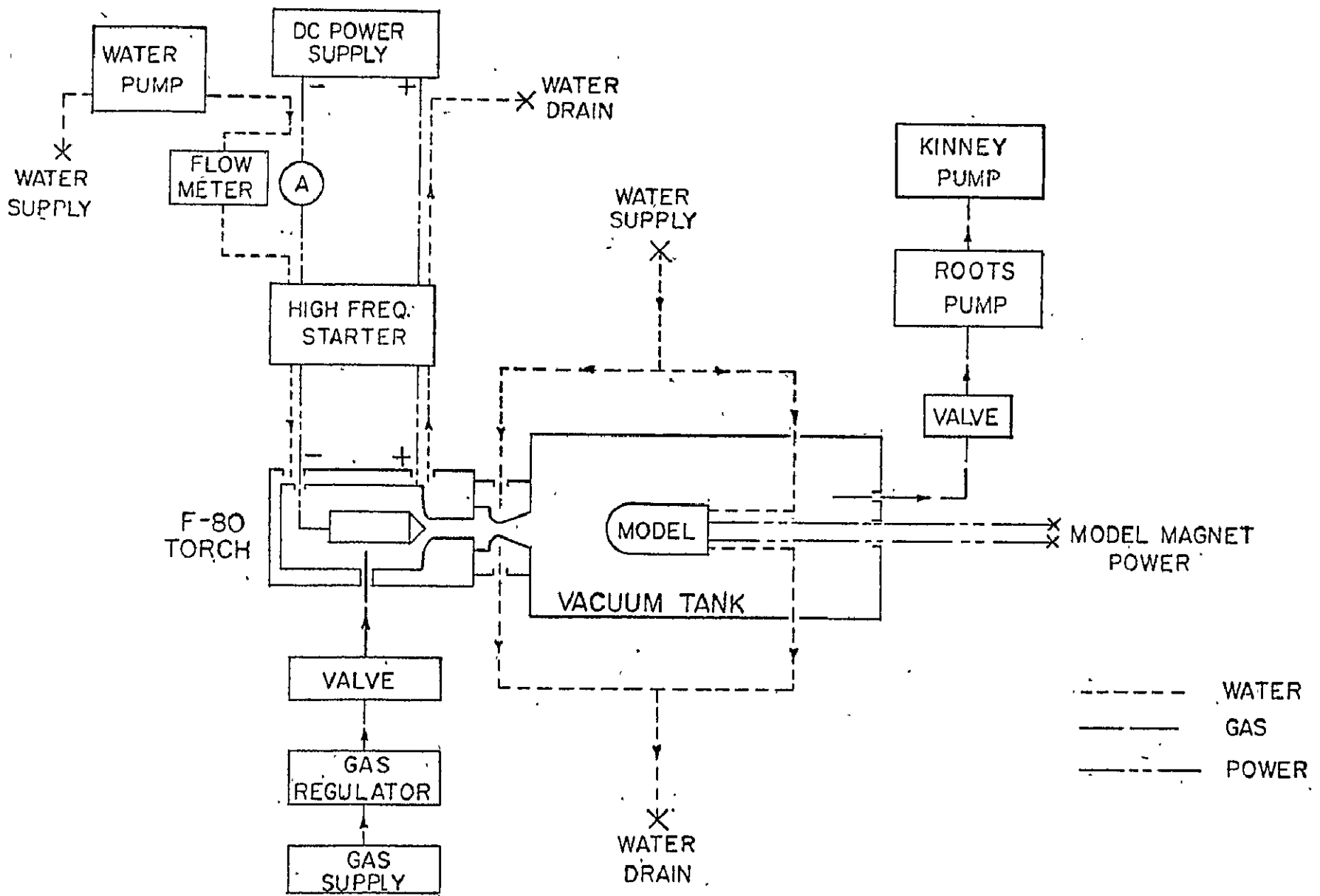
The shock stand-off distance is plotted versus magnetic field squared. These measurements were made by analyzing photographs of the flow using a scanning microdensitometer. We have found that the experimental measurement is severely hampered by a thickened shock under our running conditions. Nevertheless considerable alteration in the shock stand-off has been observed. Present efforts include the measurements of electron density and temperature across the shock structure spectroscopically in order to better define the shock stand-off distance.

In addition to the experimental drag studies, a program has been initiated to experimentally determine magnetoaerodynamic heat transfer to a blunt body. A thin shell, 3" diameter, hemispherical, copper model has been instrumented with thermocouples. In the presence of an argon plasma, the local net transient heat transfer rate to the model is measured with and without the presence of a magnetic field. For a thin shell the heat transfer rate to the model is proportional to the temperature - time rate ( $dT/dt$ ) of the body if temperature gradients in the body are neglected. Preliminary results with a magnetic field strength of 7700 gauss at the stagnation point yield a 26% reduction in model centerline  $dT/dt$ . However, corrections must be made to account for temperature gradients which do exist in the body during the test time.

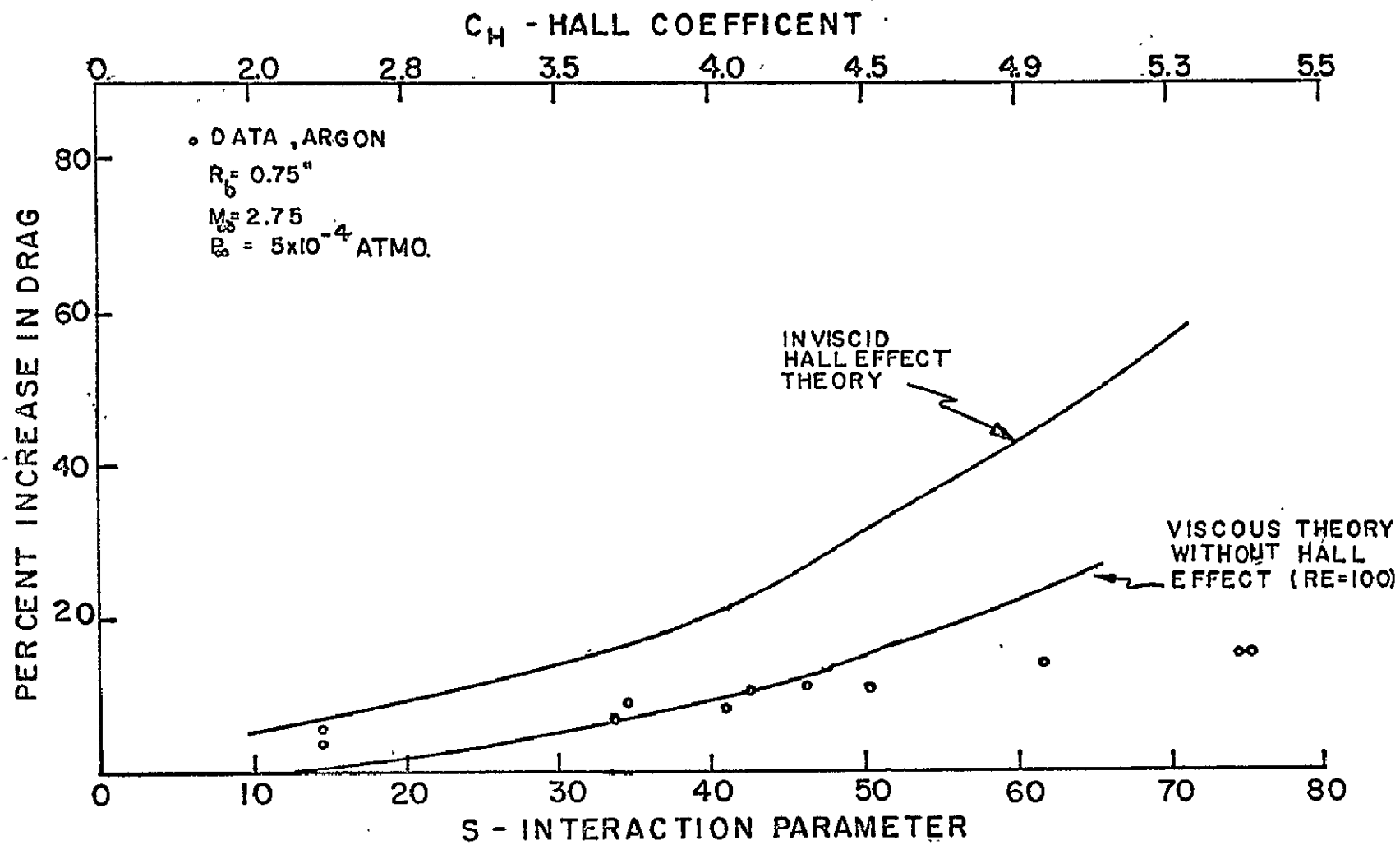
Future tests will make possible the mapping of the magnetoaerodynamic heat transfer over the surface of the body (to half angles of  $45^\circ$ ) for a range of magnetic field strengths of 8000 gauss and lower.

## PUBLICATIONS

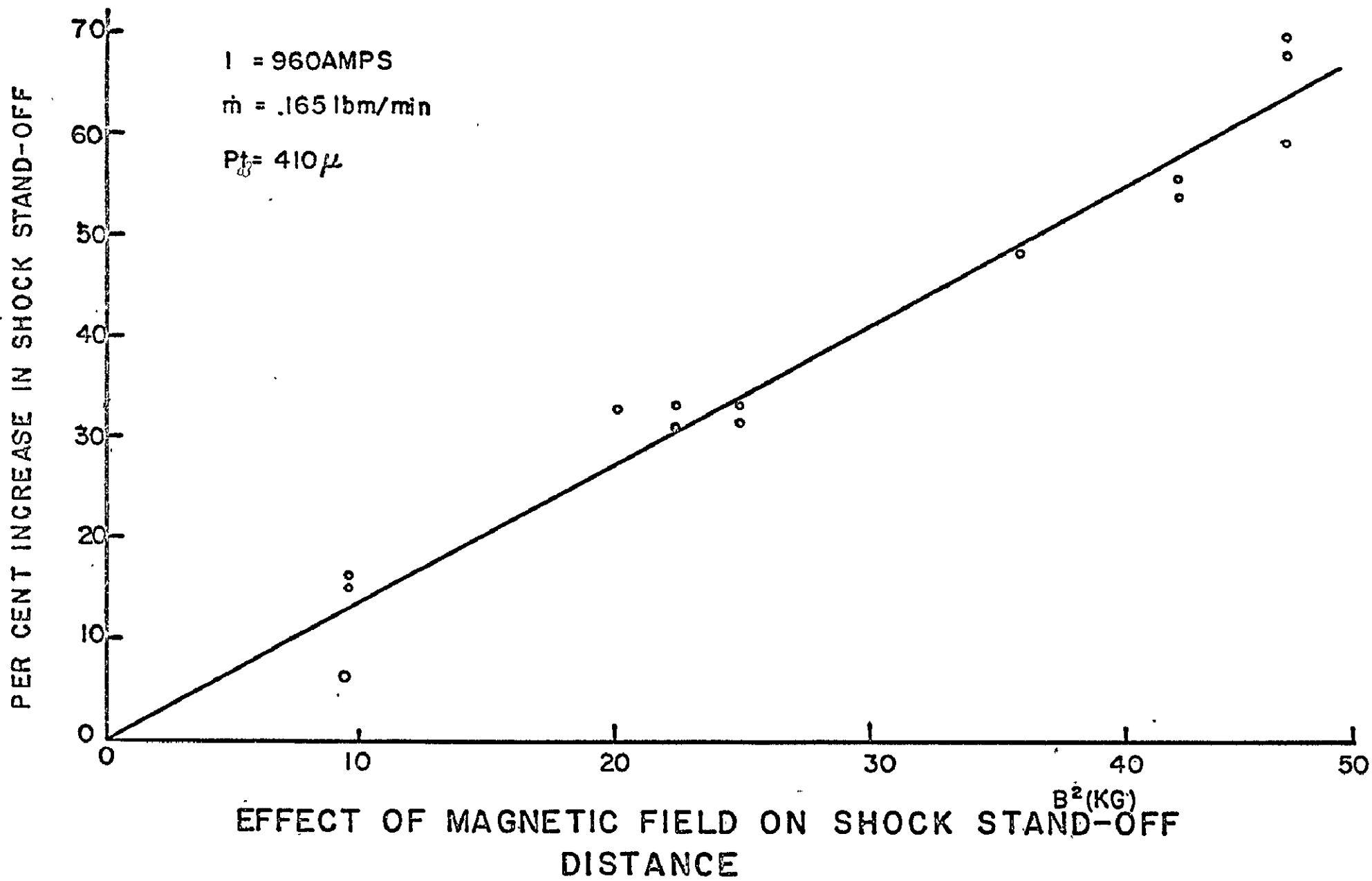
- Nowak, R., Kranc, S., Porter, R., Yuen, M. C., and Cambel, A. B., "Magneto-aerodynamic Re-entry", AIAA Plasmadynamics Conference, March, 1966.
- Anderson, T. P., and Bass, R. B., "Lorentz Drag - An Engineering Approximation", Journal of Spacecraft and Rockets", Vol. 2, #5, 1965.
- Porter, R. and Cambel, A. B., "Design Calculations for Magnetogasdynamic Drag", Report to NASA on NASA NsG 547, 1965.
- Porter, R. and Cambel, A. B., "Comment on Magneto hydrodynamic - Hypersonic Viscous and Inviscid Flow Near the Stagnation Point of a Blunt Body", AIAA Journal, (to be published).



MHD DRAG FACILITY



INCREASE IN DRAG - HALL AND VISCOUS EFFECTS IMPORTANT



Properties of a Magnetically Suspended Arc in Supersonic Flow  
by

Arnold M. Kuethe, University of Michigan

A NASA grant on which work began March 1, 1966, covers experimental and theoretical studies of the properties and structure of a dc arc suspended in mutually perpendicular electric, magnetic, and airflow fields. Previous work under an Air Force contract, in collaboration with Charles E. Bond, showed 1) that the arc can be stabilized on rail electrodes at a slant angle near the Mach angle of the flow, 2) that the "aerodynamic drag" of the arc changes with arc current in such a way that the magnetic field required to stabilize the arc is constant over a wide range of the arc current, 3) column rather than root phenomena determine the conditions for arc stability, and other gross properties of the arc.

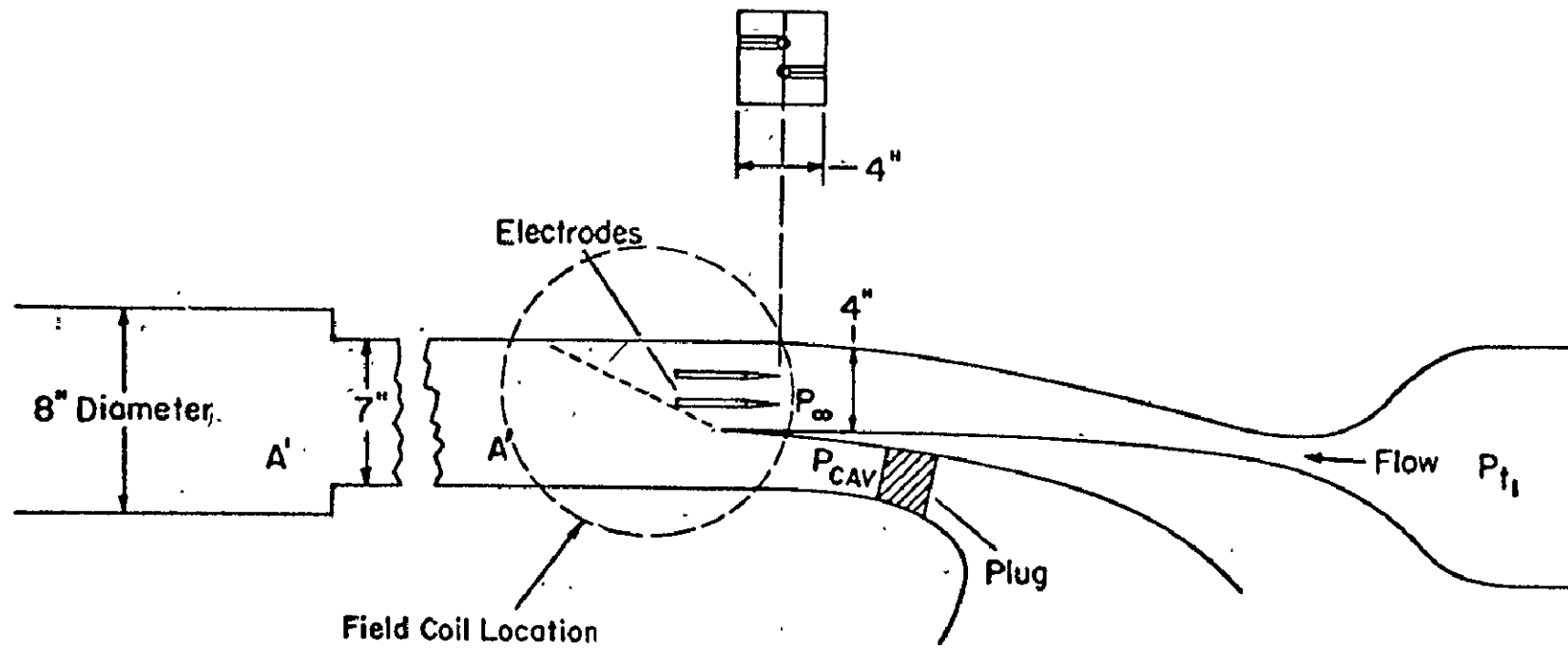
The work under the NASA grant is being directed toward the details of the fluid mechanical structure of the arc and the transfer processes by which mass, momentum, and energy are transferred to the ambient flow.

Measurements to date indicate that, over the range of the measurements (Mach numbers up to 3.5, ambient pressure down to 10 mm Hg) the arc simulates a solid cylinder with a drag coefficient between 1.0 and 1.5 balancing the Lorentz force. The solid body hypothesis is based primarily on photographic observations of an axial flow from anode to cathode of about 10 meters/sec in the Mach 2.5 arc. In addition to the axial flow, the incremental Lorentz force on any relatively hot filament, (i. e., higher conductivity and current density than the surroundings) will force it upstream to the arc boundary where it will be cooled and carried downstream with the flow along the boundary. This circulation will resemble that caused by a vortex pair, providing an upstream flow toward the stagnation point. Thus a model of the arc in agreement with the measurements and physical reasoning is as follows: The streamlines projected on a cross-section would resemble those of a distributed source at the center, a vortex pair and a distributed sink at the boundary.

The work will cover the widest possible range of Mach numbers, ambient pressures, arc current and magnetic field. Wake traverses of gas properties will be made. Theoretical analyses will include arc stability and transport phenomena.



(a) View looking downstream



(b) View looking West

Figure 2. Experimental Setup

## A CRITICAL MASS FLOW MODEL FOR THE MPD ARCJET

H. A. Hassan  
 North Carolina State University  
 Raleigh, North Carolina

NsG-363

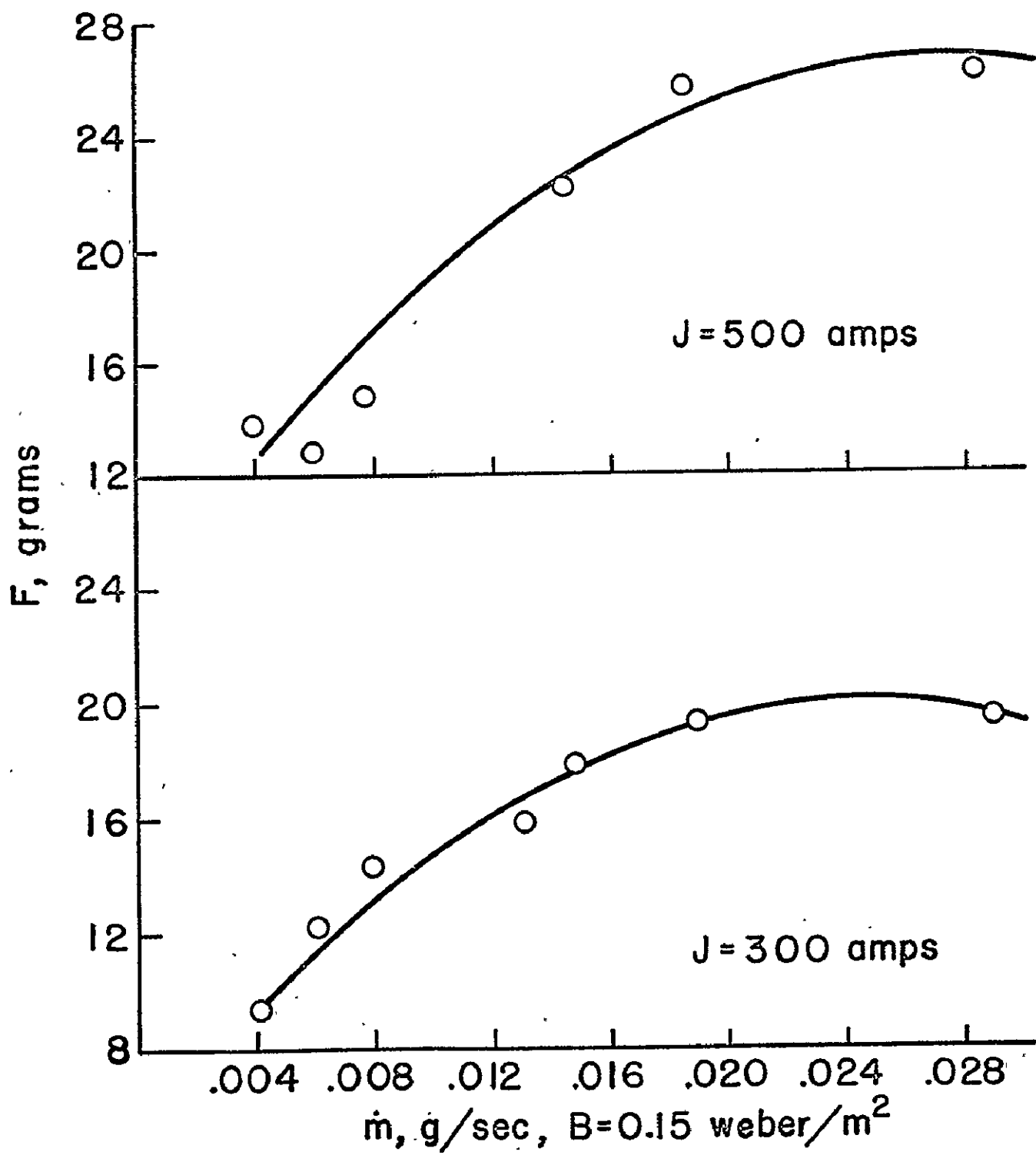
At the recent Fifth Electric Propulsion Conference a phenomenological theory describing the MPD arcjet was presented by Bennett, John, Enos and Tuchman<sup>1</sup>. The theory employs the concept of an effective mass flow rate<sup>2,3</sup> and is based on the assumption that the arc discharge will operate at an effective mass flow rate,  $\dot{m}_e$ , which minimizes the arc voltage independent of the actual mass flow rate passing through the device. As a result of this theory it is shown that, for mass flow rates greater or equal to  $\dot{m}_e$ , the maximum attainable velocity is limited by a critical velocity,  $v_c$ , given by  $v_c = (2I/m)^{1/2}$  where  $I$  is the ionization potential and  $m$  is the mass of the atom. For mass flow rates less than  $\dot{m}_e$  the maximum velocity can exceed  $v_c$ . It appears that the concept of effective mass flow rate was introduced<sup>2</sup> to explain the existence of the voltage plateau which is characteristic of rotating plasmas. Since it has been shown<sup>4,5</sup> that an interpretation of this phenomenon can be obtained from a consideration of the conservation equations, the observed behavior of the MPD arcjet should be explained without invoking any assumptions regarding the mass flow rate or the voltage.

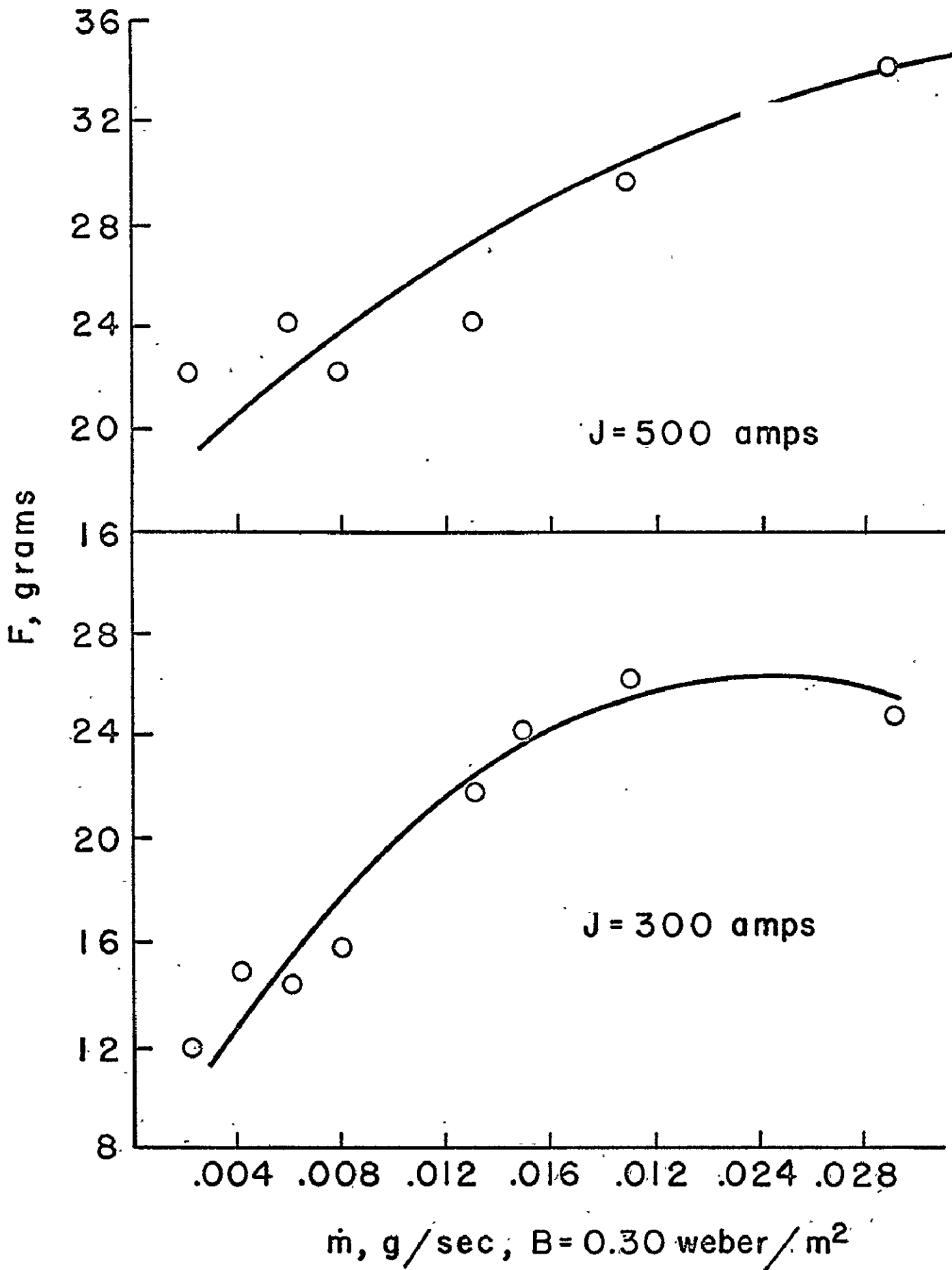
It has been established experimentally and theoretically that the voltage has the representation  $V = V_0 + CB$  where  $V_0$  and  $C$  are constants depending on the propellant and  $B$  is the magnetic field strength. Using this relation and the conservation equations, it is shown that there exists a critical mass flow rate at which the thrust is maximum. In the absence of losses, the efficiency at this critical mass flow rate is 50% and, for mass flow rates less (or greater) than the critical mass flow rate, the efficiency is greater (or less) than 50%. The critical mass flow increases with an increase in total current and/or magnetic field strength. This critical mass flow rate plays the same role played by  $\dot{m}_e$  of Ref. 1.

An experimental verification of the above theory requires thrust measurements for a given total current and magnetic field strength for a range of mass flow rates at low tank pressure. Such measurements were reported by Brockman, Hess, Bowen and Jarrett<sup>6</sup> for various tank pressures. The figures show a least-square fit of the data of Ref. 6 for low tank pressures. These figures indicate the existence of an optimum mass flow rate which increases with an increase in the total current and/or magnetic field strength in agreement with the predictions of the theory.

References

- <sup>1</sup> Bennett, S., et al. "Experimental investigation of the MPD arcjet." AIAA Paper 66-239 (March, 1966).
- <sup>2</sup> Moore, R. A., Cann, G. L., and Gallagher, L. R. "High specific impulse thermal arcjet thruster technology." AFAPL-TR-65-48, Part I. Air Force Aero Propulsion Laboratory (June, 1965).
- <sup>3</sup> Cann, G. L., et al. "Hall current accelerator." NASA CR-5470 (1966).
- <sup>4</sup> Hassan, H. A., et al. "Experiments and analysis for coaxial Hall current accelerators and the role of ionization effects." Sixth Symposium on Engineering Aspects of MHD, 83-84 (April, 1965).
- <sup>5</sup> Hassan, H. A., Hess, R. V., and Grossmann, W. "Study of coaxial Hall current accelerators at moderate pressures." To appear as a NASA TN.
- <sup>6</sup> Brockman, P., et al. "Diagnostic studies in a Hall accelerator at low exhaust pressure." AIAA Paper 65-297 (July, 1965).





## ANALYSIS OF INSTABILITIES IN A LINEAR HALL CURRENT ACCELERATOR

G. W. Garrison, Jr. and H. A. Hassan  
 North Carolina State University  
 Raleigh, North Carolina

NsG - 363

Experimental investigation of instabilities in linear Hall current accelerators with applied axial electric fields and radial magnetic fields. showed the existence of screw type instabilities<sup>1,2</sup> which show a striking resemblance to the instabilities observed in the positive column. Various attempts<sup>1,2</sup> have been made to apply the various theories developed by Kadomtsev and Nedospasov<sup>3</sup>, Simon<sup>4</sup>, Hoh<sup>5</sup> and Morse<sup>6</sup> for the study of instabilities in the positive column and crossed field geometries to the linear Hall current accelerator. However, none of the above theories was directly applicable.

Because of the observed instability in the linear Hall current accelerator is similar to that observed in the positive column, the governing equations employed here are those normally employed in the study of weakly ionized gases. These equations were also the basic equations employed in References 3-6. A normal mode analysis similar to that employed by Johnson and Jerde<sup>7</sup> for the positive column has been employed. It is shown that, regardless of the direction of the density gradient, no screw type instability exist if it is assumed that the axial magnetic field is identically zero. Since the driving mechanism of the observed instability is an  $E \times B$  drift the above result is expected because a  $B_r$  component alone does not yield a radial drift component.

Since the axial component of the magnetic field is small but never identically zero in a linear Hall current accelerator, the analysis has been carried out for a magnetic field having both a radial and axial components. An exact solution of the governing equations resulted in a density distribution with no axial or azimuthal dependence. This solution was expressed in terms of the confluent hypergeometric function. Assuming that the perturbed density and potential have the general representation  $f(r) \exp i(\omega t + k_z z + m\theta)$  where  $\omega$  is the frequency and  $k$  is the wave number a general dispersion relation has been derived. The special case of a right handed helix ( $m = -1$  mode) has been discussed in detail and the results are presented graphically. The Figures show plots of frequency, wave length, electric field for typical mobilities vs. the critical value of  $B_z/B_r$  at the stability boundary. It is seen that the dimensionless parameter  $x_0$  which depends on the ionization rate, radius of the device and radial and axial magnetic field strengths has a great influence on the stability; as the value of  $x_0$  increase the discharge becomes more and more unstable. As an illustration, the calculations show that the discharge is unstable for values of  $x_0$  between 1.5 and 2.0 when  $\delta$ , the mobility ratio, is 10. This result is somewhat interesting because the results of Ref. 1 indicate an onset of instability as soon as the magnetic field is switched on. The results also show that, at the stability boundary, the wave length is almost independent of the magnetic field strength except for a combination of high  $x_0$  and  $B_z/B_r$ . Also, an increase in  $B_r$  promotes stability.

## References

- <sup>1</sup>Hess, R. V. and J. Burlock, B. Sidney and P. Brockman, 1964. Study of Instabilities and Transition to Turbulent Conduction in the Presence of Hall Currents. International Symposium on Diffusion of Plasma across a Magnetic Field, Feldafing, Germany.
- <sup>2</sup>Jones, G. S. and J. Dockon. 1964. Experimental Studies of Oscillations and Accompanying Anomalous Electron Diffusion Occurring in D.C. Low Density Hall Type Crossed Field Plasma Accelerators. Proceedings of the Fifth Symposium on the Engineering Aspects of Magnetohydrodynamics. MIT Cambridge, Mass. pages 135-148.
- <sup>3</sup>Kadomtsev, B. B. and A. V. Nedospasov. 1960. Instability of a Positive Column in a Magnetic Field and the "Anomalous" Diffusion Effect. J. Nuclear Energy, Part C, Plasma Physics 1:230-235.
- <sup>4</sup>Simon, A. 1963. Instability of a Partially Ionized Plasma in Crossed Electric and Magnetic Fields. Physics of Fluids 6(3): 382-388.
- <sup>5</sup>Hoh, F. C. 1963. Instability of a Penning-Type Discharge. Physics of Fluids 6(8):1184-1191.
- <sup>6</sup>Morse, D. L. 1965. Low Frequency Instability of Partially Ionized Plasma. Physics of Fluids 8(7):1339-1346.
- <sup>7</sup>Johnson, R. R. and D. A. Jerde. 1962. Instability of a Plasma Column in a Longitudinal Magnetic Field. Physics of Fluids 5(8):988-993.

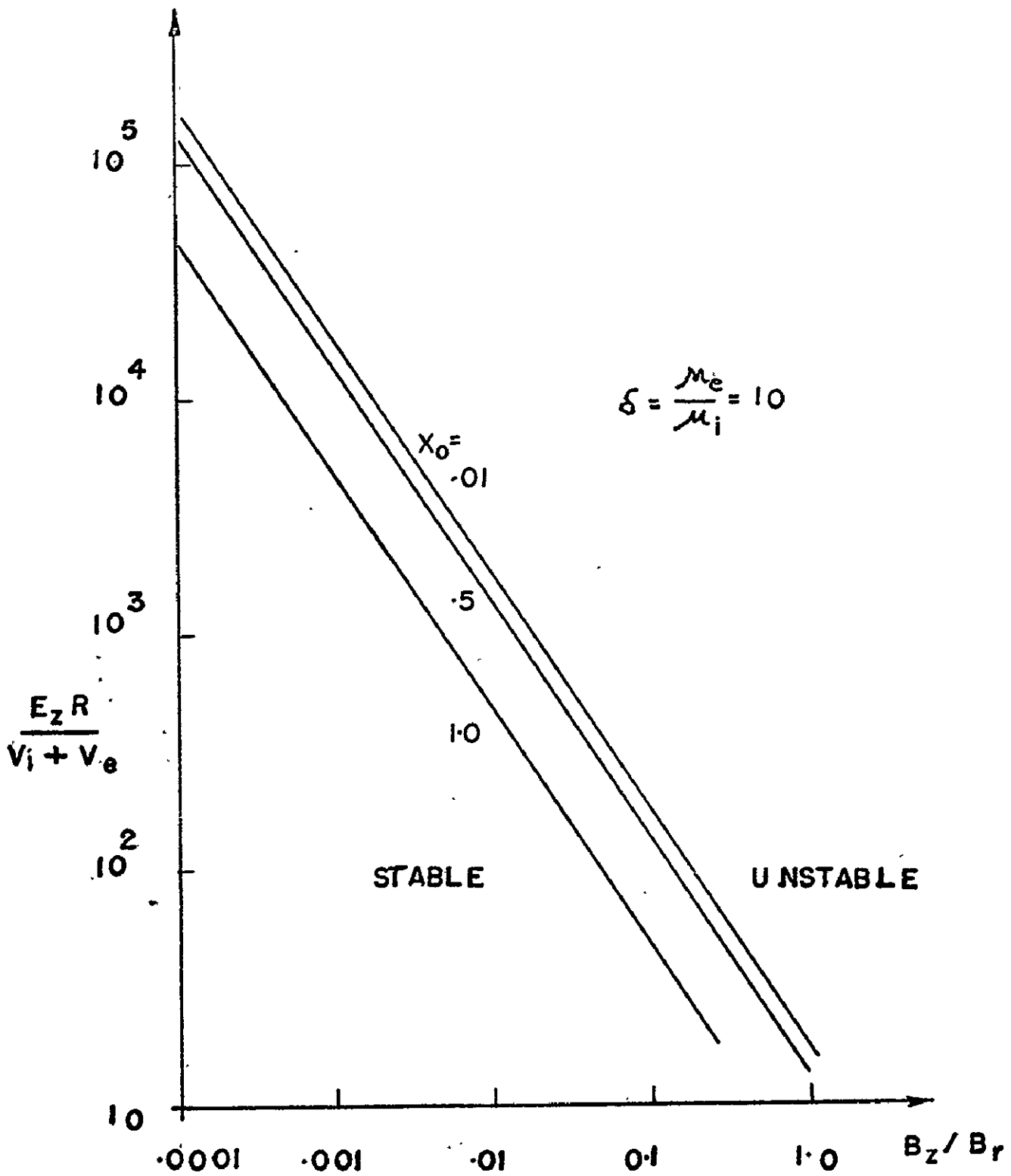


FIGURE 1. ELECTRIC FIELD vs  
MAGNETIC FIELD RATIO.



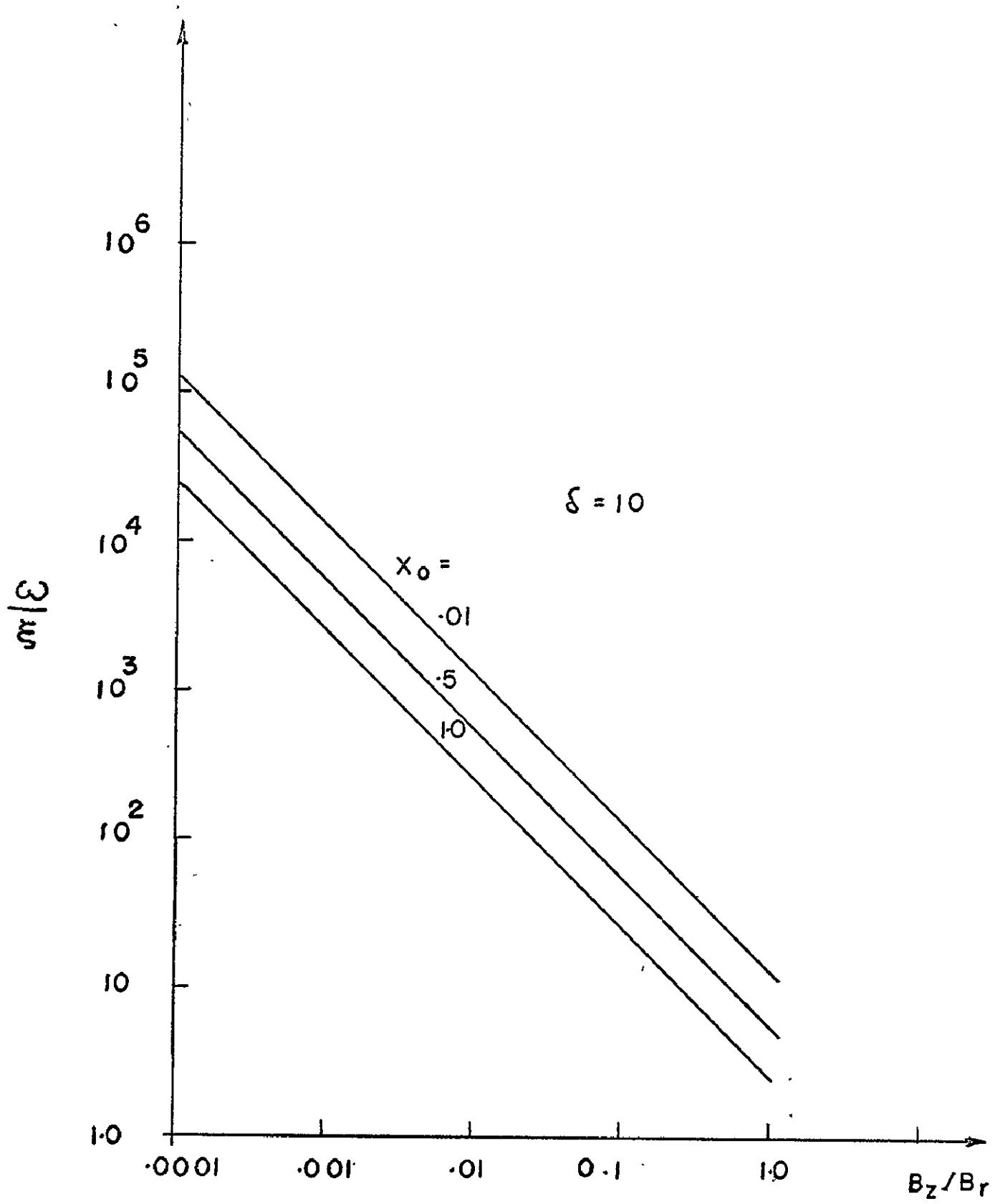


FIGURE 2. FREQUENCY vs MAGNETIC FIELD RATIO

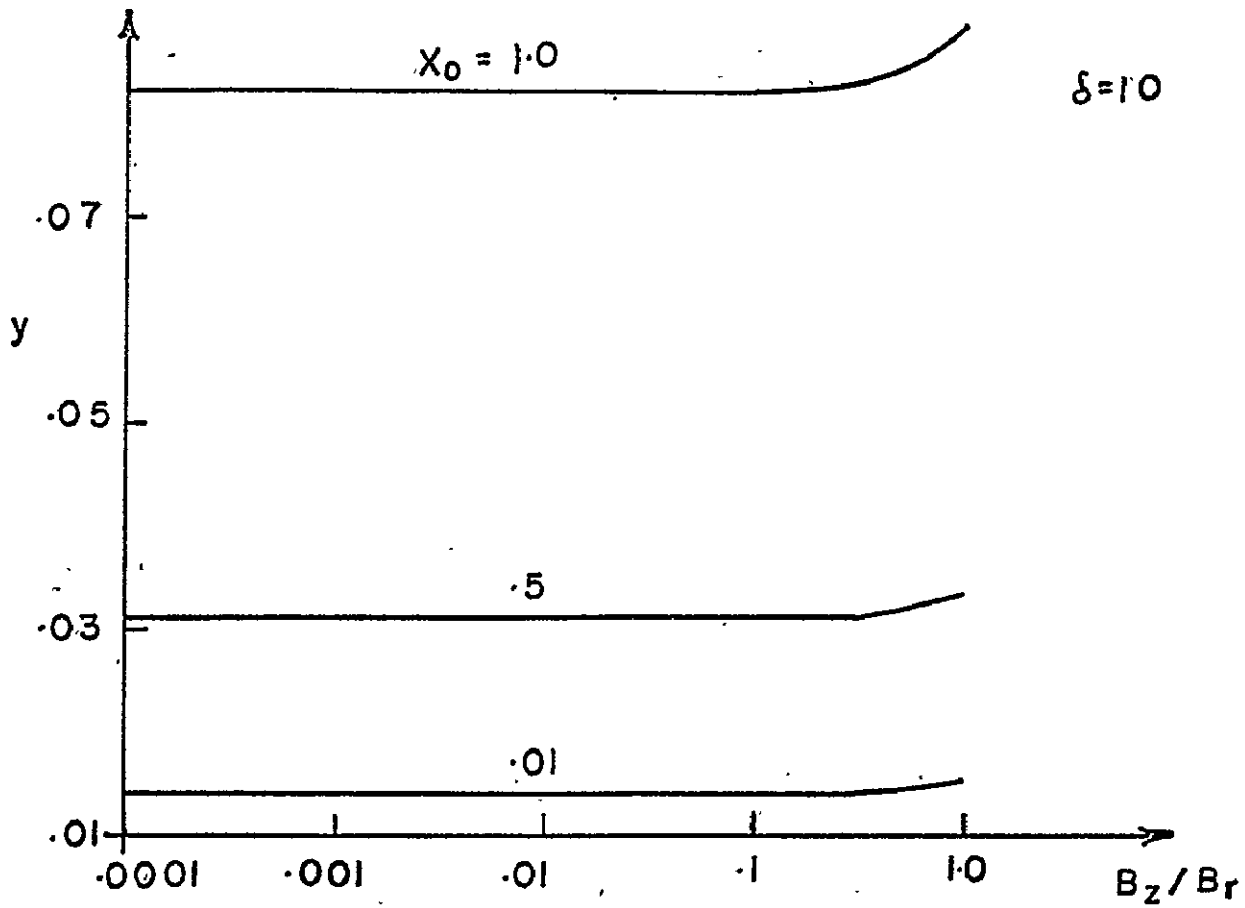


FIGURE 3.  $y$  vs MAGNETIC FIELD RATIO

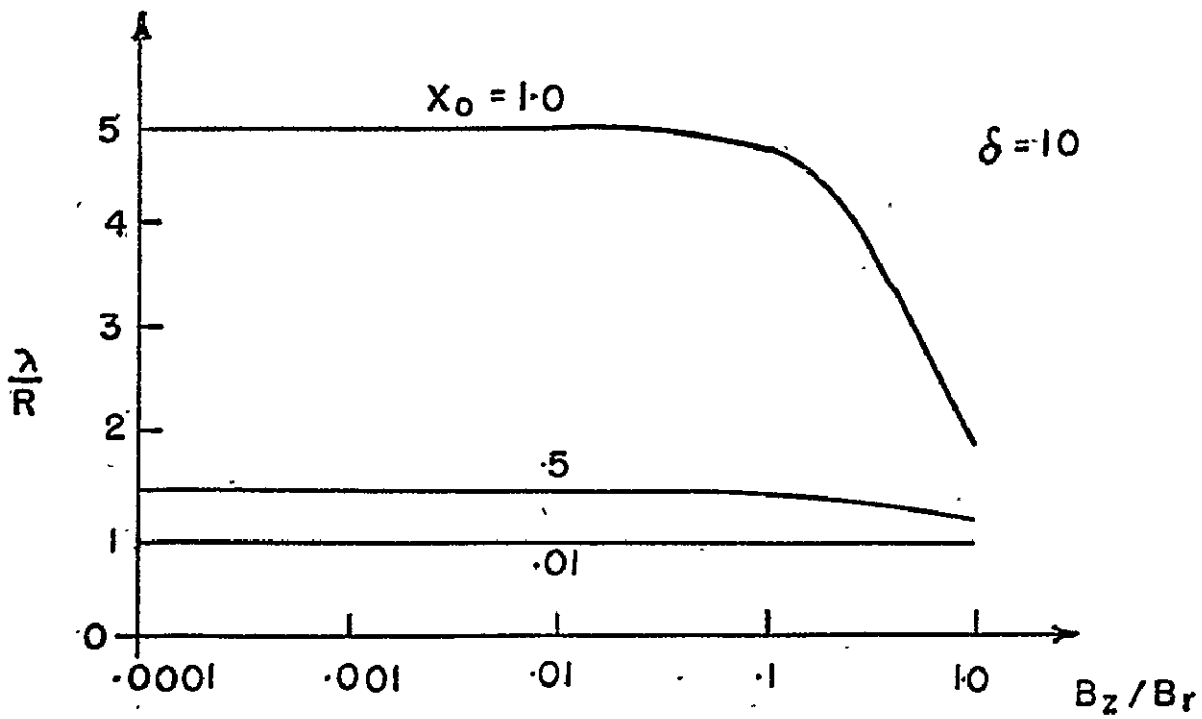


FIGURE 4. WAVE LENGTH vs MAGNETIC FIELD RATIO

EXPERIMENTAL INVESTIGATIONS OF STRONG SHOCK WAVES  
MOVING THROUGH AN IONIZED GAS

G. L. Spencer  
Case Institute of Technology  
Cleveland, Ohio

An experimental investigation of shock waves moving through a highly ionized gas is reported. The shock waves are generated in an electromagnetic T-tube. The ambient gas, helium, is highly preionized by means of an axial current discharge with the shock waves being initiated during the after-glow period of the preionization. Measurements have shown that the plasma is in local thermal equilibrium and nearly completely ionized during the early after-glow period of the preionization. Typical temperatures and electron densities are in the order of 22,000°K and  $3 \times 10^{16}$  electrons/cm<sup>3</sup>. Gasdynamic shock waves were studied and the results compared to the theory presented by Jaffrin and Probststein.\* It was possible to verify the existence of, and quantitatively measure the thickness of the first layer, as predicted by their theory. Magnetohydrodynamic effects were studied via provision of an axial magnetic field. Magnetic field jumps and currents were observed in the shock front and found to be completely stable as long as the shock wave could be observed. It was found that these effects did not appear if either the applied magnetic field or preionization were absent.

\*Jaffrin, M. Y. and R. F. Probststein, Phys. Fluids 7, 1958 (1964).

## HARMONIC GENERATION IN A MICROWAVE PLASMA

F. J. Mayer and O. K. Mawardi

Case Institute of Technology  
Cleveland, Ohio

A number of attempts have been made to estimate the harmonics generated in a microwave discharge.<sup>1</sup> These predictions have been compared with experiments.<sup>2</sup> The corroboration of the theory with the experimental observations has often been artificially improved by the arbitrary choice of parameters appearing in the theory. One such parameter is the electron temperature. Now as this temperature has a marked influence on the amplitude of the harmonics one would expect that the temperature should be found as one of the consequences of a correct theory.

Accordingly, the affect of a few parameters were studied systematically. It was demonstrated<sup>3</sup> that the temperature dependence of the collision frequency was unimportant in as far as explaining the result of Uenohara's experiment.

Work is now proceeding to investigate the effect of density gradients and ionization on the harmonic generation.

---

<sup>1</sup>B. Murphy, Phys. Fluid 8, 1534 (1965); P. Rosen, Phys. Fluid 4, 341 (1961).

<sup>2</sup>M. Uenohara, et.al., Proc. Ionization Phenomena in Gases, 2, 768 (1960).

<sup>3</sup>F. Mayer, Phys. Fluid (In Press).

A WIDE-BAND DICKE TYPE RADIOMETER  
A. T. Alper and O. K. Mawardi  
Case Institute of Technology  
Cleveland, Ohio

A wide-band Dicke type radiometer capable of operating within 2.6 to 14 KMC frequency range has been constructed. In order to achieve this extremely wide bandwidth operation double ridge waveguide instruments, such as a balanced mixer, a directional coupler, a ridged-waveguide switch, two coaxial to ridge adapters, and X and S-band to ridge waveguide transitions, have been designed and developed. Difficulties have been encountered in achieving uniform frequency response of the balanced mixer due to matching of mixer "E" and "H" planes to the balanced arms. Aside from 4.5 - 5 KMC frequency bandwidth, the radiometer has been calibrated in the range of 2.6 to 9 KMC using argon and fluorescent noise sources. The radiometer sensitivity, equivalent to a minimum detectable temperature change of 1.6°K has been computed.

With wide-band capability of this radiometer, electron cyclotron radiation intensity measurements in a plasma have also been made by sweeping local oscillator of the radiometer from 2.6 to 9 KMC.

The radiometer is planned to be used in a series of investigations dealing with electron cyclotron harmonic generation in a plasma.

EXPERIMENTAL STUDY OF THE INTERACTION OF ENERGETIC ELECTRON  
AND A PLASMA

W. B. Johnson and M. R. Smith  
Case Institute of Technology  
Cleveland, Ohio

An experimental determination is made of the distribution of energy losses suffered by a beam of energetic test electrons traversing a dense, high temperature plasma. The test electron energy is 3,000 electron volts and the plasma density varies from  $5 \times 10^{15}$  to  $1 \times 10^{16}$   $\text{cm}^{-3}$  at a temperature of  $\sim 40,000^\circ\text{K}$ . The experiment was designed to produce data on single electron interactions and not on beam-plasma effects. The experimental average energy loss is observed to be larger than the theoretical prediction, indicating a minimum discrepancy of at least an order of magnitude between theory and experiment. The theory includes the effects of binary collisions and collective interactions. The discrepancy probably is explained by the neglect in the theory of higher order terms in the plasma kinetic equations. The experimental average energy loss and spread in energy are both found to vary proportional to the plasma electron density.<sup>1,2</sup>

---

Reported in detail in:

- <sup>1</sup>"A Measurement of Energetic Test Electron Interaction with a Plasma", M. R. Smith and W. B. Johnson, Plasma Research Program T.R. A-38, June, 1965; Case Institute of Technology.
- <sup>2</sup>"Collisional Interactions of Energetic Test Electrons with a Plasma", M. R. Smith, Plasma Research Program T.R. A-39, July, 1965; Case Institute of Technology.

A BEAT FREQUENCY INTERFEROMETER FOR PLASMA DIAGNOSTICS\*

W. B. Johnson, A. B. Larsen, and T. P. Sosnowski

Case Institute of Technology

Cleveland, Ohio

A laser method has been developed for the diagnostics of plasmas with electron densities greater than about  $10^{11}$  electrons/cm<sup>3</sup>. A spatial resolution of about one microsecond, is calculated for the particular apparatus which has been used. The range of sensitivity corresponds favorably to that achieved by microwave methods, but the spatial resolution is much superior to that afforded by microwaves. The method depends on the detection of the shift in frequency of a laser when a plasma is introduced into the optical cavity.

If a cavity of length  $L$  is employed to probe a plasma of length  $l$  internal to the cavity, then a frequency shift  $\Delta\nu$  is expected which is given by

$$\Delta\nu = \frac{1}{2} \nu \frac{\omega_p^2}{\omega^2} \frac{l}{L} - \nu \frac{l}{L} (n_0 - 1) \quad (1)$$

where  $\omega_p^2 = 4\pi n e^2/m$  is the square of the plasma frequency,  $\nu$  is the oscillatory frequency of the laser, and  $n_0$  is the index of refraction of all other particles in the plasma. To separate the effects of plasma, the frequency shift must be measured at two laser frequencies. Conveniently He-Ne lasers operate well at both 6328 Å and 11,523 Å. At the first wavelength, the expected plasma contribution for a density of  $10^{11}$  electrons/cm<sup>3</sup> is 4.3 kc/s for  $l/L = 1/2$ . Observed frequency shifts are about two orders of magnitude higher, which shows the necessity for making the dual measurement. FM detector techniques have been used with frequency differences up to about 5 mc/s. For larger shifts, spectrum analyzer methods could be employed out to the limit of photomultiplier tubes. Thus these techniques complement both microwave and other laser methods for the measurement of plasma electron densities.

Experimentally a system has been constructed which employs two laser cavities; one laser serves as the probe and the other the "local oscillator" laser. Each of the lasers is isolated optically and electronically but coupled together mechanically to assist in the cancellation of mechanical and thermal drifts. The output beams from each laser are made to coalesce by a beam splitter and are allowed to illuminate the surface of a photomultiplier. Two channels are thus available to make measurements simultaneously at the two wavelengths, 6328 Å and 11,523 Å. Using these techniques and others to be described in the paper, excellent overall system stability has been achieved in standard laboratory surroundings. Beat frequencies of  $\pm 150$  kc/s for at least three minutes. The former corresponds to a stability of the total optical path length to about  $\pm 0.1$  Å. Short-term stability measurements therefore show that plasmas in the order of  $10^{11}$  electrons/cm<sup>3</sup> can be probed. Experimental data on argon discharge tubes will be presented.

It is felt that with a better environment that it should be possible to improve on this stability by an order of magnitude.

---

\*Also published in:

Journal of Quantum Electronics, April, 1966, Vol. QE-2, Paper 8C-8 Pg. 1x.



## TURBULENCE IN A RAREFIED PLASMA

C. M. Tchen

National Bureau of Standards, Washington, D. C.

A theory is developed on the damping process in a turbulent plasma (nonlinear Landau damping). The Vlasov-Poisson equations, describing the turbulent fluctuations, generate a chain of equations for their correlations. If the fourth order correlation is degenerated into lower orders, the chain becomes closed. The result shows that the decay of the electrostatic wave energy is governed by the sum of two damping coefficients: (1) a linear Landau damping coefficient which is independent of the amplitude, and (2) a turbulent damping coefficient dependent on the amplitude. Correspondingly the dielectric coefficient consists of a linear part and a turbulent part. On the same basis a kinetic equation is derived in the generalized form of the Fokker-Planck equation.

## PLASMA VORTICES AND THEIR MOTION IN INHOMOGENEOUS MAGNETIC FIELDS

Winston H. Bostick  
Stevens Institute of Technology

In the laboratory experiment of plasma flow over a magnetic dipole the breakup of the plasma front into plasma vortices has been observed by magnetic and electric field probes and by image-converter photography. (See figure 1). Recent image-converter photographs now show quite clearly the formation of these columnar type vortices in pairs. One can make a plausible model for the formation of these pairs out of the flutes which grow in Rayleigh Taylor instability. (See figure 2). One can also now understand on the same basis why the plasma proceeding across a magnetic field from a small two-wire button plasma gun is in the form of columnar plasma vortices two abreast.

The photographed trajectories of plasma from a two-wire button plasma gun fired in inhomogeneous magnetic fields shows clearly that the plasma vortices "bounce off" of the region of increasing field.

The force-free type of vortices with helical magnetic fields observed by Wells have been studied by one of our students Robert Small, at Grumman. He confirms with density-flow probes, magnetic and electric field probes that the conical theta-pinch generates a train of such force-free vortices which proceed along a guide field and coalesce with time.

The plasma coaxial accelerator operated with a hexagonally shaped center conductor generates two such force-free vortices on each flat side of the hexagon. We now understand qualitatively the process whereby these pairs of vortices, one corotating, the other counterrotating, are generated. (See figure 3).

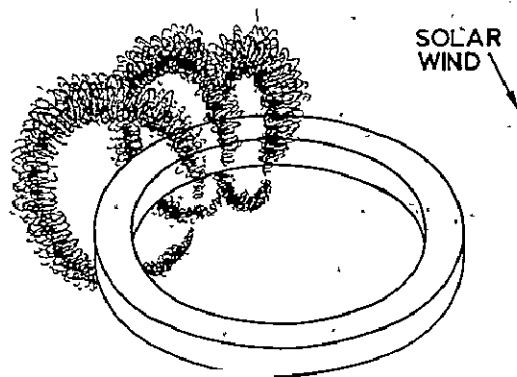


FIG. 1

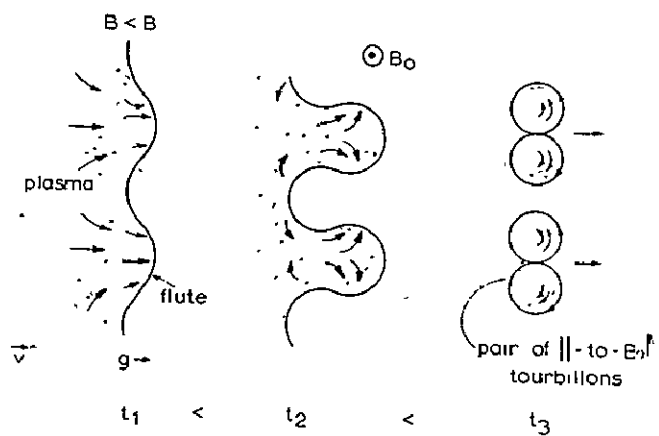


FIG. 2

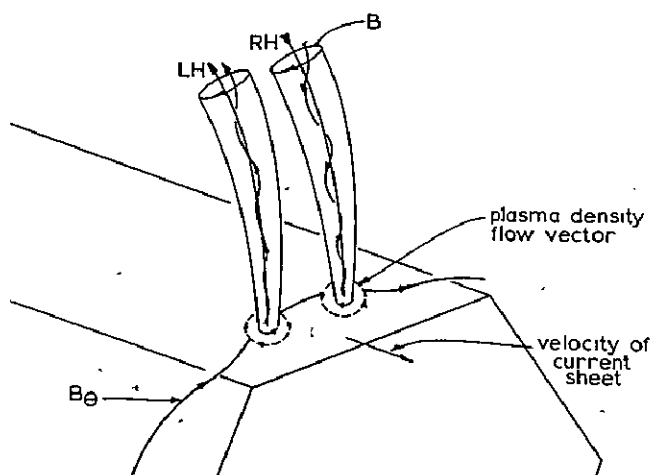


FIG. 3

## Addendum to Report

Pair Production of Plasma Vortices, W. H. Bostick et. al.

The only vectors in figure 5 whose directions (i.e. the signs) have been experimentally measured or inferred thus far are:

- a. The general direction of  $B_0$  in the coaxial accelerator, resulting from a negative center conductor and positive outer conductor.
- b. The direction of  $B$  along each of the radial plasma filaments (see figure 3).
- c. The plasma density flow vector along the filaments is inferred from general plasma flow patterns in previous coaxial accelerators and also from the fact that figure 2 shows a piling up of the plasma at the locations where the radial filaments intersect the outer conductor (anode).

In figure 5 the plasma density flow vectors circumferential to the filaments and magnetic fields circumferential to the filaments have been only surmised with consistency being observed in righthandedness and lefthandedness for both magnetic and velocity vectors. A serious criticism of the directions chosen for these vectors in figure 5 is that the current along the filaments would be in the opposite direction to the general current in the coaxial accelerator. An alternative and probably preferable choice is that shown in figure 6 in this addendum. The true determination of the directions of these vectors must await further measurements with coupling loops and density flow probes. These measurements are now in progress.

## ERRATA

1. Page 2 line 12 should read ( $\sim B_0$  in the coaxial accelerator) and show that these these fields are of opposite -----
2. Page 9 figure 5 caption - delete last line.

Winston H. Bostick

Winston H. Bostick  
Stevens Institute of Technology  
Hoboken, New Jersey  
5 April 1966

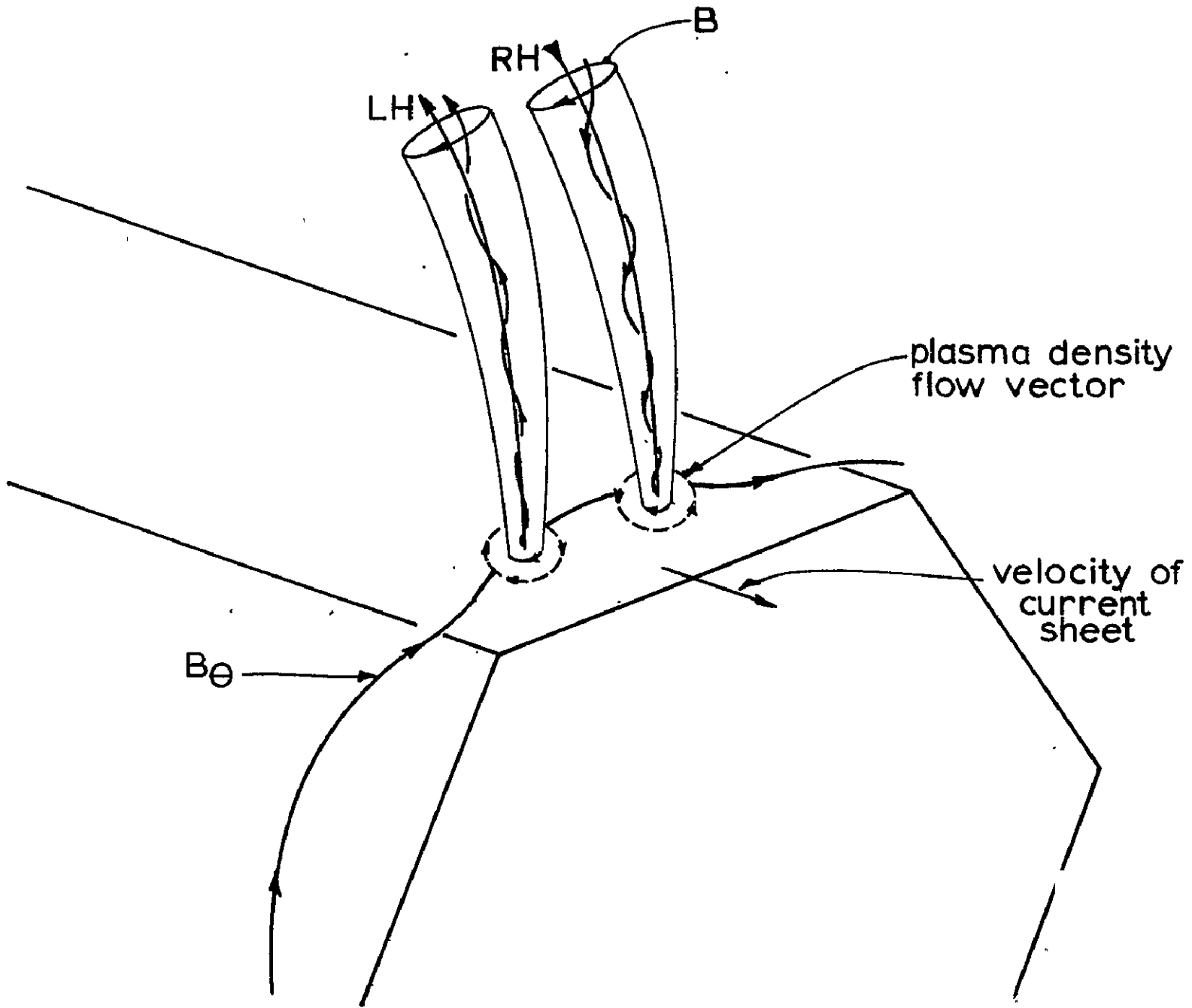


Figure 6`

EXPERIMENTAL INVESTIGATION OF THE FUNDAMENTAL  
MODES OF A COLLISIONLESS PLASMA

Contract Number NAS7-275  
General Atomic Division  
General Dynamics Corporation  
P. O. Box 608, San Diego, California 92112

Principal Investigator: John H. Malmberg  
Associates: David L. Book  
Norris W. Carlson  
T. K. Fowler  
C. Dave Moore  
T. O'Neil  
Charles B. Wharton  
Norman Rostoker

Objective

To measure the dispersion, damping, and beam induced growth of plasma waves near the electron cyclotron frequency, and to develop theoretical dispersion relations for plasma waves in non-uniform plasmas. This work is part of a project to investigate experimentally and theoretically the turbulence resulting from the growth of waves in a collisionless plasma, and to study the effect of the turbulence on properties of the plasma (e.g., transport coefficients).

Background

The behavior of plasmas is, in many circumstances, dominated by dynamic effects which do not depend on the existence of large-angle collisions. In these collisionless plasmas the usual collisional dissipative mechanisms are absent and the dynamics of such plasmas are completely different from the dynamics of a fluid. Among the most basic properties of a collisionless plasma, from a theoretical point of view, are those embodied in the dispersion relations which determine the character of the waves which can propagate in the plasma. If any of these waves are unstable, they grow to some limit determined by the non-linear theory of plasma dynamics, and the wave spectrum in the final state (i.e., the turbulent end-result of the growth) determines many of the plasma properties of practical interest. For example, the transport properties, the microwave scattering cross section, and the equilibrium density in a containing field (e.g., the earth's magnetic field) are likely to be dominated by the turbulence of the plasma.

The dynamics of a collisionless plasma is described by the collisionless Boltzmann equation combined with Maxwell's equations. These equations, combined with the definition of charge and current, constitute a complete set of equations and thus, if boundary conditions are specified, are in principle a complete description of the collective motions of the plasma. However, the equations are non-linear and cannot be integrated directly. To obtain solutions the set of equations is usually linearized by investigating the effect of a small disturbance on some initial state, i.e., using perturbation theory. By carrying the perturbation theory to second order ("quasi-linear theory") a description of the turbulence resulting from the wave growth is obtained, and from what amounts to a third order calculation, the ultimate dissipation of

the turbulence is predicted. Experimental confirmation of the theory is almost completely lacking, partly because it has only recently been possible to make laboratory plasmas which match the assumptions of the theory.

### Progress and Results

The principal theoretical effort in the program has been devoted to developing the theoretical techniques necessary for the application of the linear theory of plasma waves to the geometries encountered experimentally, where the size is finite, and the density a function of position. In particular, methods have been developed for predicting the dispersion and damping of electron cyclotron waves in the geometry of the turbulence machine from first principles.

The turbulence machine at General Atomic (developed under other programs) provides a quiescent, collisionless plasma which matches the assumptions of the theory. Included in the installation are a variety of highly developed diagnostic instruments for wave propagation experiments. Many of the plasma properties are known in detail from other experiments. Using this facility, the propagation of waves near the electron cyclotron frequency has been investigated. The dispersion and damping of the waves has been measured, and their growth due to an electron beam injected into the plasma has been observed. Some of the waves are wave-guide modes perturbed by the plasma. The wave of most interest for these measurements is electron cyclotron wave. This is a backward wave which propagates between the cyclotron frequency and the upper hybrid frequency. The measurements have been made for a variety of plasma parameters.

Addition of a cusp magnetic field to the usually uniform magnetic field near the plasma source reduces the anomalous diffusion of the plasma by an order of magnitude. We hypothesize that this geometry decreases random electric fields in the plasma by reducing communication with the source, and thus results in reduced diffusion.

### Future Plans

We intend to continue the investigation of the waves. We want to compare the observed dispersion relations with theory using independently measured plasma properties in the theory for comparison. The damping measurements need better precision, and much better growth data would be desirable. After the dispersion, damping, and linear growth of these waves is measured and compared to theory, the next step along the road to understanding the ultimate turbulence and diffusion associated with them is to investigate the non-linear limit of their growth. Further measurements will also be made to establish whether our hypothesis on how the cusp field reduces diffusion is correct.

### References

- C. B. Wharton and J. H. Malmberg, Bull. Am. Phys. Soc. II, 10, 2, 199 (1965)  
 "Cyclotron Waves in a Collisionless Plasma"
- D. L. Book, General Atomic Internal Report, GAMD-5917, "Landau Damping of Electrostatic Modes with Finite System Effects"

## STABILITY OF PLASMAS SUBJECT TO CONVECTIVE INSTABILITIES

E. H. Holt and D. A. Huchital

Rensselaer Polytechnic Institute, Troy, N.Y.

A transverse magnetic field which is weak relative to the main longitudinal magnetic field applied to a positive column plasma has the effect of increasing the range of plasma parameters over which the plasma remains stable against the well known Kadomtsev or convective instability. Kadomtsev and Nedospasov<sup>1</sup> have shown that a perturbation of the form

$$\bar{n}(r) = J_1(\beta r) \exp(im\phi + ikz + i\omega t)$$

will grow provided the criterion

$$Ak^4 + Ck^2 + G_o + G_m \leq mHk\mu_e E_z / T_e \quad (1)$$

is satisfied, where the coefficients are functions of the longitudinal magnetic field defined in reference 1. We have modified equation (1) to include a transverse field, by writing it in the form<sup>2</sup>

$$Ak^4/P^2 + Ck^2/P + G_o + G_m \leq mHk\mu_e E_z / PT_e \quad (2)$$

where  $P = 1 + (\mu_e B_T)^2$ . Clearly equation (2) reduces to equation (1) in the limit  $B_T = 0$ .

The two criteria are compared in Figure 1, in terms of the parameter  $\theta = \tan^{-1} B_T/B_L$ . It can be seen that the plasma becomes more stable as  $B_T$  increases. Experimental confirmation of this result has been obtained. A further consequence of finite  $B_T$  is shown to be the suppression of  $m = 1$  in favor of  $m = 2$  instabilities.<sup>3</sup>

Results of experiments aimed at stabilizing the plasma by means of quadrupole magnetic fields are illustrated in Figure 2. Stabilization of solid state plasmas in InSb has been successfully achieved in this way by Ancker-Johnson.<sup>4</sup> In our case, modest currents through the stabilizing windings are shown to quench the instability oscillations quite effectively.

The convective type of instability is likely to occur in a number of different plasma types covering a wide range of plasma parameters. Guest and Simon<sup>5</sup> have suggested that an entirely similar mechanism operates in the low pressure arc due to streaming of particles along the magnetic field. Hoh<sup>6</sup> and Simon<sup>7</sup> have proposed that a variation of the Kadomtsev instability is present in a reflex discharge. Finally, Cherrington<sup>8</sup> has shown that longitudinal gradients of density and temperature can trigger the Kadomtsev instability, thus suggesting an explanation for the anomalies observed in an rf discharge by Powers.<sup>1</sup> A systematic approach, based upon the techniques we have developed in studying the positive column, is expected to yield important information concerning the instability mechanism in this wide variety of plasmas.



1. B. B. Kadomtsev and A. V. Nedospasov, *J. Nucl. Energy*, C1, 230 (1960).
2. D. A. Huchital, J. F. Reynolds and E. H. Holt, Paper 66-157, AIAA Plasmadynamics Conference, Monterey, California, March 1966.
3. D. A. Huchital and E. H. Holt, *Phys. Rev. Letters*, 16, 677 (1966).  
D. A. Huchital and E. H. Holt, Submitted to *Appl. Phys. Letters*.
4. B. Ancker-Johnson, *Phys. Fluids*, 7, 1553 (1964).
5. G. Guest and A. Simon, *Phys. Fluids*, 5, 503 (1962).
6. F. C. Hoh, *Phys. Fluids*, 6, 1184 (1963).
7. A. Simon, *Phys. Fluids*, 6, 382 (1963).
8. B. E. Cherrington and L. Goldstein, Air Force Cambridge Research Laboratories, Report No. AFCRL-65-257.

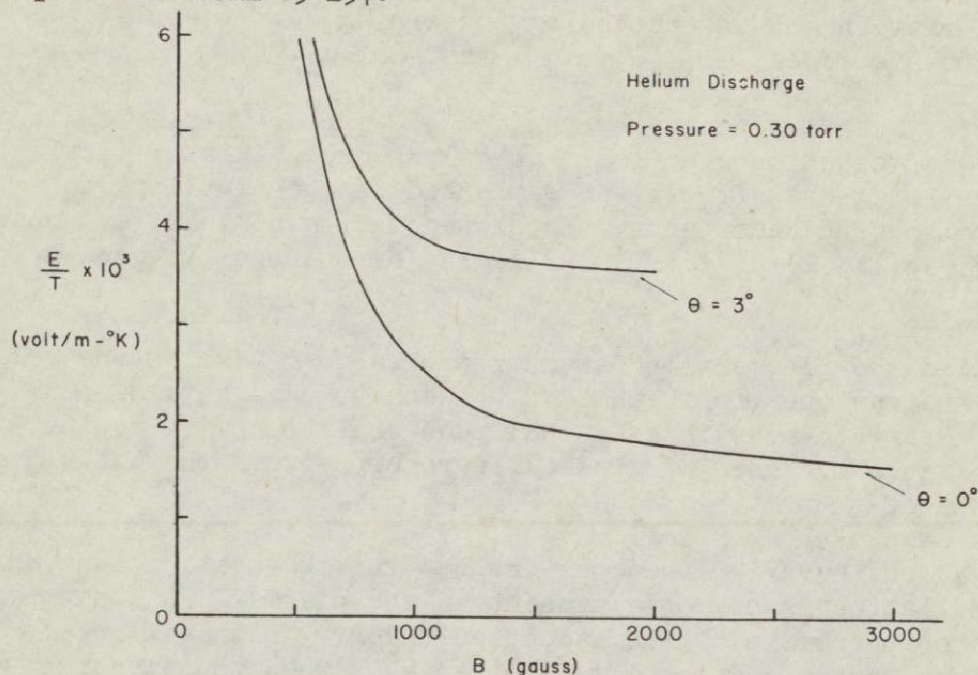


Figure 1. The Stability Criterion for a Positive Column Showing the Effect of a Transverse Component of the Magnetic Field.  
 $(\tan \theta = B_{\text{transverse}}/B_{\text{longitudinal}})$

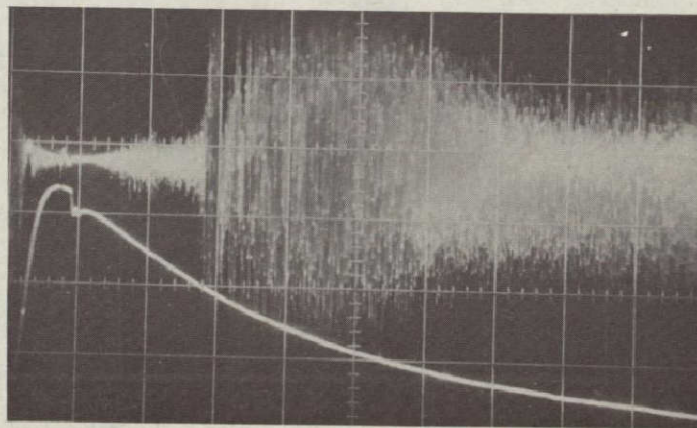


Figure 2. Stabilization of the Discharge by a Quadrupole Magnetic Field.  
 Top trace: AC voltage picked up on a probe (1 volt/cm)  
 Bottom trace: Current through the quadrupole windings (20 amp/cm)  
 Time scale: 10 milliseconds/cm



## MODES OF THE KADOMTSEV INSTABILITY

D. A. Huchital and E. H. Holt

Rensselaer Polytechnic Institute, Troy, N.Y.

We have carried out a systematic experimental study on the modes of the Kadomtsev instability of a collision dominated magnetoplasma which has resulted in new information and understanding concerning the presence and dominance of the separate modes,  $m = 0$ ,  $m = 1$  and  $m = 2$ .

Anomalous effects were reported by Lehnert<sup>1</sup> to appear when a longitudinal magnetic field,  $B_L$ , impressed on a dc positive column exceeded a critical value,  $B_c$ . The onset of these effects was explained by the stability considerations of Kadomtsev and Nedospasov<sup>2</sup> who showed that a helical perturbation of the form  $J_1(\beta r) \exp(im\phi + ikz + i\omega t)$  will grow exponentially when  $B_L > B_c$  and  $m \geq 1$ .

We have studied the plasma with Langmuir probes to determine the relative importance of the various possible modes.<sup>3</sup> We have used sets of four probes inserted  $90^\circ$  apart to measure azimuthal phase relations. A typical result is shown in Figure 1. The  $90^\circ$  phase difference between the two signals verifies the presence of the  $m = 1$  mode.

Our investigations have included the interesting observation that an  $m = 0$  class of oscillation is commonly present in the plasma. This new result cannot be explained on the basis of the Kadomtsev theory. Data will be presented to show that the  $m = 0$  oscillation vanishes when the electric field in the column is precisely aligned with the main magnetic field. Transverse components of magnetic field as small as 0.5 gauss are sufficient to generate  $m = 0$  oscillations of appreciable amplitude. Experimental and theoretical results will be presented to show that the  $m = 0$  oscillation is an important non-linear effect resulting from the interaction of the helical  $m = 1$  mode with the transverse magnetic field.

When the transverse magnetic field is increased to the order of several tens of gauss, the  $m = 2$  mode is observed to become the dominant oscillation. However, the experiment is incapable of distinguishing between a genuine  $m = 2$  instability and a non-linear effect similar to that associated with  $m = 0$ . We have developed a new experimental technique<sup>4</sup> that considers the response of the plasma to externally impressed perturbations while the magnetoplasma is operating in the sub-critical ( $B_L < B_c$ ) regime.

Figure 2 shows the signal detected at probe set B as a function of the frequency of the source connected to probe set A. It is shown that as the critical magnetic field of 2100 gauss is approached a distinct resonance representative at the  $m = 1$  instability is excited. Experimental results obtained by this technique will be presented to establish the independence of the  $m = 2$  instability and to confirm the non-linear nature of the  $m = 0$  mode.

1. B. Lehnert, Proc. 2nd U. N. Conference on Peaceful Uses Atomic Energy, 32, 349 (1958).
2. B. B. Kadomtsev and A. V. Nedospasov, J. Nuc. Energy, C1, 230 (1960).
3. D. A. Huchital and E. H. Holt, Phys. Rev. Letters, 16, 677 (1966).
4. D. A. Huchital and E. H. Holt, Submitted to Applied Physics Letters.

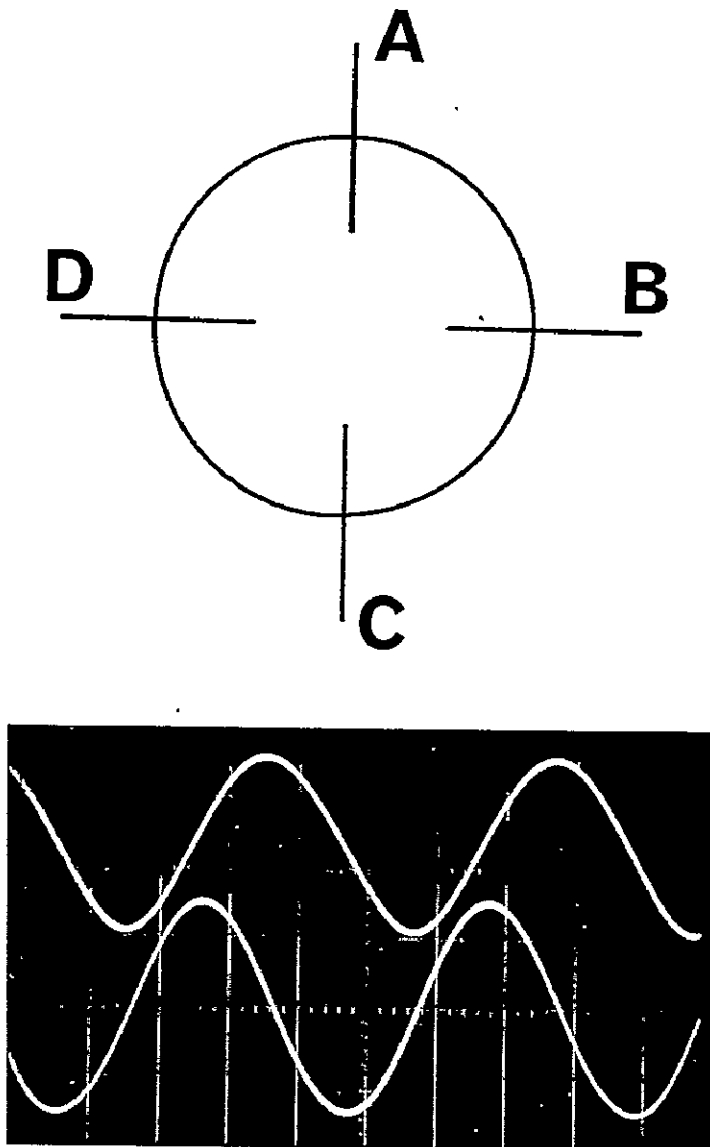


Figure 1. Probe Signals Illustrating the Helical Mode of the Instability. Top trace:  $V_A - V_C$ . Bottom trace:  $V_B - V_D$ . Time scale:  $20 \mu\text{s}/\text{cm}$ .

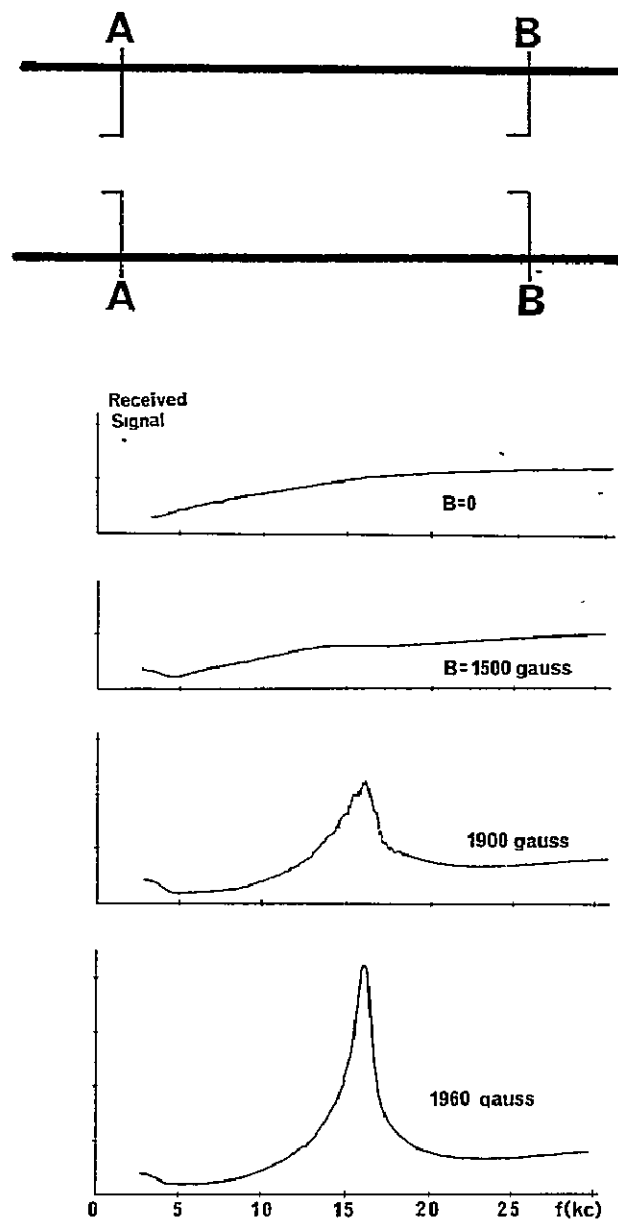


Figure 2. Signal Received at Probe Set B as a Function of the Frequency of the Source Connected Across Probe Set A. At the critical magnetic field strength (2100 gauss), the plasma exhibited self sustaining oscillations at 16.3 kilocycles.

PLASMA RADIATION AND THE DETECTION OF NON-MAXWELLIAN  
ELECTRON VELOCITY DISTRIBUTIONS\*

J.H. Noon, P.R. Blazuk, E.H. Holt

Rensselaer Polytechnic Institute, Troy, N.Y.

A gated microwave radiometer<sup>1</sup> and a specially constructed magnetoplasma waveguide cell<sup>2</sup> have been used in this laboratory to monitor the radiation temperature of electrons in an afterglow plasma and to examine departures from a Maxwellian electron velocity distribution. The cell is also suitable for a study of anomalous diffusion in a pulsed magnetoplasma,<sup>3</sup> or for measuring noise radiation near the critical magnetic field for plasma instability, although these measurements have not as yet been carried out.

Microwave radiometers have been used by a number of workers<sup>4,5</sup> to detect the thermal noise radiation from electrons in a collision-dominated nitrogen plasma and thus to determine the electron temperature, assuming a Maxwellian electron velocity distribution exists in the plasma. This assumption is not necessarily valid always as shown by our results which are reported below. If a longitudinal magnetic field is applied, measurement of the noise power from the plasma, as a function of magnetic field, for a range of field strength such that the electron cyclotron frequency is close to the microwave observational frequency, may be analyzed<sup>6</sup> to determine departures from a Maxwellian distribution. A sample of our experimental results in a nitrogen discharge showing noise radiation temperature as a function of applied magnetic field, are shown in Figure 1, and distribution function parameters giving best fit to the data are shown in Figure 2. These results show clearly that for a short time after the cessation of the pulsed DC discharge the nitrogen afterglow is relatively rich in high energy electrons, then becomes deficient in high energy electrons, then relaxes back to a Maxwellian distribution. This also manifests itself as an apparent maximum in the radiation temperature at post-discharge times of order 25 microseconds, and by a relatively slow rate at which the electrons relax back to room temperature. The magnitude of both these effects depends somewhat on the energy input into the discharge as shown in Figure 3. Time resolved studies of the active discharge itself have also been carried out and it appears that a time of the order of 10 microseconds after application of the DC voltage to the electrodes is required before a Maxwellian electron velocity distribution exists in the nitrogen discharge.

These results can be used both to provide information about energy loss processes in the plasma and also to indicate the regime in which the magnetoplasma becomes unstable above a critical magnetic field.

Further measurements planned with the magnetoplasma cell will be outlined.

\* Work supported by NASA under grant no. Nsg 48.

1. W. C. Taft, K. C. Stotz, E. H. Holt, I.E.E. Trans. on Instrumentation and Measurement, IM 12, 90, (1963).
2. J. H. Noon, E. H. Holt, J. F. Reynolds, Rev. Sci. Instr. 36, 622, (1965).
3. V. E. Golant, A. P. Zhilinskii, Sov. Phys. Tech. Phys. 5, 669, (1961).

4. D. Formato, A. Gilardini, Ionization Phenomena in Gases. (Proc. of Fifth Internat. Conf.) Vol. 1, p. 660, North Holland, (1962).
5. M. H. Mentzoni, R. V. Row, Phys. Rev. 130, 2312, (1963).
6. H. Fields, G. Bekefi, S. C. Brown, Phys. Rev. 129, 506, (1963).

Figure 1. Radiation noise temperature  $T_r$  as a function of applied magnetic field  $B$ . When  $\Delta(B) = 0$ ,  $B$  is such that the electron cyclotron frequency  $\omega_b$  is equal to the microwave observational frequency  $\omega$ .

$$\Delta(B) = 10^{-18} ((\omega - \omega_b)/P_0)^2 \quad (\text{cycles/sec torr})^2$$

Figure 2. Variation of distribution function parameter  $l$  with time in the afterglow. Assuming  $f(v) \propto \exp(-bv^l)$ ,  $l = 2$  corresponds to a Maxwellian and  $l = 4$  to a Druyvestyn distribution.

Figure 3. Radiation noise temperature in the afterglow period for different energy input conditions in the active discharge.

$\times = 0.5A$ ,  $\bullet = 5A$ ,  $\circ = 7A$ , and all are 20 microsecond pulses.

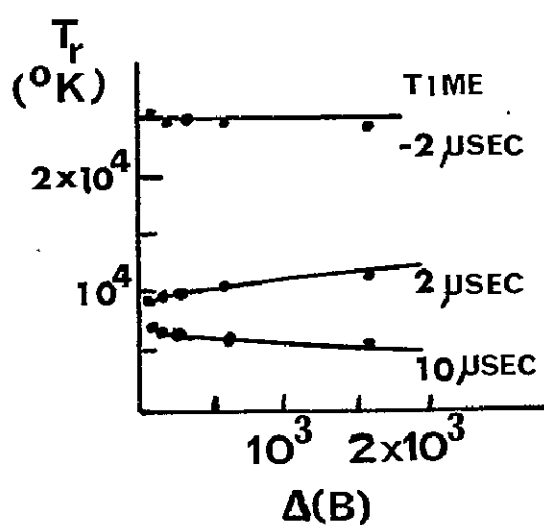


FIG 1

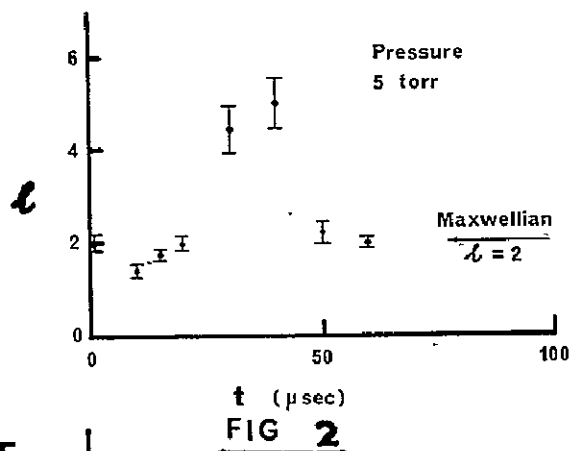


FIG 2

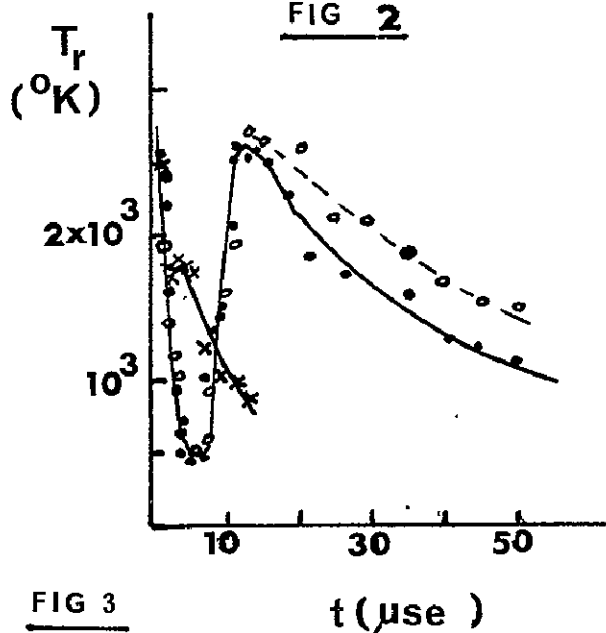


FIG 3



## PLASMA MEASUREMENTS FROM 3 TO 120 KILOBARS OF PRESSURE

James W. Robinson

The University of Michigan, Ann Arbor, Michigan  
Grant No. NsG-415

The purposes of the research have been to make basic measurements of the properties of very dense plasmas and to check the accuracy of theories which might be applicable to a description of these plasmas. Measurements of temperature, pressure, resistivity, and energy density were obtained in the range of pressures from 3 to 120 kilobars. The Debye shielding theory often used for theoretical studies of plasma was found to be very inadequate at these high pressures.

Although high density plasmas occur in various experiments involving exploding wires and hypervelocity guns, for example, little has been known about the properties of such plasmas. E. A. Martin of the University of Michigan introduced techniques which have been extended to form the basis of the present research into the properties of plasmas at high pressure.

The experimental work was conducted in two phases. First, with a refinement of Martin's methods, plasmas were studied in the range of pressures from 3 to 15 kilobars. These plasmas were formed by discharging a capacitor bank between electrodes submerged in water. From measurements of radiation intensity, measurements of the electrical discharge characteristics, and photographs, the desired data was computed. The pressure was a function of the rate of current rise in the column of plasma formed by the discharge. In the second phase, the discharge was formed in water which had been compressed by a chemical explosive to 100 kilobars of pressure. The data was recorded similarly and variations of pressure from 100 to 120 kilobars also depended upon the rate of current rise.

The diameter of the discharge column and the current flowing through the column increase nearly linearly with time. As the column grows, energy is supplied from the discharge circuit so as to maintain a nearly constant energy density in the plasma. Likewise the other intensive properties of the plasma are nearly constant with time. Energy lost from the plasma through expansion against its surroundings and through radiation is a small fraction of the total energy supplied to the plasma. The best data are taken late in the interval of observation when the variables are in the most accurate ranges of the instrumentation, that is in the interval from 0.8 to 1.0  $\mu$ sec.

The magnetic pinch effect is important in the calculation of pressure. For a uniform radial current distribution the pinch pressure varies from zero at the boundary of the discharge to a peak on the cylindrical axis. The volume average of the pinch pressure which is half of

the peak is added to pressure produced by the inertial restraint of the water surrounding the column to obtain total pressure. Since the resistivity of the plasma has been found to decrease with increasing pressure, the radial pressure gradient tends to concentrate current at the center, causing an even greater pinch than has been estimated.

Without exception, the temperatures of the plasmas formed without explosives were about 35 000°K while the temperatures with explosives were about 10 000°K. The variations with pressure of the energy density  $u$  and the resistivity  $\rho$  are plotted in Fig. 1 and Fig. 2:

A system of equations based upon the Debye shielding theory was used to predict particle density and energy density from temperature and pressure for the case without explosive. The predictions of energy density were found to be about one-fifth of the measured values, while the measurements are considered accurate to within 20 percent. The failure of the Debye theory was not surprising because the Debye radius was smaller than the average interparticle spacing. In place of the Debye theory, a semiquantitative theory based upon the distortion of electron quantum levels was found to provide a much better explanation of the energy density measurements. For the case with explosive, the Debye theory predicted an unreasonably low level of ionization because of the low temperature, and the analysis was not carried further. The concept of excluded volume was introduced into calculations for the higher pressure. From the theoretical considerations, the density of atoms for a 100 kilobar plasma was estimated to be  $10^{23} \text{cm}^{-3}$  and for a 7 kilobar plasma to be  $10^{22} \text{cm}^{-3}$ .

#### Publications

Robinson, James W.: Measurement and Interpretation of Plasma Properties to 100 Kilobars of Pressure, To be published as a NASA Contractor Report, CR-446.

Robinson, James W.: Plasma Measurements at 100 Kilobars of Pressure. Appl. Phys. Letters, vol. 8, no. 8, 15 April 1966.

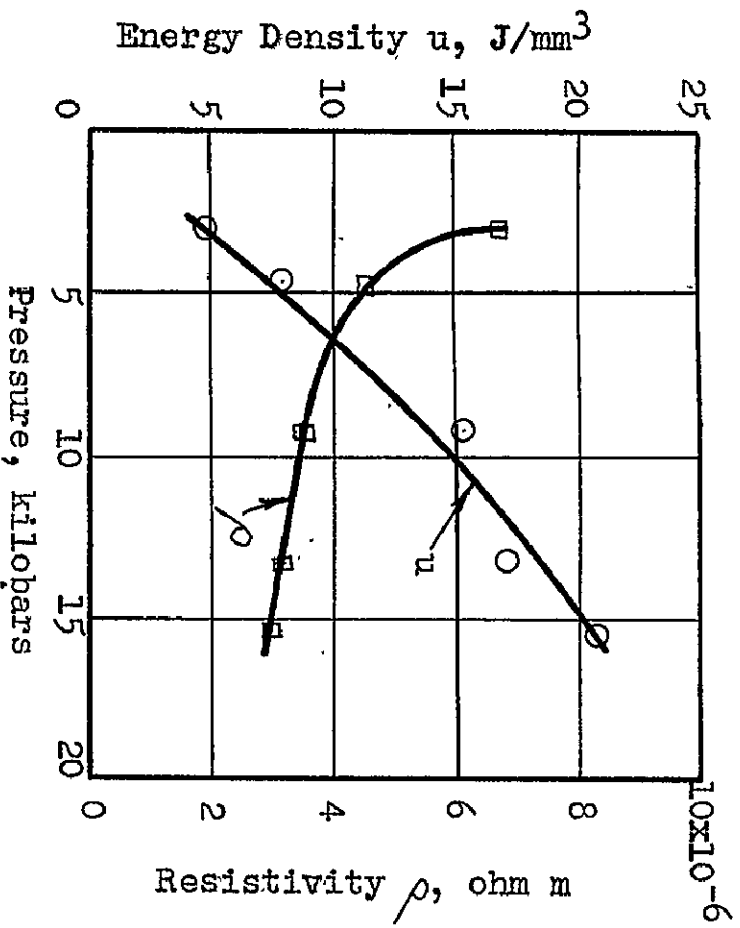


Fig. 1. Results without explosive at 35 000°K.

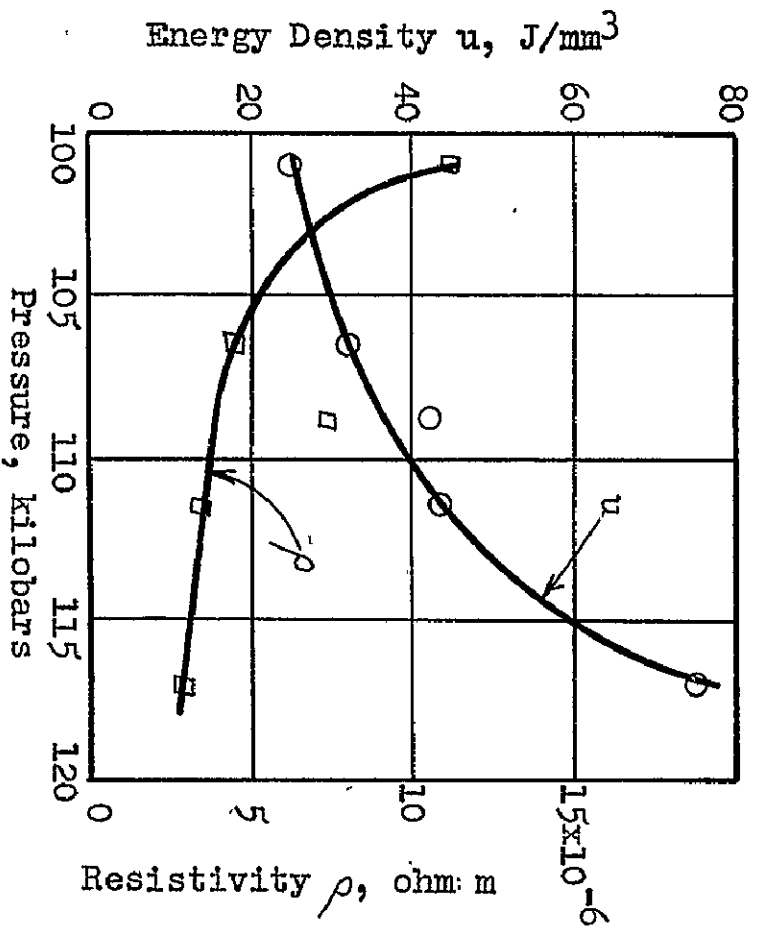


Fig. 2. Results with explosive at 10 000°K.



INVESTIGATIONS ON THE MECHANISM OF THE MATERIAL RELEASE  
IN THE HIGH VACUUM BREAKDOWN

by  
Richard T. Schneider  
Department of Nuclear Engineering Sciences  
University of Florida

ABSTRACT

The program to be reported started on May 1, 1966; therefore, it is necessarily still in the planning stage. However, preliminary experiments for orientation purposes have been made. The program is aimed to make a contribution to the understanding of the mechanism of the high voltage vacuum breakdown. Special emphasis is placed on the mechanism of material release from the electrodes. It is desirable to find means to predetermine the material release, and perhaps initiate it by magnetic ignition. The information obtained should be useful for electric propulsion using metal plasmas.

The measurements will be made in a vacuum as low as  $10^{-10}$  Torr. The electrode configuration will be parallel plates for electrode conditioning and repeatability tests. Other configurations are planned to favor or suppress one or more of the many processes which take part in the vacuum breakdown. These processes are (1) electron frees positive ion at the anode, (2) photon frees electron on the cathode, (3) electron frees photon on the anode, (4) positive ion frees electron at the cathode, (5) negative ion frees positive ion at the anode. Using appropriate electrode configurations, with auxiliary electrostatic or magnetic fields, it should be possible to suppress or enhance some of these processes in order to study their influence on the mechanism of the vacuum breakdown.

Spectroscopic studies of the inter-electrode plasma are planned. The object is to determine the temperature, density and ionization degree of the material released from the electrode. In order to do this, methods of short-time spectroscopy have to be applied. The discharge time is in the order of  $1 \mu\text{sec.}$  or shorter. Therefore, it is worthwhile to investigate whether the inter-electrode plasma has a defined temperature. Our point of interest will be to find out if the material released from the electrodes is released in the form of ions or if it is released as atom vapor by thermal vaporization, or if it is released in larger units (clumps) by mechanical stress or impact.

Time integrated spectroscopy can be used to determine how much material from which electrode is released. This will be aided by making anode and cathode of different materials.

Some results of the preliminary experiments will be shown at the meeting.

SYNTHESIS AND CHARACTERIZATION  
OF MAGNETIC FLUIDS

R.E. Rosensweig  
Avco Corporation  
Research and Technology Laboratories  
Wilmington, Massachusetts

In the present research program we endeavor to synthesize fluids having a strong magnetic response, and to characterize their properties and discover the laws and relationships which govern their response to an applied magnetic field.

Background Information

All known materials that are strongly magnetic like iron--the ferromagnetic metals, alloys and compounds--are solids. While theoreticians do not rule out the possibility of true ferromagnetic liquids, none is known at present. It is, however, possible to make a stable suspension of a finely divided ferromagnetic solid in a carrier liquid, to produce a fluid that reacts strongly when a magnetic field is applied to it, and we are engaged in studies of such fluids.

The pressure distribution in these fluids can be independently controlled by an applied magnetic field. The fluid response then takes several basic forms, opening up a wide range of possibilities in viscous dampers, inertial sensors, heat engines, fluid computers, fluid modelling studies, medical technology, and other technological areas.

Investigation of the basic fluid mechanical processes which govern the response of a magnetizable fluid to a source of magnetic field leads to an augmented Bernoulli principle in which a magnetic pressure-like term is additive to the usual pressure, speed, and gravitational terms.

$$p + \frac{1}{2} \rho q^2 + \rho gh - \int_0^H I dH = \text{constant}$$

The various terms in this equation along with consistent c.g.s. units are,  $p$  = pressure (dynes/cm<sup>2</sup>),  $\rho$  = density, assumed constant (gm./c.c.),  $q$  = speed (cm./sec.),  $h$  = elevation (cm.),  $I$  = magnetic moment per unit volume (pole-cm.) =  $M/4\pi$  where  $M$  is expressed in gauss ( $M = B-H$ ), and  $H$  = applied field (oersteds). The initial three terms taken in various combinations describe fluid mechanically a number of familiar technological processes as categorized in an accompanying figure. The magnetic term then combines to yield additional classes of fluid dynamic and static phenomena laden with possibilities for technological application. These furnish a portion of the motivation for these studies.

### Program Activities

Much of the work under the program has concentrated on the preparation and study of magnetic fluids composed of ferrite solid particles dispersed in an organic liquid. The carrier fluids are chosen on the basis of viscosity, chemical nature, and boiling point. Dispersants are selected on the theory that a suitable molecular structure contains a chainlike nonpolar tail and a polar end group. Both magnetite and a lower Curie temperature, manganese zinc ferrite are used as the solid, magnetic constituent. Dispersion into colloidal form is accomplished by wet ball milling of the solid material in the presence of the carrier liquid and the dispersant.

Screening tests are conducted to determine systems that lead to the successful production of colloid. Then study is made of the effects of initial charge and the grinding time on the formation of colloid and its physical nature. The successful fluids are characterized by their properties of magnetism, viscosity, temperature dependence of viscosity, density, stability, and particle size and shape. The fluids are modified by vacuum distillation or addition of solvents and study is made of the modified fluids so obtained.

Correlations are studied of the inter-relationship between the various measured properties and known parameters such as dispersant chain length and attempt is made to feed back this information into the synthesis of additional fluids having accented properties.

### Presentation of Results

Stable magnetic fluids are produced in which the typical particle size is 100 angstroms. The number of colloidal particles per cubic centimeter is enormous, and characteristically ranges from  $10^{15}$  to  $10^{20}$ . Oleic and linoleic acids have proven successful as dispersing agents and so has another class of dispersants consisting of succinic acid derivatives. Fluids prepared in this manner are strongly attracted to a magnet and volumes of the fluid may be suspended against the force of gravity. The magnetic particles experience a constant attraction in the direction of an applied field gradient but at the same time are free to move through the fluid, hence the persistence of a stable suspension requires explanation. It is believed that at equilibrium the terminal motion of the particles equals the diffusional transport of particles due to a (small) concentration gradient. Then the stable diameter  $d$  is less than the value computed from

$$d^3 = 24 \frac{kT}{M \frac{dH}{ds}}$$

where  $k$  = Boltzmann's constant =  $1.38 \times 10^{-16}$  erg/particle  $^{\circ}K$ ,  $T$  = absolute temperature in Kelvin unit,  $M$  = ferric induction in gauss,  $H$  = applied field in oersted, and  $s$  is length-- $d$  is then given in centimeters.

Suspended in the fluid each particle is analogous to a molecule of a paramagnetic gas. The Langevin equation of statistical mechanics then relates  $\bar{\mu}$  the average magnetic moment per particle averaged over all thermally induced orientations to  $\mu$  the true magnetic moment of a

particle,  $H$  the applied field, and  $T$  the temperature. Unlike a paramagnetic gas molecule, for a particle of the magnetic fluid  $\chi = \chi(T)$ . An extended form of the equation has been obtained to deal with the actual particle size distribution function.

The experimentally determined dependence of viscosity upon the loading is correlated with theoretical predictions. The earliest theory was derived by Einstein who solved the flow field of pure strain as perturbed by the presence of a sphere. His result relates mixture viscosity  $\eta_s$  to solvent viscosity  $\eta_0$  and solids fraction  $\phi$  :

$$\frac{\eta_s}{\eta_0} = 1 + 2.5 \phi .$$

However, this relationship is valid only for dilute colloidal mixtures; a better expression, correct for high solids loadings, has the form:

$$\frac{\eta_s}{\eta_0} = \frac{1}{1 - 2.5 \phi + 1.55 \phi^2}$$

This relationship predicts solidification corresponding to spheres in the hexagonal close-packed arrangement. In using this relationship, the thickness  $\delta$  of the monolayer coating on each particle must be considered in the computation of  $\phi$  .

Another important consideration is the prevention of particle agglomeration or flocculation. The important mechanisms are the magnetic forces and van der Waal's attractions (which tend to flocculate) and repulsion forces arising from deformation of an adsorbed layer of dispersing agent. The energies of two adjacent particles are found to be:

$$\text{Magnetic energy: } E_m = -2 \left( \frac{M}{4\pi} \right)^2 \frac{v^2}{R^3}$$

$$\text{Van der Waal's: } E_L = -\frac{A}{6} \left[ \frac{2}{h^2+4h} + \frac{2}{(h+2)^2} + \ln \frac{h^2+4h}{(h+2)^2} \right]$$

(London's model)

$$\text{Entropic repulsion: } E_R = \begin{cases} NkT \left( 1 - \frac{hr}{2\delta} \right) & \frac{hr}{2\delta} < 1 \\ 0 & \frac{hr}{2\delta} > 1 \end{cases}$$

Where  $N$  is the number of adsorbed molecules per unit area,  $\delta$  is the length of the hydrocarbon chain, and  $h$  is the relative separation of particle surfaces,  $h = H/r$  where  $H$  = surface to surface separation.

For stability against flocculation the three energies must produce a superimposed energy distribution having a barrier or energy hump at least several times greater than  $kT$ , the thermal energy of a particle.

At the beginning of this program, magnetic fluid with viscosity less than ten centipoise was limited to a ferric induction at saturation of little more than 100 gauss. The relationship between viscosity and ferric induction is presented in the accompanying figure which also illustrates the advance in the state of the art. Fluid is now produced whose ferric induction exceeds 1000 gauss. The remaining figure presents data that permits correlation of the initial permeability of the fluids with the ferric induction at saturation,  $M_s$ , according to

$$\mu_i = \left(1 + \frac{M_s}{600}\right) \quad M_s > 100 \text{ gauss}$$

This tells that the present fluids yield permeabilities in the range  $1 < \mu_i < 3$  which, although it is extraordinarily large compared to the permeabilities of normal liquids, is still rather small compared to the permeabilities of solid ferromagnetic materials. The obtaining of stable magnetic fluids having a much greater permeability is one of a number of challenging problems in this work where the solution in probability depends upon an understanding of surface physics and chemistry, magnetostatics, and the behavior of matter in general.

#### Background References

Rosensweig, R.E., Nestor, J.W., and Timmins, R.S., "Ferrohydrodynamic Fluids for Direct Conversion of Heat Energy" A.I.Ch.E.-I. Chem. E. Symposium Series No. 5, London, p. 104 (1965).

Neuringer, J.L. and Rosensweig, R.E., "Ferrohydrodynamics" The Physics of Fluids 7 No. 12, p. 1927, December (1964).

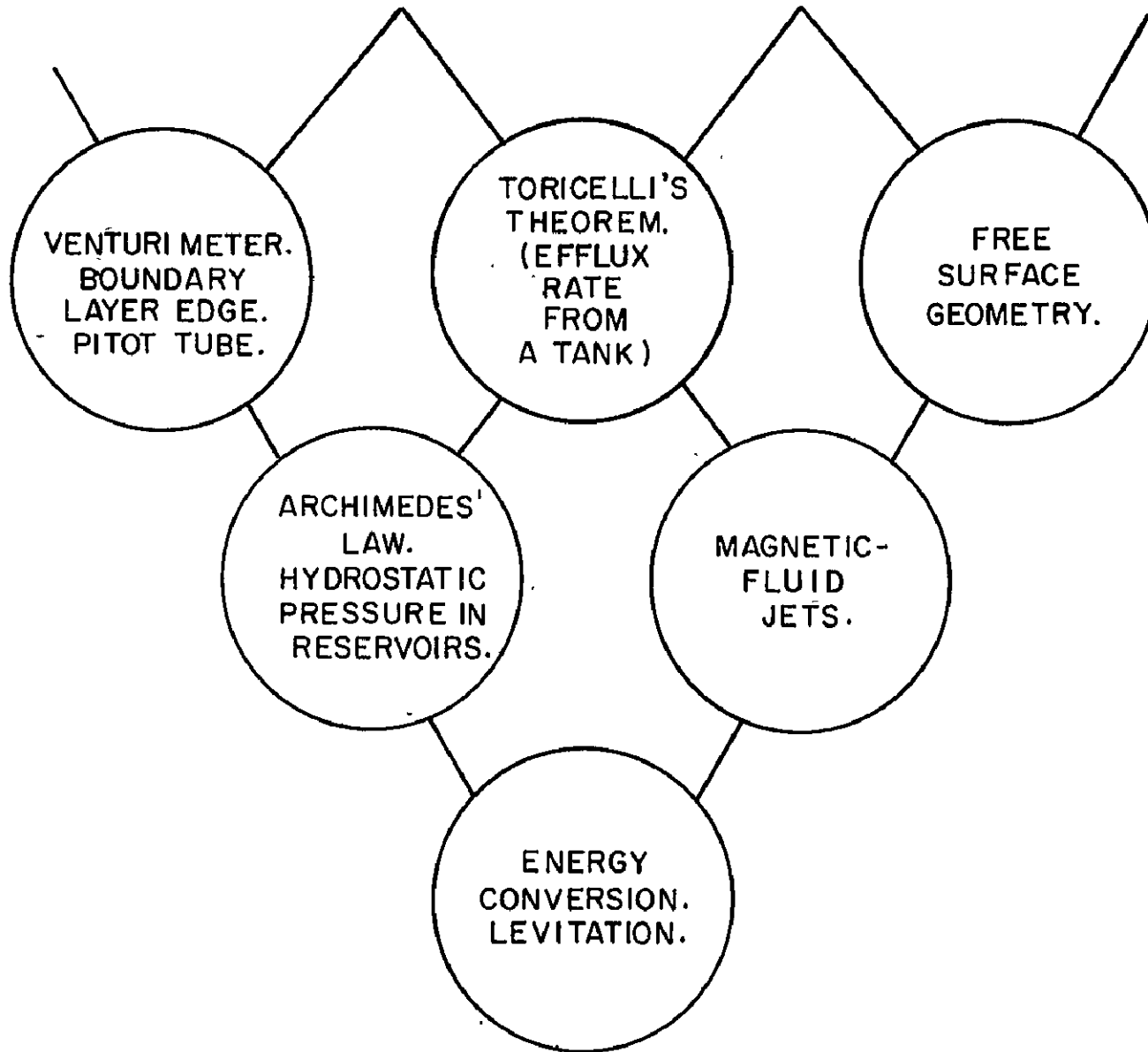
Rosensweig, R.E., "The Fascinating Magnetic Fluids" New Scientist p.146 January 20, 1966.

#### Publications Generated During This Research

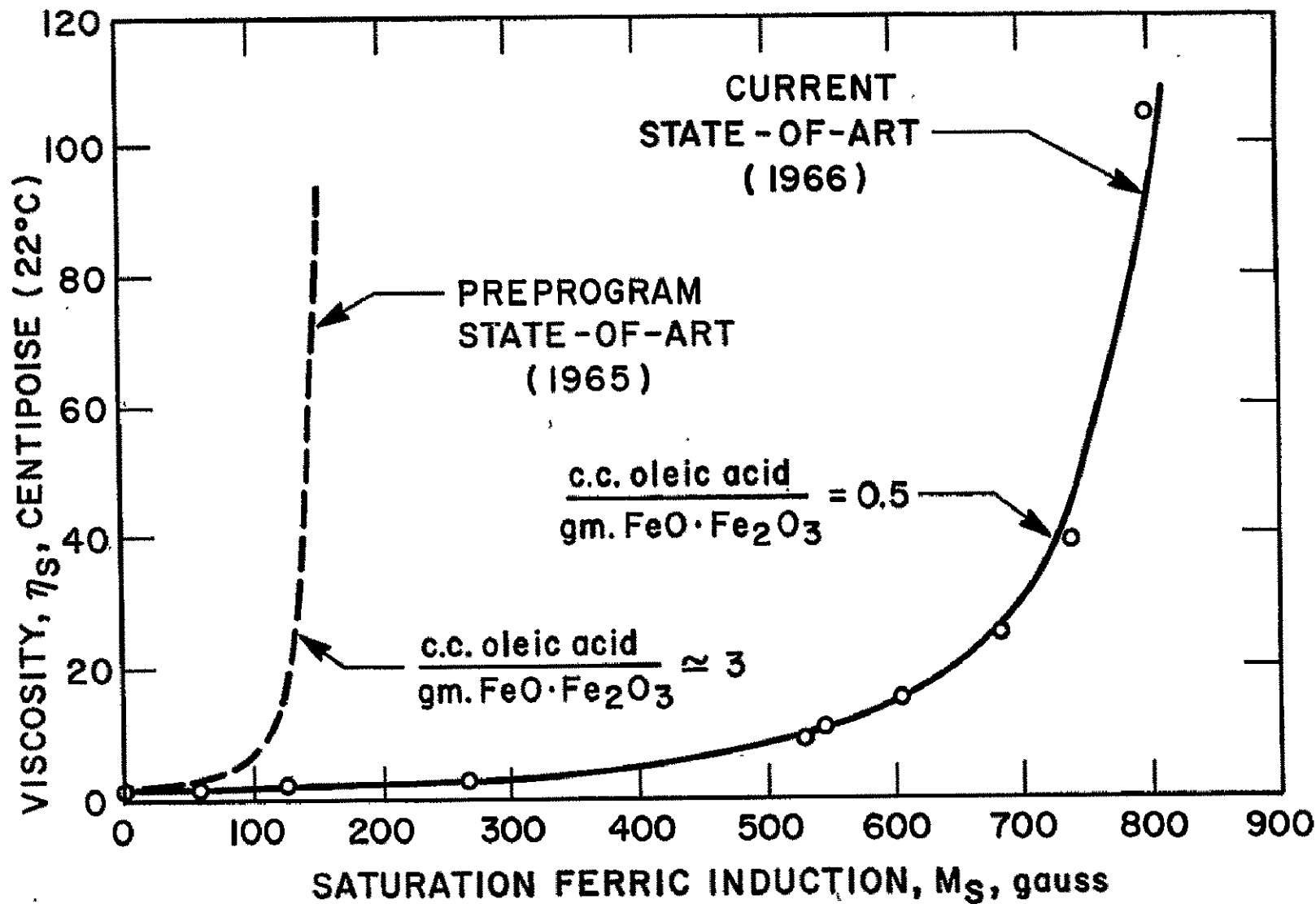
Rosensweig, R.E., "Buoyancy and Stable Levitation of a Magnetic Body Immersed in a Magnetizable Fluid." Accepted for publication in Nature, A Weekly Journal of Science.

Neuringer, J.L., "Magnetic Effects on the Diffusion of Ferromagnetic Colloidal Particles Dispersed in a Current-Carrying Fluid Medium." To appear in The Physical Review Part I in May (1966).

$$p + \frac{1}{2} \rho q^2 + \rho g h - \int_0^H \rho dH = \text{CONSTANT}$$

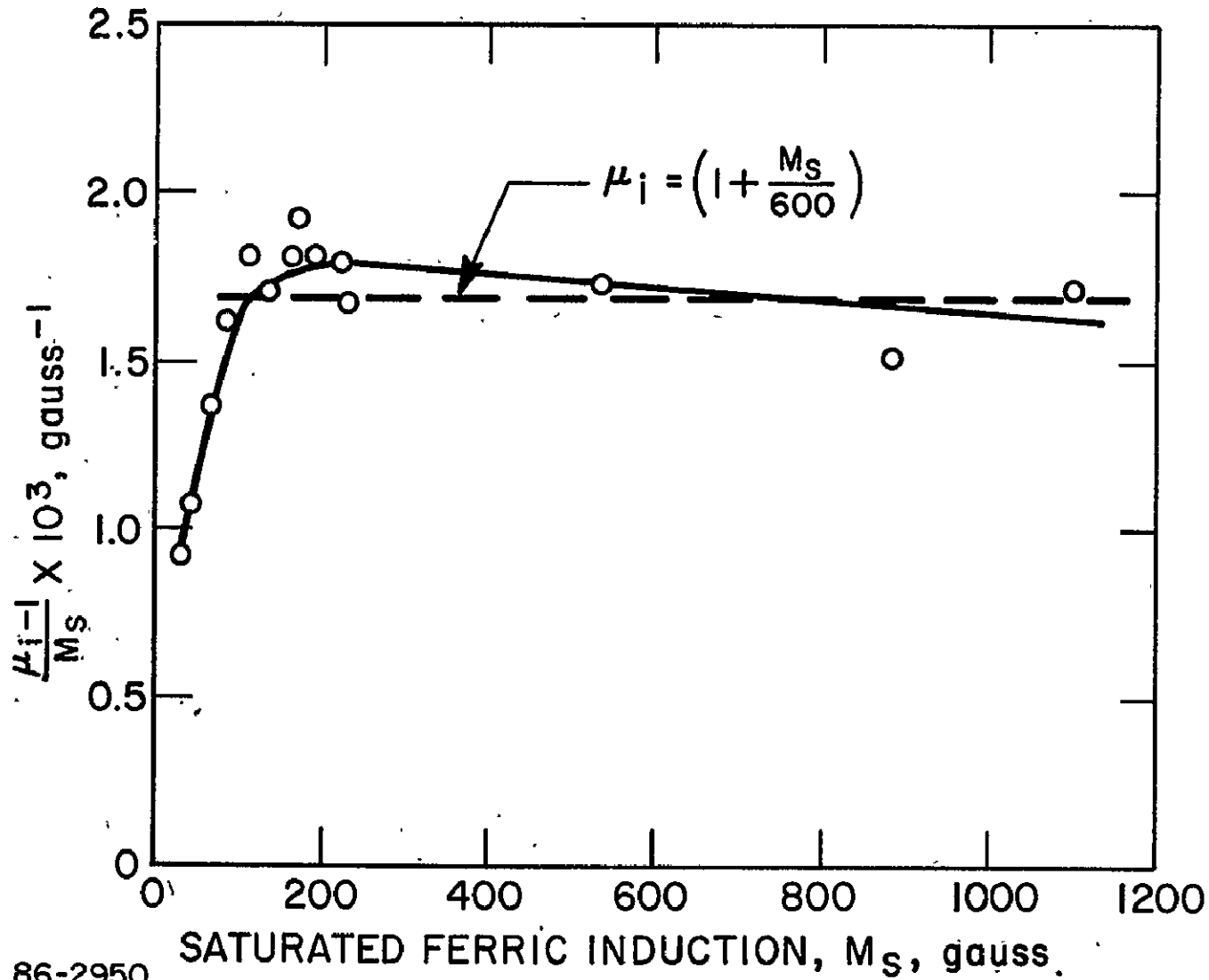


# VISCOSITY OF MAGNETITE COLLOID AS A FUNCTION OF THE FERRIC INDUCTION AT SATURATION





INITIAL PERMEABILITY OF MAGNETITE COLLOID AS  
 A FUNCTION OF THE FERRIC INDUCTION AT  
 SATURATION.  $\mu_i = (\partial B / \partial H)_{H=0}$



86-2950

PROPAGATION AND DISPERSION OF HYDROMAGNETIC AND  
ION CYCLOTRON WAVES IN PLASMAS IMMERSSED IN MAGNETIC FIELDS\*

Professor Arwin A. Dougal, The University of Texas, Austin 78712

The long range challenges for exploration and exploitation of space requires that ever increasing, technological and scientific attention be given towards the realization of extremely light, almost infinitely long-lived, and efficient power sources. Within very recent years the technological community has recognized the vast potential power production realizable from the fusion products of reacting light nuclei as the ultimate source. Almost overwhelming power output per unit fuel mass is afforded by the reacting light nuclei. Two million kilowatt hours of energy are foreseen to be extractable through fusion of as little as 0.06 pounds of deuterium nuclei. An immense technological problem to be overcome is the requirement for the production and heating of deuterium ions in the gaseous plasma state to several hundred million degrees temperature to which this research work and its continuation are addressed. Experimental and analytical findings from our recent research work on ion cyclotron resonance heating show definite promise towards future realization of increasingly super-high ion temperatures. These findings are supported by relatively recent reports from those few research groups throughout the world who have had the foresight to initiate studies on ion cyclotron resonance heating and to realize the major experimental facility for effective experimental work.

Most earlier and existing attempts to elevate plasma temperatures into the desired range have resulted in high electron temperatures but relatively low ion temperatures which are inadequate. Both theory and experiment have recently confirmed that effective heating, propagation, and dispersion of ion cyclotron waves in plasmas immersed in magnetic fields are possible. Deposition of power into a plasma through radio frequency fields at an angular frequency  $\omega$  requires consideration of characteristic frequencies associated with the plasma and its magnetic field configuration. The characteristic frequency  $\Omega_i$  of an ion in a magnetic field is given by  $\Omega_i = \frac{q_i B}{m_i}$ , where  $q_i$  and  $m_i$  are the ionic charge and mass respectively. Theory and experiments show that effective heating of plasma ions occurs through ion cyclotron wave interactions.

Experimental research on ICRH has been performed by research groups at NASA-Lewis, Princeton University, Lawrence Radiation Laboratory at the University of California at Berkeley, Physicotechnical Institute at Khar'kov USSR, The University of Texas, the Massachusetts Institute of Technology, and the Institute of Plasma Physics at Nagoya University, Japan.

The experimental arrangement at The University of Texas is shown in Fig. 1. Both hydrogen and/or deuterium gas can be leaked into the plasma tube: The vacuum

---

\*Sponsored by the National Aeronautics and Space Administration Grant NsG-353.

base pressure is better than  $10^{-8}$  torr. VacSorb and VacIon pumps are used in order to reduce impurities in the system. The overall length of the magnetic field coil system is presently 150 cm. Rf power is coupled into the plasma through a Faraday shielded "Stix" coil located in a uniform field region of maximum 10.6 kG. A "magnetic beach" region on one side of the "Stix" coil is used for wave propagation studies. Maximum incident rf power is presently over 30 kW. The incident and reflected rf power is measured with adjustable, calibrated directional couplers. The rf driver is crystal controlled at 5.8 MHz. A 27 MHz, 1 kW, preionizer is used in all experiments. A fairly extensive study of the design of the "Stix" coil and associated electrostatic shields was undertaken. The present coil and shield combination gives an  $E_{\theta}$  field which is almost sinusoidally varying in the axial direction and an  $E_{z}$  field which is substantially reduced. The number of coil turns and their relative spacing was determined using a digital computer. The Faraday shield consists of 9 strips of copper, .020" thick by 0.5" wide along the discharge tube under the Stix coil.

A new and previously unreported wave phenomenon was observed in this experimental investigation of ion cyclotron resonance heating of hydrogen and deuterium plasmas. For certain gas pressures the ion cyclotron waves propagate for frequency ( $f$ ) greater than the ion cyclotron frequency ( $f_1$ ), and attenuate at harmonics of the ion cyclotron frequency with a resulting increase in the transverse temperature-density product ( $nKT_{\perp}$ ). In this experimental investigation the frequency ( $f$ ) of the driver was kept constant and the other parameters, such as gas pressure and magnetic field strength, were varied. Decreasing the magnetic field strength is effectively the same as increasing the frequency of the driver ( $f$ ), and vice versa. The wave magnetic field components were measured with movable, shielded, magnetic probes located near the end of the magnetic beach.

For low hydrogen pressures ( $p < 2$  millitorr) an ion cyclotron wave was observed to propagate for  $B > B_C$ , where  $B_C$  is the ion cyclotron resonance magnetic field for the driver frequency ( $f$ ). The ion cyclotron wave was observed to attenuate quite sharply near  $B = B_C$  as expected. As the gas pressure was increased, a wave was observed to propagate for  $B < B_C$ , which was unexpected. Closer investigation revealed that the wave attenuates near  $B_C/N$ , where  $N$  is an integer. Thus, the wave propagates for  $f > f_1$  (the ion cyclotron frequency) and attenuates at harmonics of  $f_1$ . The value of  $N$  was found to depend upon the gas pressure such that  $N$  increased for higher pressures. The same general effects were observed in deuterium plasmas. In deuterium, the effects are more pronounced since the separations between the various  $B_C/N$  are larger due to the larger deuterium ion mass. Fig. 2 shows these effects as measured in a deuterium plasma. The region of abrupt wave attenuation moves to lower magnetic fields as the gas pressure increases. The attenuation regions are very close to the harmonic resonance fields.

The question arises whether the observed wave field attenuation of harmonics of  $f_1$  is due to a wave cut off or to actual wave damping near the critical fields. Diamagnetic probe measurements indicate that the waves are damped and that energy is transferred from the waves to the plasma particles. Additional measurements on

wave propagation and wave attenuation are in progress. An analytical explanation for these observed effects is being developed.

#### Publications

1. A. G. Engelhardt and A. A. Dougal, "Dispersion of Ion Cyclotron Waves in Magnetoplasmas," *Physics of Fluids*, 5, pp. 29-37, 1962.
2. Y. J. Seto and A. A. Dougal, "The Wave Equation and the Green's Dyadic for Bounded Magnetoplasmas," *Journal of Mathematical Physics*, 5, pp. 1326-1334, 1964.
3. M. Kristiansen and A. A. Dougal, "Ion Cyclotron Resonance and Wave Propagation in Magnetoplasma," *Bull. Am. Phys. Soc., Ser. II*, 10, pp. 159-160, 1965.
4. M. Kristiansen and A. A. Dougal, "High Power RF Plasma Heating and Wave Propagation Near the Ion Cyclotron Resonance Frequency," Paper E5, Abstracts of the Proc. of VII Annual Meeting, Div. of Plasma Physics, American Physical Society, November 8-11, 1965.

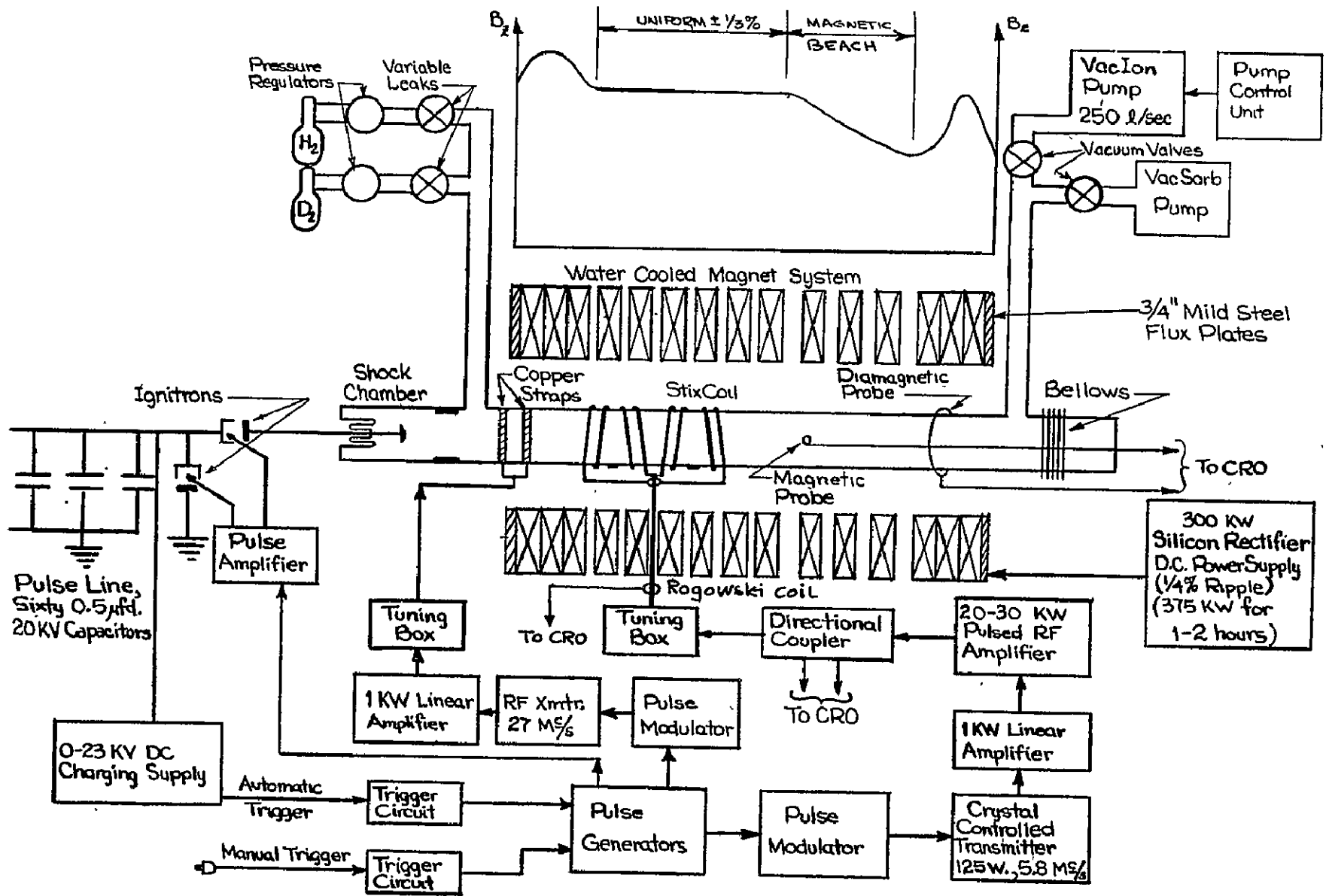


Fig. 1. Block Diagram of Ion Cyclotron Resonance and Wave Propagation Experiment

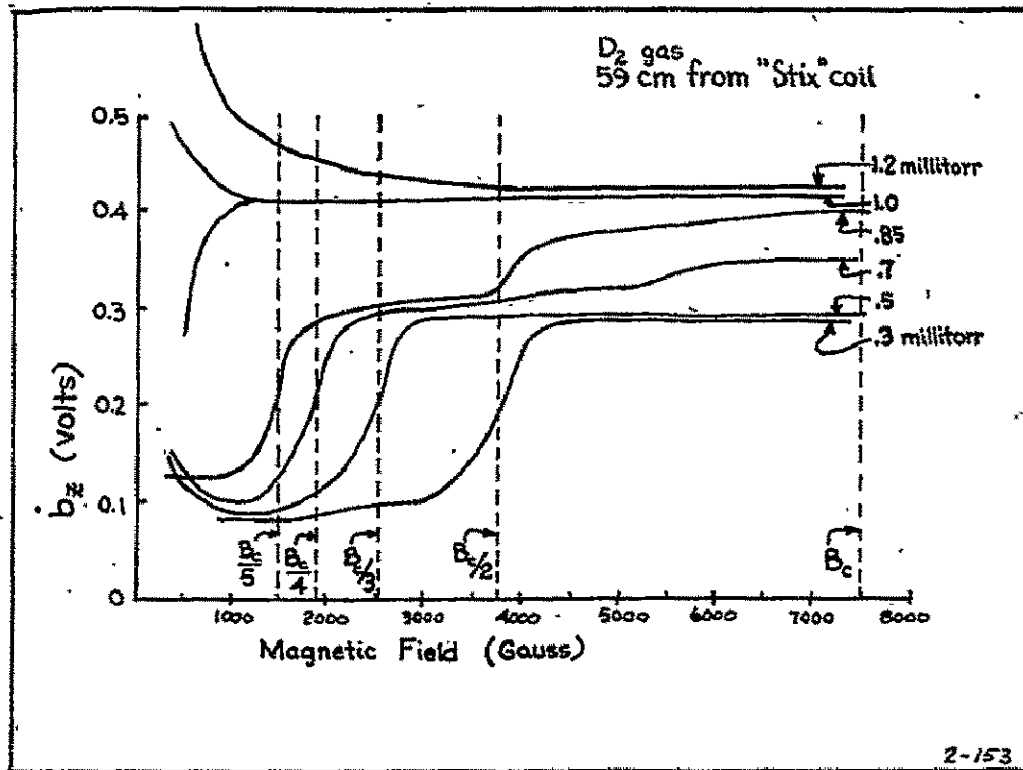


Fig. 2. Pressure Dependent Wave Attenuation at Harmonics of the Ion Cyclotron Frequency

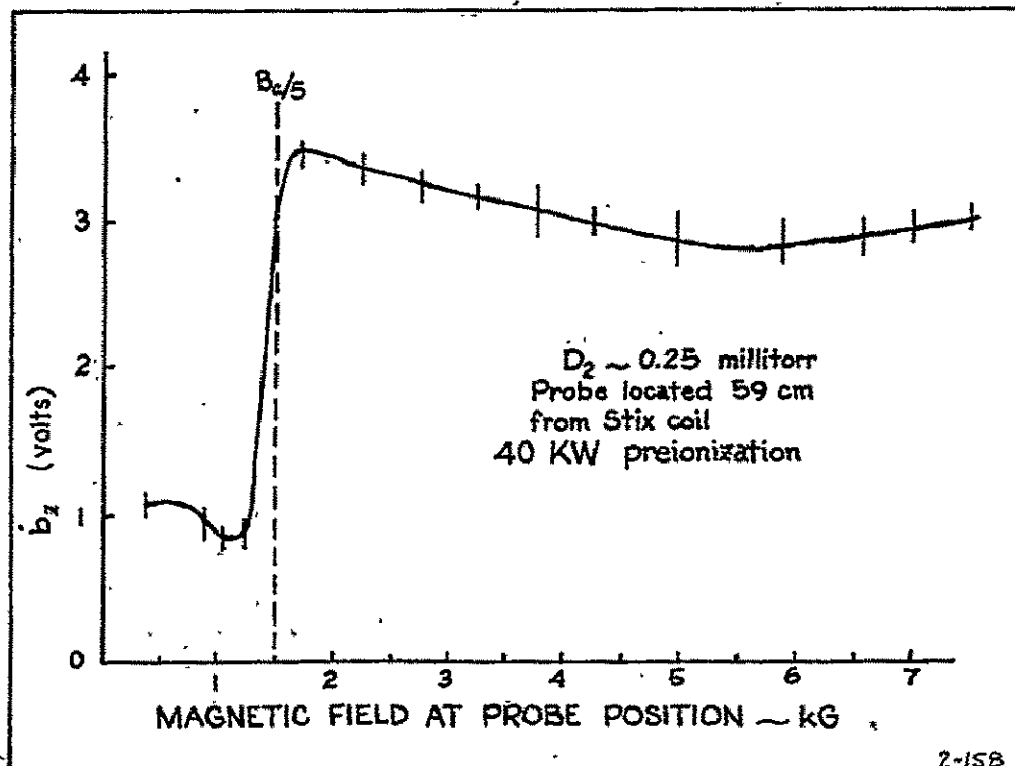


Fig. 3. Wave Attenuation at a Harmonic of the Ion Cyclotron Frequency for Strong Preionization

## A-C POWER GENERATION THROUGH WAVE-TYPE INTERACTIONS

by

G. L. Wilson

Department of Electrical Engineering  
Massachusetts Institute of Technology

The purpose of this project is to investigate schemes which directly generate A-C electric power through magnetohydrodynamic interactions in plasmas. The method under current study is one, in which standing magnetoacoustic waves in a flowing plasma interact with an artificial or lumped transmission line, which is magnetically coupled to the gas. Magnetoacoustic waves are disturbances which propagate in a conducting gas at velocities greater than the sound speed in the medium. This greater propagation velocity is due to currents which are induced through the compression of magnetic field lines within the conductor. These currents interact with the applied magnetic field to produce forces which aid compressional forces.

The proposed generator is shown in Figure 1, in which the coils of an artificial transmission line are coupled to the magnetic field  $B$  associated with the waves in a convecting plasma. For a velocity  $V_0$  greater than the magnetoacoustic velocity, there will be two forward waves in the gas. By adjusting the transmission line parameters such that the phase velocity on the transmission line is equal to the velocity of the slow wave in the gas, an interaction between the two systems occurs, which results in unstable bulk oscillations in the plasma and unstable voltages and currents on the transmission line. By coupling to this system in a variety of ways, net electric power can be coupled out of the system at the expense of the thermal and kinetic energy of the plasma.

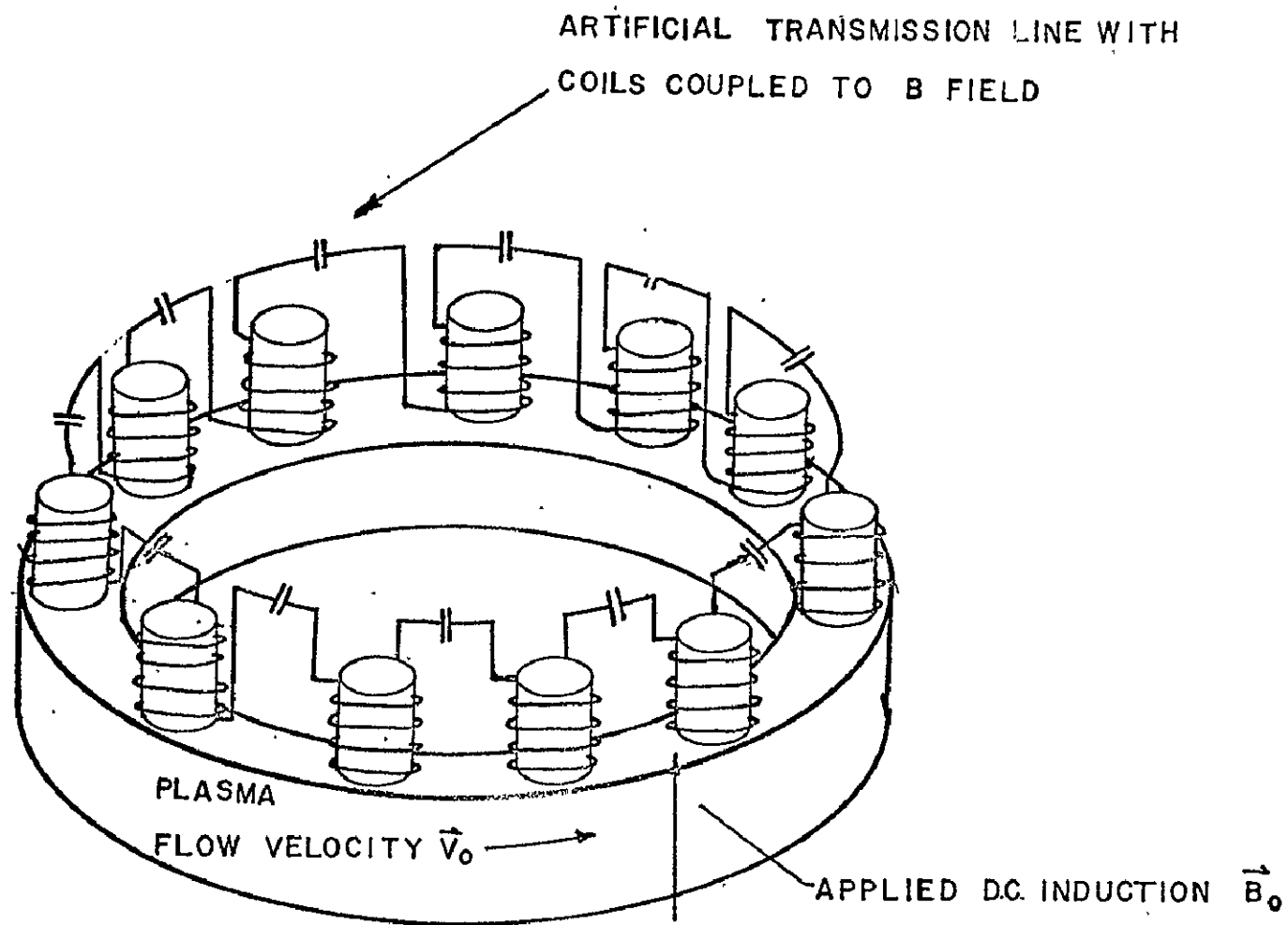
Experiments are in progress in which a helium plasma is heated and accelerated in a circular channel through electric heating and  $\vec{J} \times \vec{B}$  forces. The gas is accelerated to velocities on the order of 20,000 meters/second and is heated to temperatures in excess of 18,000°Kelvin. The experiment lasts for one millisecond at input powers on the order of 3 megawatts. A two-dimensional Hartmann flow theory for the accelerator has been developed and compares very favorably with measured values of the accelerator parameters. The results of these measurements are presented in Figure 2.

Measurements of gas temperature and velocity profiles are in progress to further check the Hartmann flow model.

The accelerator is used to provide proper gas conditions for study of magnetoacoustic wave oscillations. Magnetoacoustic waves have been successfully excited and detected in this medium and the acoustic-magnetoacoustic transition region as a function of electric conductivity has been observed. The measured frequencies of the standing wave oscillations as a function of input power to the accelerator is shown in Figure 2, and compared with theoretical predictions. This experiment represents the first instance in which magnetoacoustic waves in a flowing medium and their dependence on electrical conductivity have been observed.

Preparations are presently in progress for the final phase of the study; that is to experimentally observe the interaction of an artificial transmission line with the waves and to extract electric power from the system.

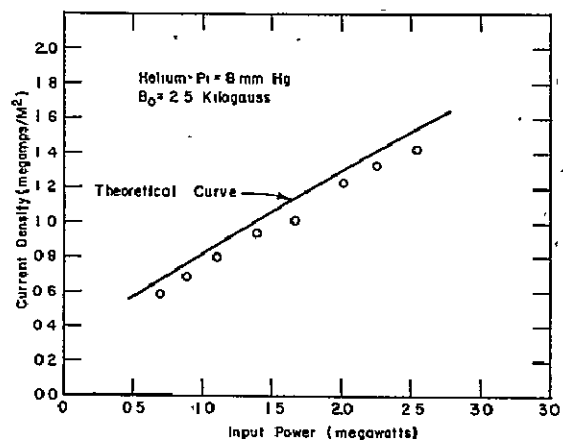




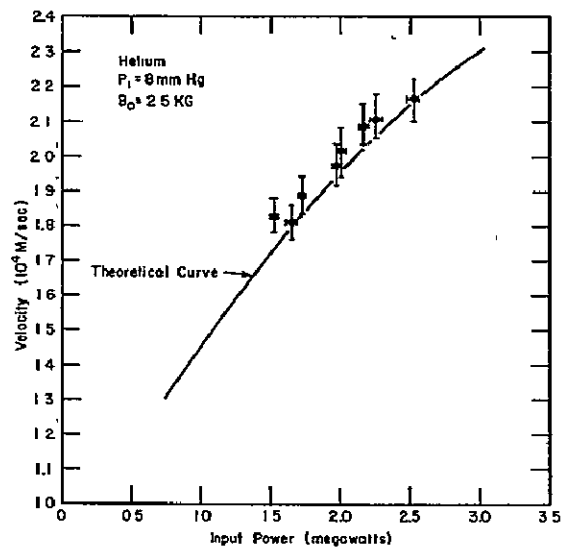
## STANDING-WAVE MHD GENERATOR

Figure 1.

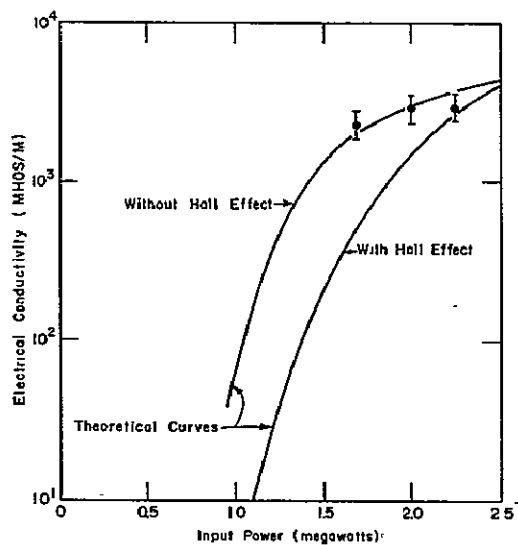
PRECEDING PAGE BLANK NOT FILMED



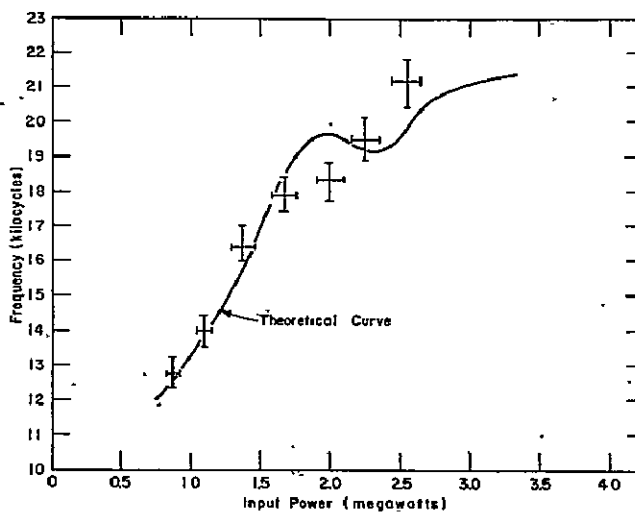
Current Density vs Input Power Data



Velocity vs Input Power Data



Electrical Conductivity vs. Input Power



Eigenfrequency vs Input Power

Figure 2 Collective Illustration of Experimental Measurements

ANODE OSCILLATIONS IN CESIUM PLASMAS  
Harry S. Robertson, Department of Physics,  
University of Miami, Coral Gables, Florida

Self-excited oscillations in otherwise quiescent cesium arcs have been found to originate at the anode surface. These oscillations appear to be similar to those observed in cesium diodes and in Q-machines with ion-rich sheaths. The suggestion that the oscillations in cesium diodes might provide a means for direct conversion of thermal to a.c. power on the one hand, and the experimental evidence that some of the instabilities seen in Q-machines originate in the anode sheath have motivated the study of these oscillations in an experimental facility that permits a variety of observations.

The experimental facility consists of a pyrex discharge tube with (usually) a thermionic cathode, usually about 30cm from one or more of a variety of anode structures. A cesium reservoir in its own oven determines the vapor pressure, and the discharge tube is operated in a transparent pyrex furnace at a temperature usually 50°C or more above that of the reservoir. The neutral cesium pressure may be varied from about  $10^{-3}$  Torr to 1 Torr; the current from a few milliamperes to 1 ampere; the electron temperature is a few tenths of 1 eV, and the fractional ionization in the plasma is usually less than 1%. Anodes may be plane, cylindrical, or spherical, and multiple anodes recessed in cylindrical pyrex tubes are sometimes used. Both rubidium and potassium have been studied, but the most extensive work has been in cesium.

Oscillation amplitudes may be as high as several volts, and periods vary from a few microseconds to a few milliseconds. Photoelectric observations of the emitted light shows that the oscillations are localized to the region within a few millimeters of the anode surface.

Theoretical and experimental analyses lead to the following qualitative understanding of the phenomenon. Neutral atoms incident on the anode surface are ionized because the work function of the anode is greater than the ionization potential of the atom, but they are lightly bound to the anode surface by image forces. A rising electric field at the anode results in a burst of emitted ions from the surface, accompanied by release of electrons from the sheath edge to maintain neutrality. The resulting enhanced conductivity of the anode sheath leads to an abrupt fall in tube volts and

local electric field, while the locally increased ion or electron densities lead to a sharp increase in the emission of both recombination radiation and excitation radiation. Then, as the burst of ions and electrons dissipates, principally by diffusion and conduction, but in part by recombination, the electric field begins to rise. During the low-field part of the cycle, more neutrals have been absorbed on the anode surface, and when the field increases sufficiently, a new cycle begins.

The oscillations will exist, then, whenever the steady-state electric field is within a range such that it is great enough to cause some field emission of anode surface ions and not so great that it steadily removes them as fast as they are formed. Frequency is determined principally by the diffusive and convective loss rate.

The greatest difficulty in comparing theory and experiment is that ion emission usually occurs at one or more spots on the surface where the local electric field must be a bit larger than anywhere else, so brightly glowing spots are seen on the anode, and the firing of one spot triggers that of others.

Attempts are in progress to control the formation of spots and otherwise alter the behavior of these oscillations by choice of anode geometry, material, finish, temperature, and geometry of the surrounding region.

## Transverse Stream Instabilities in Plasmas

Dr. W. Bennett  
North Carolina State Univ.

The objective in this project is to produce a steadily running undriven pinch and to examine the instabilities which may exist in such streams.

The project is supported by the Electrophysics Branch of the National Aeronautics and Space Administration and involves the production of high current high voltage electric pinches in small diameter beams and to observe the transition of these beams into a simultaneous electric and magnetic pinch. Studies are being made of: (1) the physical processes in these two kinds of pinch; (2) the onset of beam instabilities as the magnetic pinch becomes dominant; (3) the interaction of these beams with their associated plasmas.

In earlier work, it was found that undriven electron beams do not readily accumulate ions from low density residual gas and retain them in sufficient quantity to neutralize the space charge and permit the magnetic pinch to set in. For this reason, it was decided to undertake to increase the intensity of electrically pinched beams sufficiently to provide the essential conditions for the magnetic pinch to become predominant.

In order to undertake this kind of investigation properly, it has been necessary to develop a directional plasma probe with which velocity distributions can be measured. The basic principle used in this probe is similar to that in a probe which has been successfully flown on a rocket in some earlier space research. The probe in its present form consists of two knitted 0.0005 in. tungsten grids and a 15° conical collector. The outer grid is attached to a metal sleeve which surrounds the rest of the probe. The leads to the interior parts of the probe are glass covered. The outer grid and sleeve core are held at the potential at which the probe

least disturbs the surrounding plasma. For measurements of the electron velocity distribution in the direction of the probe axis, the inner grid is held at positive potential sufficient to turn back all positive ions which enter through the outer grid. The electron current to the conical collector is measured with a full feed back amplifier based at potentials which are swept through a range of negative values to cover the range of electron velocities in that direction. Corrections must be made for secondary emissions from the collector and for currents due to ionization inside the probe. For measurements of the positive ion distributions, the inner grid is set at a negative potential sufficient to turn back all electrons which pass the outer grid, and the base potential of the amplifier is swept through a range of positive values to cover the range of ion velocities in the direction of the probe axis.

A tube has been built for examining electrically pinched streams by measuring velocity distributions of electrons and ions with directional probes, magnetic stream deflections, stream attenuation, and other characteristics as a function of vapor density, beam current, beam voltage and tube diameter.

Methods have been developed in the gun design for protecting coated cathodes from deterioration due to back bombardment by positive ions. In essence, the procedure is to use a "grid" aperture as near the cathode as possible which is held at a more positive potential than any other potential further down stream. In order to go to the high voltage streams which will be required in the later phases of this project, where much more positive potentials will be necessary beyond the end of the gun, it will be necessary to design the gun to strongly defocus the back-streaming positive ions before they can reach the coated cathode, or else to use bare cathodes instead of the coated cathodes and to use narrow-band optical filters in order to see the beam while focusing it.

## PULSED PLASMA PROPULSION

R. G. Jahn and W. von Jaskowsky  
Princeton University, Princeton, New Jersey

Despite the advanced state of development of ion propulsion devices, and the very promising early performance of steady magnetoplasmadynamic arc thrusters, continued interest in the inherently more complex pulsed mode of plasma acceleration is sustained by four potentially profitable basic characteristics. Specifically, passage of the current through the plasma in intermittent intense pulses may be expected (1) to provide higher average thrust density than by steady consumption of the same electric power; (2) to involve less heat transfer loss and electrode erosion than equal power steady arc devices; (3) to minimize undesirable kinetic thermalization within the accelerating plasma; and (4) to generate various unsteady electromagnetic field effects which aid in the acceleration and containment of the plasma.

Practical implementation of these potential advantages requires detailed understanding of the participating phenomena. Any pulsed plasma accelerator must execute the following controlled sequence of physical processes: (a) the appropriate amount of electrical energy must be accumulated in the external circuit, e.g. in a high performance capacitor; (b) a proper distribution of propellant gas must be established in the accelerator channel; (c) the circuit must be completed by a discharge across the channel electrodes, in the proper geometric location at the proper time in the cycle; (d) this discharge must rapidly intensify to a self-accelerating current sheet which covers the entire channel cross-section, is impermeable to ambient gas ahead of it and its self-magnetic field behind it, and can accelerate over the full channel length stably and with total-ambient gas entrainment; (e) when the accelerated mass of gas and plasma reaches the end of the channel, it must be ejected with a minimum of thermal and electromagnetic loss; (f) finally, the entire gasdynamic and electromagnetic system must recover its initial situation, prior to initiation of a new cycle.

Over the past four years our laboratory has carried out a spectrum of basic experiments and related analytical studies encompassing all of the six phases of the pulsed plasma acceleration cycle outlined above. The apparatus has been developed primarily from the standpoint of controlled, reproducible experimentation with maximum diagnostic accessibility, rather than focusing on any particular thruster geometry. At present we have operative five different discharge chambers driven by a variety of capacitor banks, pulse-forming networks and special energy storage units. Peak discharge currents up to  $10^6$  amp at 10 KV may be attained, and pulse lengths from 1/2 to 100  $\mu$ sec are available. Diagnostic equipment employed includes electric and magnetic probes, voltage dividers, D loops and Rogowski coils, streak and Kerr cell cameras, a grating monochrometer and gas laser, high speed piezoelectric transducers and 4 mm. microwave bridges and interferometers. Vacuum facilities include a 3' dia. x 6' long Plexiglas tank capable of evacuation to  $10^{-5}$  torr. (32,35)

For purposes of this presentation we will illustrate the program with two of the currently active studies: the production of various driving current waveforms and their effect on the development of the plasma acceleration process; (33,34) and the distribution of current density and magnetic field in exhaust plumes from one

type of accelerator. (18,20,21,29,32) With regard to the former we begin by noting that while it is quite conventional to drive pulsed accelerators with free-ringing lumped capacitor banks, this is far from an ideal source for this purpose. Associated with each reversal of the damped sinusoidal current pattern is a secondary "crowbar" breakdown in the discharge chamber which effectively uncouples the primary current sheet from the energy source, leaving it to dissipate itself over the remainder of its motion down the channel. (2,4,5) These secondary breakdowns also badly complicate the experimental diagnosis of the discharge-acceleration events by the techniques outlined above. Both problems have been eliminated by replacing the lumped capacitor bank with a pulse-forming line capable of providing a variety of high current waveforms at the operator's discretion. Essentially the device is an L-C ladder network formed by two parallel collector plates, along which stock capacitors may be attached at arbitrary locations. As suspected, the driving current waveform is found to have a profound influence on the effectiveness of the discharge acceleration process. Sweeping efficiency and terminal velocity of current sheets in a given accelerator can be changed by an order of magnitude by proper distribution of the same total electrical energy in the current-pulse. Figure 1 shows four example current waveforms constructed by this facility and corresponding streak photographs of an 8" diameter, linear pinch discharge in argon driven by them.

The importance of the plasma exhaust phase to the over-all performance of a pulsed thruster is evident enough; whatever energy is expended in ejecting the plasma slug, or remains trapped within it in various thermal modes, detracts from the total thrust efficiency. Although it is difficult to reduce this problem to concise elements for systematic study, any information about the development of current density and magnetic field patterns in the plume will provide some insight into the ejection mechanisms. For this purpose, a special discharge chamber with 4" dia. orifice, driven by a 6500 joule pulse line, (32) is allowed to eject plasma into a large Plexiglas vacuum tank. (35) Here the development of the luminous pattern of the exhaust plume may be determined by Kerr cell photography, and the distribution of magnetic fields and current densities mapped with magnetic probes and Rogowski loops. Typical patterns are shown in Fig. 2. Substantial currents are found to extend far out into the plume, and the sense of the local  $\mathbf{j} \times \mathbf{B}$  body force is predominantly favorable to continued expansion or detachment of the plume. One significant result of such studies is the identification of a transient phase of ejection, wherein discrete current sheets propagate through the plume, "sweeping" gas along much as they do within the discharge chamber, followed by a more steady phase wherein the current patterns stabilize and revert to a "pumping" mode of gas acceleration much like that of the steady magnetoplasmadynamic arcs. A second result of interest is a demonstrated sensitivity of some aspects of plume development to relatively small changes in ambient gas pressure in the exhaust tank, emphasizing the importance of test environment to this phase of the acceleration process.



## REFERENCES

1. "Proposed Studies of the Formation and Stability of an Electromagnetic Boundary in a Pinch." Proposal for NASA Research Grant NsG-306-63, 5 March 1962.
2. First Semi-Annual Progress Report for the period 1 July 1962 to 31 December 1962, Research Grant NsG-306-63, Aeronautical Engineering Report No. 634, Princeton University, Princeton, New Jersey.
3. "The Plasma Pinch as a Gas Accelerator," AIAA Electric Propulsion Conference, 11-13 March 1963, Preprint No. 63013.
4. Second Semi-Annual Progress Report for the period 1 January 1963 to 30 June 1963, Research Grant NsG-306-63, Aeronautical Engineering Report No. 634a, Princeton University, Princeton, New Jersey.
5. "Structure of a Large-Radius Pinch Discharge," AIAA Journal 1, 8, 1809-1814, (1963).
6. "Gas-Triggered Inverse Pinch Switch," Review of Scientific Instruments 34, 12, 1439-1440 (1963).
7. "A Gas-Triggered Inverse Pinch Switch," Technical Note, Aeronautical Engineering Report No. 660, Princeton University, Princeton, New Jersey, August, 1963.
8. "Pulsed Electromagnetic Gas Acceleration," Paper No. II, 8, Fourth NASA Intercenter Conference on Plasma Physics in Washington, D. C., 2-4 December 1963.
9. "Current Distributions in Large-Radius Pinch Discharges," AIAA Aerospace Sciences Meeting, 20-22 January 1964, AIAA Preprint No. 64-25.
10. "Current Distributions in Large-Radius Pinch Discharges," AIAA Bulletin 1, 1, 12 (1964).
11. "Current Distributions in Large-Radius Pinch Discharges," AIAA Journal 2, 10, 1749-1753 (1964).
12. Third Semi-Annual Progress Report for the period 1 July 1963 to 31 December 1963, Research Grant NsG-306-63, Aeronautical Engineering Report No. 634b, Princeton University, Princeton, New Jersey.
13. "Pulsed Electromagnetic Gas Acceleration," Renewal Proposal for 15 months extension of NASA Research Grant NsG-306-63, Princeton University, Princeton, New Jersey, dated 15 January 1964.
14. Fourth Semi-Annual Progress Report for the period 1 January 1964 to 30 June 1964, Research Grant NsG-306-63, Department of Aerospace and Mechanical Sciences Report No. 634c, Princeton University, Princeton, New Jersey.
15. "Gas-Triggered Pinch Discharge Switch," Princeton Technical Note No. 101, Department of Aerospace and Mechanical Sciences, Princeton University, Princeton, New Jersey, July 1964.
16. "Gas-Triggered Pinch Discharge Switch," The Review of Scientific Instruments 36, 1, 101-102 (1965).

## REFERENCES-cont'd

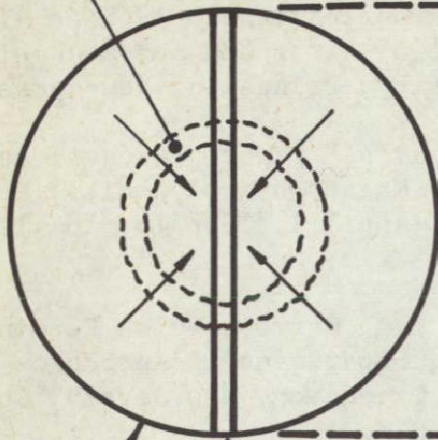
17. "Double Probe Studies in an 8" Pinch Discharge," M.S.E. Thesis of J. M. Corr, Department of Aerospace and Mechanical Sciences, Princeton University, Princeton, New Jersey, September 1964.
18. "Exhaust of a Pinched Plasma from an Axial Orifice," AIAA Bulletin 1, 10, 570 (1964).
19. "Exhaust of a Pinched Plasma from an Axial Orifice," AIAA Second Aerospace Sciences Meeting, New York, New York, 25-27 January 1965, Paper No. 65-92.
20. "Ejection of a Pinched Plasma from an Axial Orifice," AIAA Journal 3, 10, 1862-1866 (1965).
21. Fifth Semi-Annual Progress Report for the period 1 July 1964 to 31 December 1964, Research Grant NsG-306-63, Department of Aerospace and Mechanical Sciences Report No. 634d, Princeton University, Princeton, New Jersey.
22. "On the Dynamic Efficiency of Pulsed Plasma Accelerators," AIAA Journal 3, 6, 1209-1210 (1965).
23. "Linear Pinch Driven by a High-Current Pulse-Forming Network," AIAA Bulletin 2, 6, 309 (1965).
24. "Linear Pinch Driven by a High Current Pulse-Forming Network," 2nd AIAA Annual Meeting, San Francisco, California, 26-29 July 1965, Paper No. 65-336.
25. "The Design and Development of Rogowski Coil Probes for Measurement of Current Density Distribution in a Plasma Pinch," M.S.E. Thesis of Edward S. Wright, Department of Aerospace and Mechanical Sciences, Princeton University, Princeton, New Jersey, May 1965.
26. "The Design and Development of Rogowski Coil Probes for Measurement of Current Density Distribution in a Plasma Pinch," Department of Aerospace and Mechanical Sciences Report No. 740, Princeton University, Princeton, New Jersey, June 1965.
27. "Pulsed Electromagnetic Gas Acceleration," Renewal Proposal for 12 months extension of NASA Research Grant NsG-306-63, Princeton University, Princeton, New Jersey, dated 7 June 1965.
28. "Miniature Rogowski Coil Probes for Direct Measurement of Current Density Distributions in Transient Plasmas," The Review of Scientific Instruments 36, 12, 1891-1892 (1965).
29. Sixth Semi-Annual Progress Report for the period 1 January 1965 to 30 July 1965, Research Grant NsG-306-63, Department of Aerospace and Mechanical Sciences Report No. 634e, Princeton University, Princeton, New Jersey.
30. "Cylindrical Shock Model of the Plasma Pinch," M.S.E. Thesis of Glen A. Rowell, Department of Aerospace and Mechanical Sciences, Princeton University, Princeton, New Jersey, February 1966.
31. "Cylindrical Shock Model of the Plasma Pinch," Department of Aerospace and Mechanical Sciences Report No. 742, Princeton University, Princeton, New Jersey, February 1966.

## REFERENCES-cont'd

32. Seventh Semi-Annual Progress Report for the period 1 July 1965 to 31 December 1965, Research Grant NsG-306-63, Department of Aerospace and Mechanical Sciences Report No. 634f, Princeton University, Princeton, New Jersey.
33. "Pulse Forming Networks for Propulsion Research," paper presented at the Seventh Symposium on Engineering Aspects of Magnetohydrodynamics, Princeton University, Princeton, New Jersey, March 30-April 1, 1966 (p. 10-11 of Symposium Proceedings).
34. "Dynamics of a Pinch Discharge Driven by a High Current Pulse-Forming Network," Ph.D. Thesis of Neville A. Black, Department of Aerospace and Mechanical Sciences, Princeton University, Princeton, New Jersey, April 1966.
35. "A Large Dielectric Vacuum Facility," Technical Note to appear in the AIAA Journal 4, 6 (June 1966).

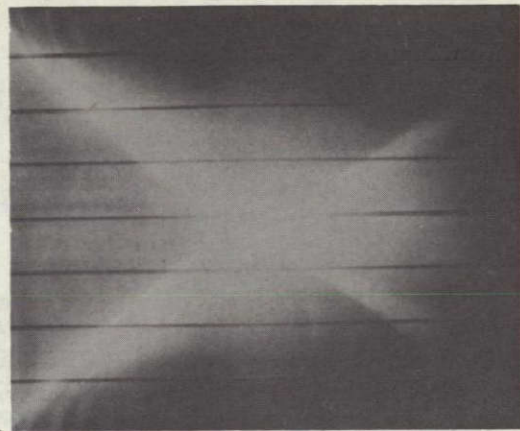


DISCHARGE DURING  
RADIAL CONTRACTION

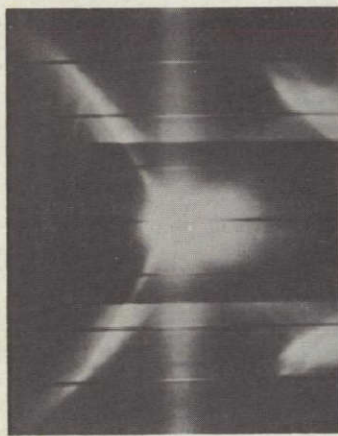
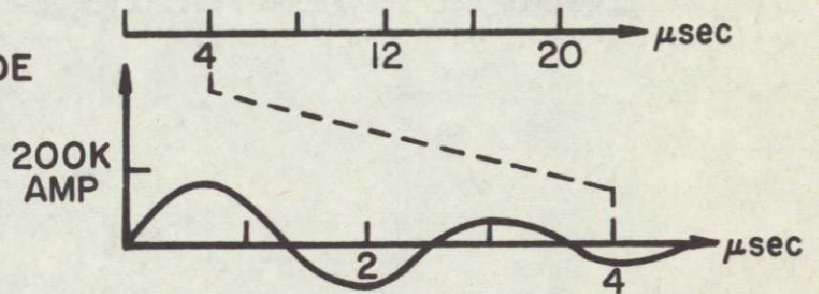


PINCH DISCHARGE  
CHAMBER

SLIT IN  
ELECTRODE



T185

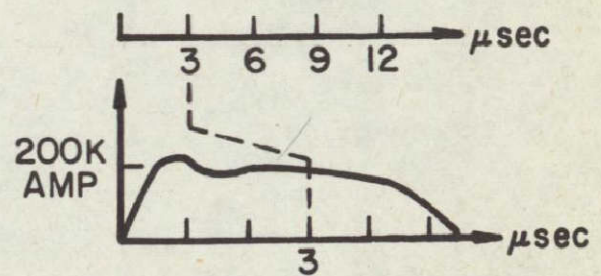
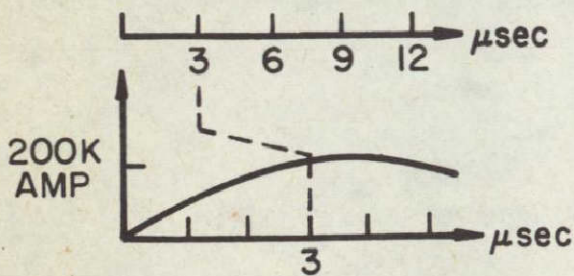


T833



T828

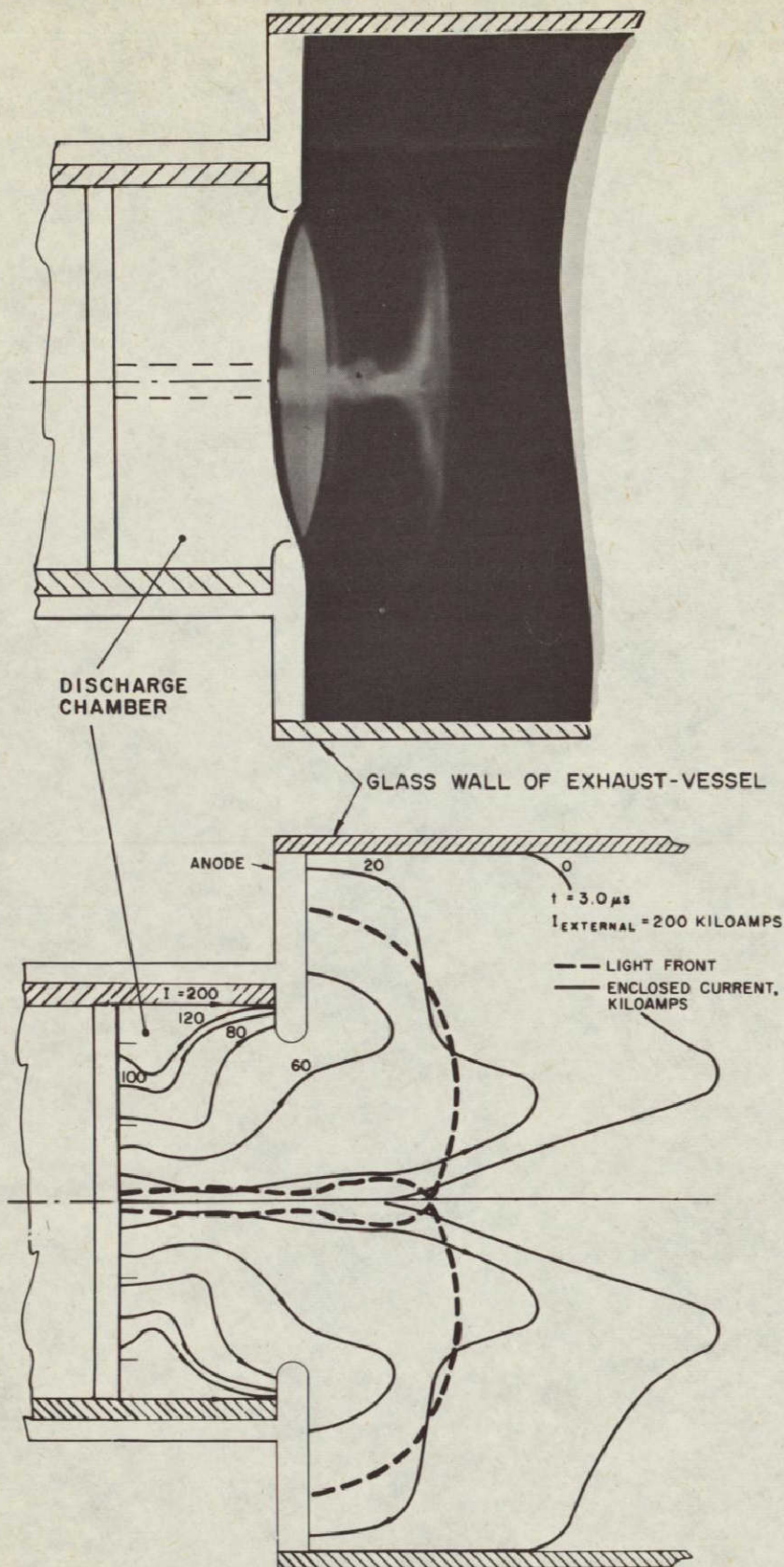
NOT REPRODUCIBLE



EFFECT OF VARIOUS DRIVING CURRENTS ON 100 μ ARGON DISCHARGE

FIGURE I





PHOTOGRAPH OF EXHAUST, & CURRENT PROFILES OF PINCH DISCHARGE IN  $120 \mu$  ARGON

## PULSED PLASMA ACCELERATOR

P. Gloersen, B. Gorowitz, and T. W. Karras

General Electric Space Sciences Laboratory, King of Prussia, Pa.

Problem Definition

This program was initiated for the purpose of developing an efficient reliable, lightweight device for ionizing and accelerating gaseous substances to velocities the order of  $5 \times 10^4$  meters/second. A coequal part of the program is the generation of experimental data which will permit a better understanding of the acceleration mechanisms involved in a coaxial gun.

Background

The motivation for this research is the requirement for thrusters with specific impulse characteristics higher than available from chemical or nuclear rockets to permit higher payload fractions in interplanetary space missions with intermediate characteristic lengths (the order of  $3 \times 10^6$  Km), acceptable payloads for deeper solar system exploration (characteristic lengths up to  $5 \times 10^9$  Km), and economically feasible solar system escape. With respect to competing electric thruster concepts, pulsed plasma devices offer the potential of much higher average thrust per unit area than electrostatic devices ( $\nu \tau B^2 / 2 \mu_0$  vs  $\epsilon_0 E^2 / 2$ ) and much higher peak thrust (with possibly resulting higher coupling efficiency) at a given average power level than steady-state MPD arcs.

Approach

The program consists of the construction of various accelerator configurations based on current understanding of acceleration mechanisms, measurement of the gross performance characteristics (thrust, mass flow, power input) of such configurations, confirming measurements and detailed plasma diagnostics (exhaust stream calorimetry, particle velocity and energy probe, magnetic field probe, current probes, particle density probes, terminal measurements, and spectroscopy) on the most promising of these configurations, and the updating of the understanding of the acceleration mechanism. (See Figure 1)

## Results

In terms of gross performance measurements, the best numbers consistently generated to date are an overall efficiency ( $\eta_o = T^2/2\dot{m} P$ ) of 70% or more at a specific impulse ( $I_{sp} = T/\dot{m} g$ ) of 5000 seconds. The power-to-thrust ratio at this point is about  $3.6 \times 10^4$  meters/second (160 KW/pound) and is constant within 5% of this value from 3300 to 5400 seconds specific impulse.

The most complete diagnostics to date exist for an operating point attained earlier, which was  $\eta_o = 57\%$ ,  $I_{sp} = 4800$  seconds, obtained at a mass flow rate of  $2.96 \times 10^{-7}$  Kg/sec, a capacitance of 144.5 mfd, a potential of 950 volts, a pulsing rate of  $10 \text{ sec}^{-1}$ , xenon propellant, and the A-7D gun configuration (see Figures 2-4). The relations

$$\eta_o' = \eta_E \eta_m \frac{\frac{2}{\bar{v}}}{\frac{2}{v^2}} \frac{1}{\cos^2 \alpha}$$

$$I_{sp}' = \bar{v} / g$$

were used to generate second values for  $\eta_o$  and  $I_{sp}$  for comparison with the results of the gross performance measurements.  $\eta_E$  was obtained by the use of a water-cooled calorimeter placed in the exhaust stream during repetitive operation of the accelerator under conditions equivalent to those cited. An upper limit to  $\eta_m$  was obtained by measuring the fraction of gaseous propellant available to the discharge by means of a small, fast ionization gauge pressure sensor (See Figure 5) used to map the propellant density prior to discharge as a function of both time after injection and position in the discharge region (See Figures 6-8). The factors  $\bar{v}$ ,  $\frac{2}{v^2}$ , and  $\cos^2 \alpha$  were obtained by means of the particle velocity and energy probe (See Figures 9-13), taking into account the  $\eta_m$  of the device. The values obtained are  $\eta_E = 72\%$ ,  $\eta_m = 90\%$ ,  $\bar{v} = 4.8 \times 10^4$  meters/sec,  $\frac{2}{\bar{v}} / \frac{2}{v^2} = 86\%$ , and  $\frac{1}{\cos^2 \alpha} = 97\%$ . Thus, the agreement between  $\eta_o$  and  $\eta_o'$  is within 10%, as is the agreement between  $I_{sp}$  and  $I_{sp}'$  which is remarkable in view of the estimated cumulative measuring accuracy of 20%. An accounting of current distributions both inside and outside of the accelerator added credence to these results, as did the operating background pressure level of about  $10^{-5}$  mm and an extended run of 10 hours under equivalent operating conditions with no degradation of performance.

## Future Plans

The mainstream of the next contractual effort will be to adapt the coaxial gun to the use of metal vapor propellant and determine the performance of this combination. Additional studies using xenon propellant are in progress.

- P. Gloersen, B. Gorowitz, and J. T. Kenney, "Energy Efficiency Trends in a Coaxial Gun Plasma Engine System", AIAA J. 4, 436 (1966).
- T. Karras, B. Gorowitz, and P. Gloersen, "Neutral Mass Density Measurements in a Repetitively Pulsed Coaxial Plasma Accelerator", AIAA Second Annual Meeting, San Francisco, California, AIAA Paper No. 65-341, July 1965.
- B. Gorowitz, T. Karras and P. Gloersen, "Performance of a Two-Stage Repetitively Pulsed Coaxial Plasma Engine", AIAA 2nd. Annual Meeting, San Francisco, California, Paper No. 65-342 (Revised) July 1965.
- B. Gorowitz, P. Gloersen, and T. Karras, "A 20 KW Solar Powered Pulsed Plasma Engine", AIAA 3rd. Aerospace Sciences Meeting, New York, Paper No. 66-114, January 1966.
- B. Gorowitz, P. Gloersen, and T. Karras, "Steady State Operation of a Two-Stage Pulsed Coaxial Plasma Engine", AIAA 5th. Electric Propulsion Conference at San Diego, California, Paper No. 66-240, March 1966.
- P. Gloersen, T. Karras and B. Gorowitz, "Diagnostic Observations of a Repetitively Pulsed Coaxial Accelerator", AIAA 5th. Electric Propulsion Conference, San Diego, California, Paper No. 66-197, March 1966.
- T. Karras, B. Gorowitz, and P. Gloersen, "Propellant Injection into a Coaxial Plasma Accelerator", AIAA 5th. Electric Propulsion Conference, San Diego, California, Paper No. 66-241, March 1966.



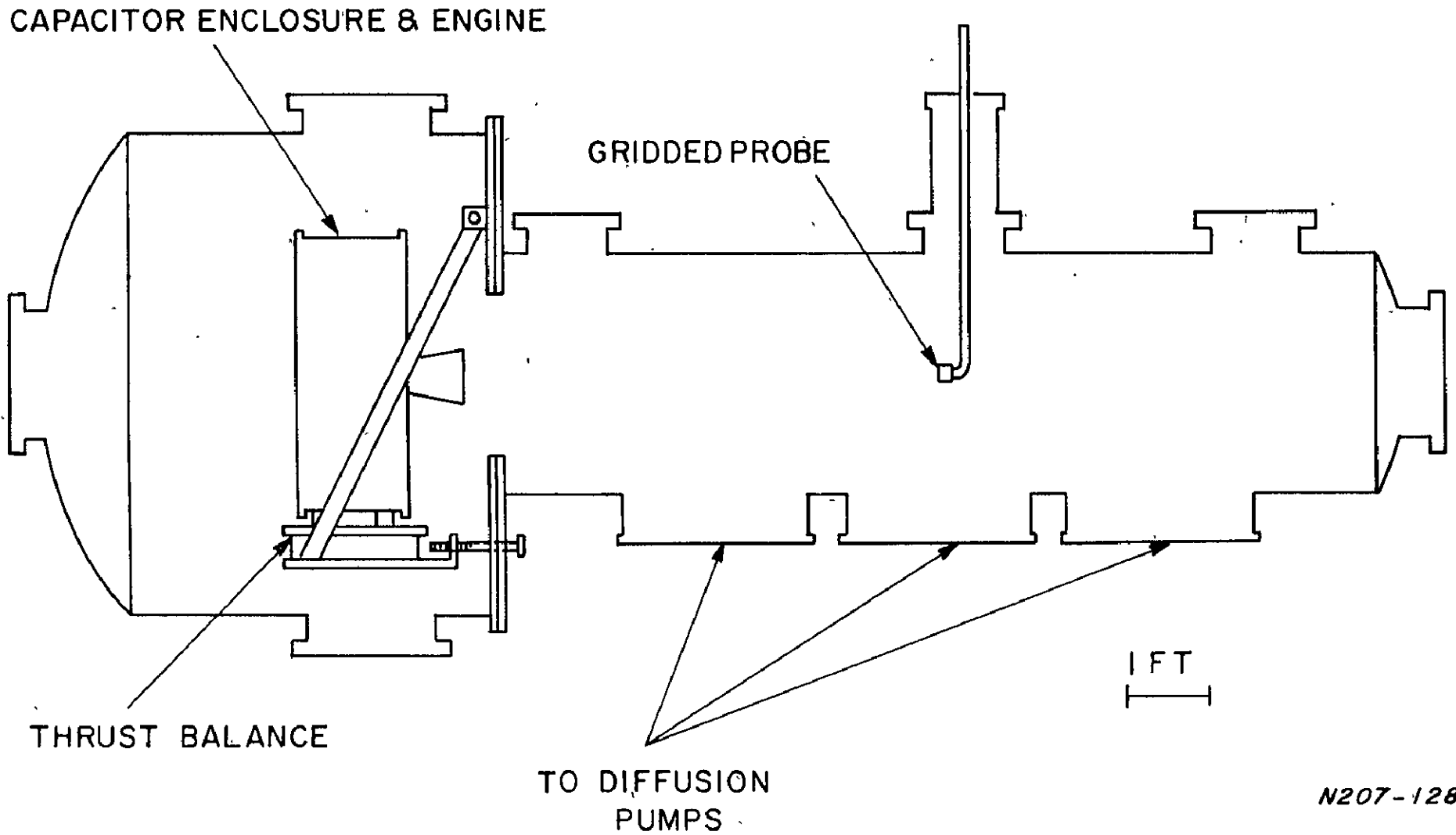


Figure 1. Outline of Plasma Accelerator Test Facility

N207-128

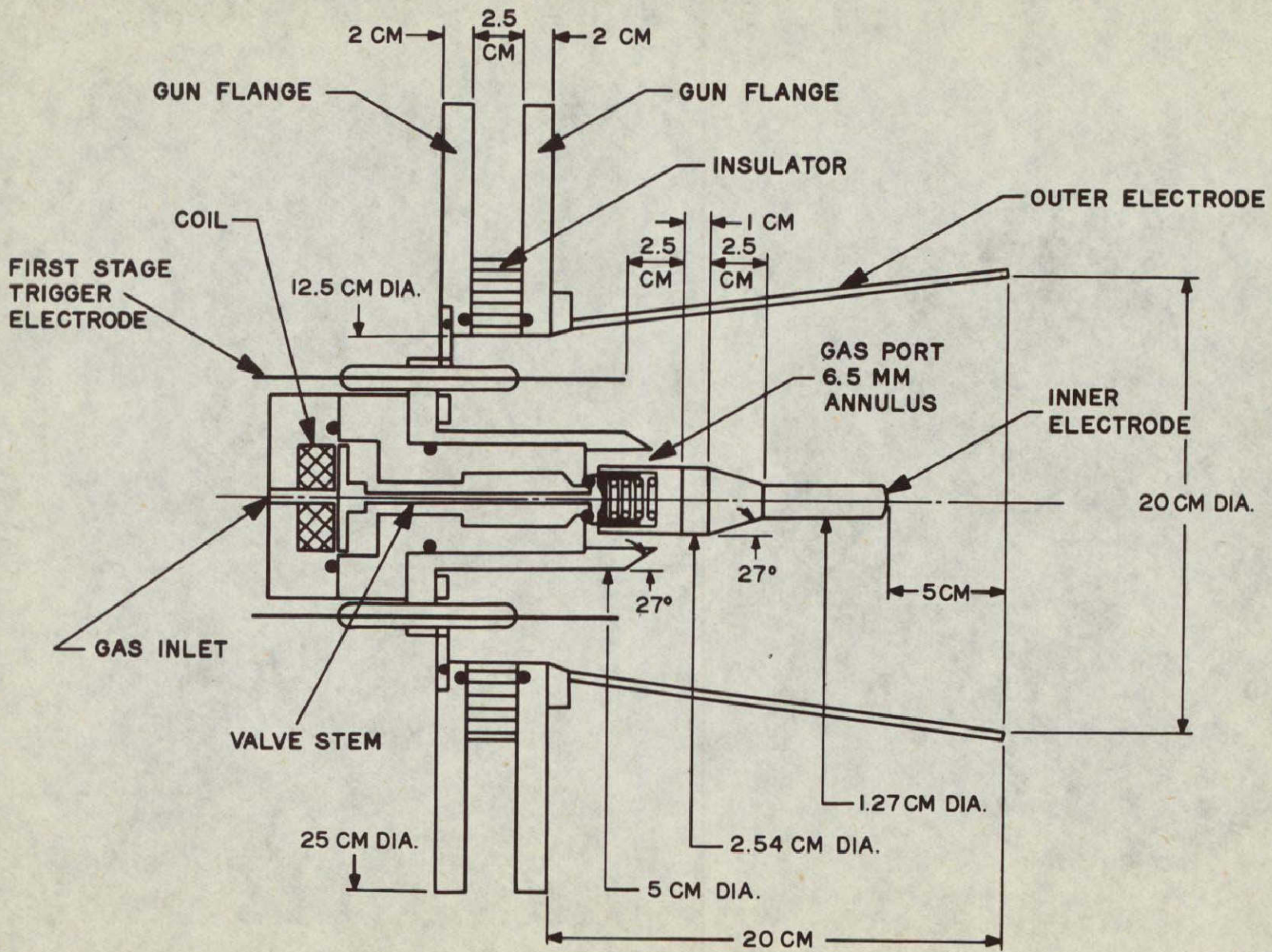
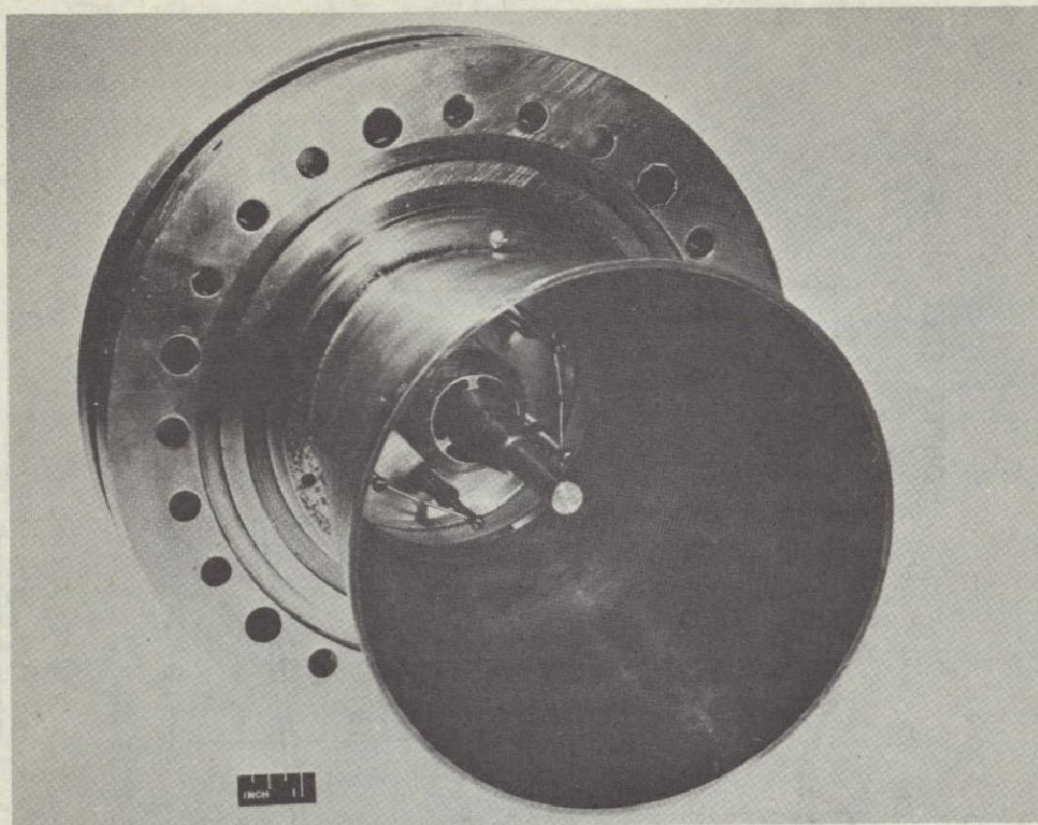
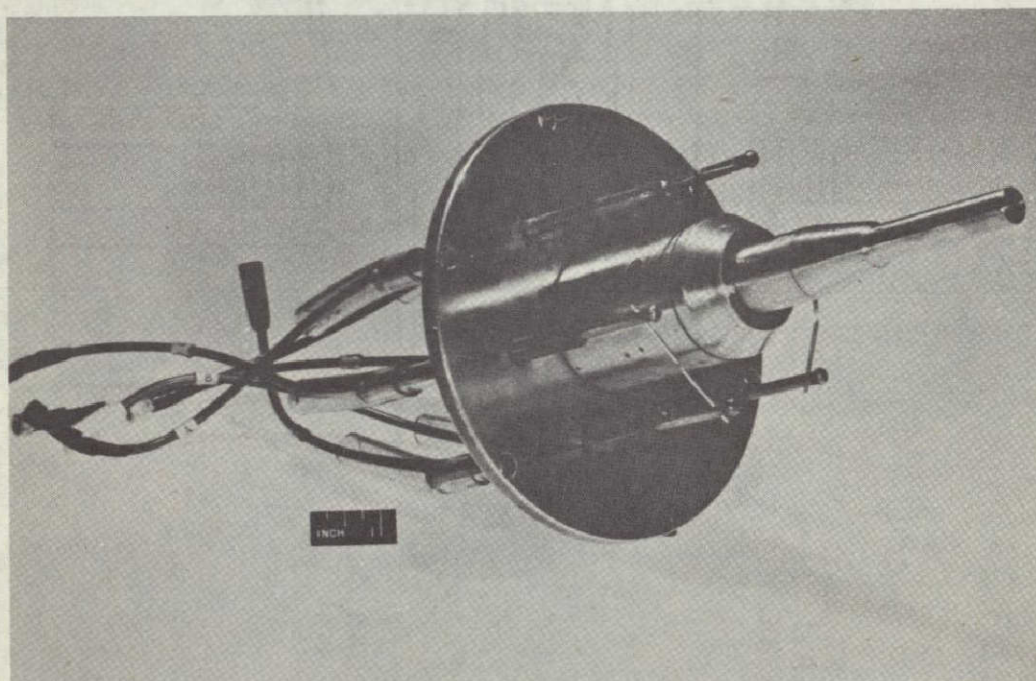


Figure 2. A-7D Accelerator





(a)



(b)

Figure 3. (a) A-7D Accelerator, (b) A-7D Accelerator Central Electrode Assembly



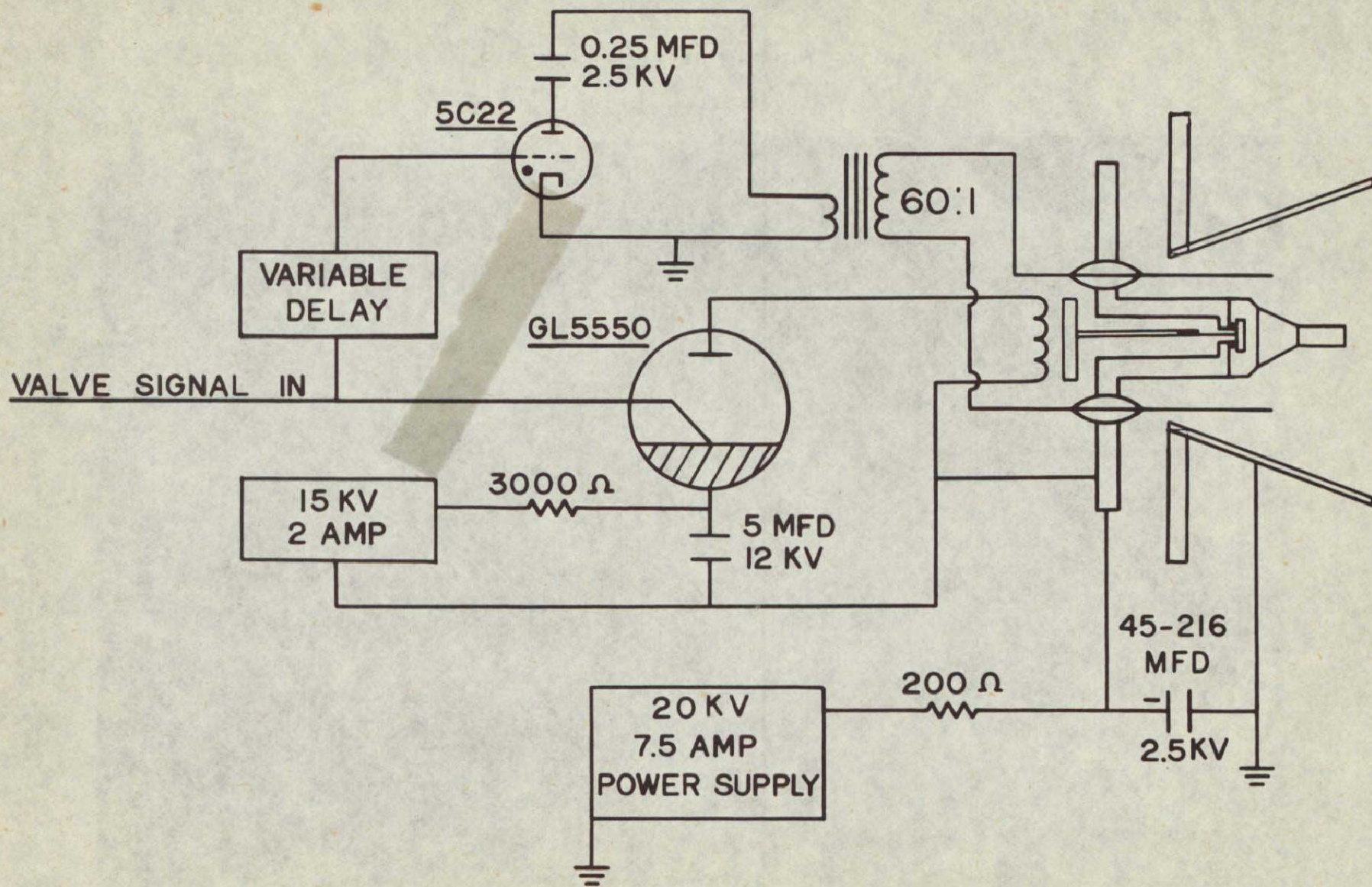


Figure 4. Circuit Diagram of the A7-D Accelerator



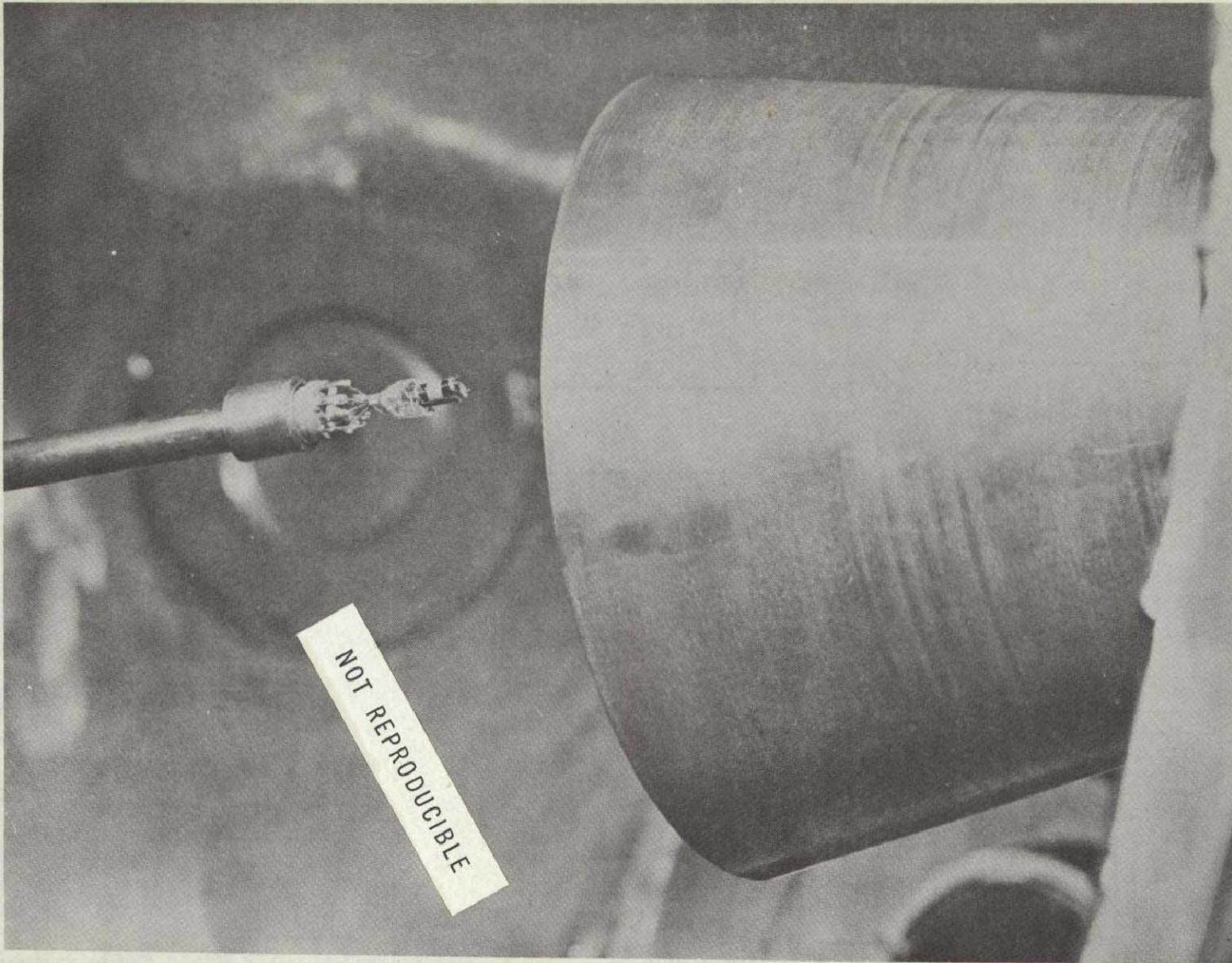


Figure 5. Gas Density Probe

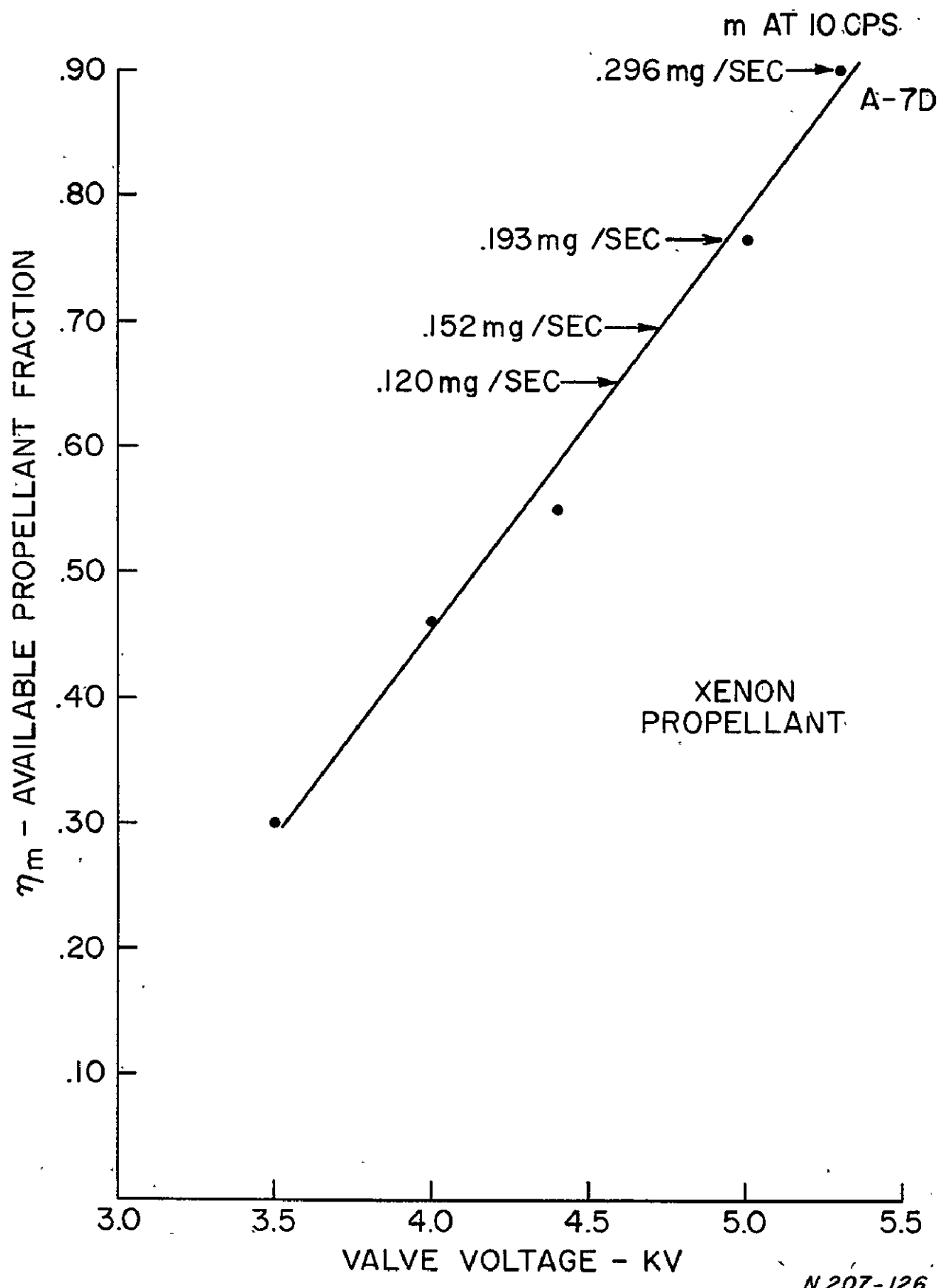


Figure 6. Propellant Mass Fraction vs Valve Voltage for Mod A-7D Gun

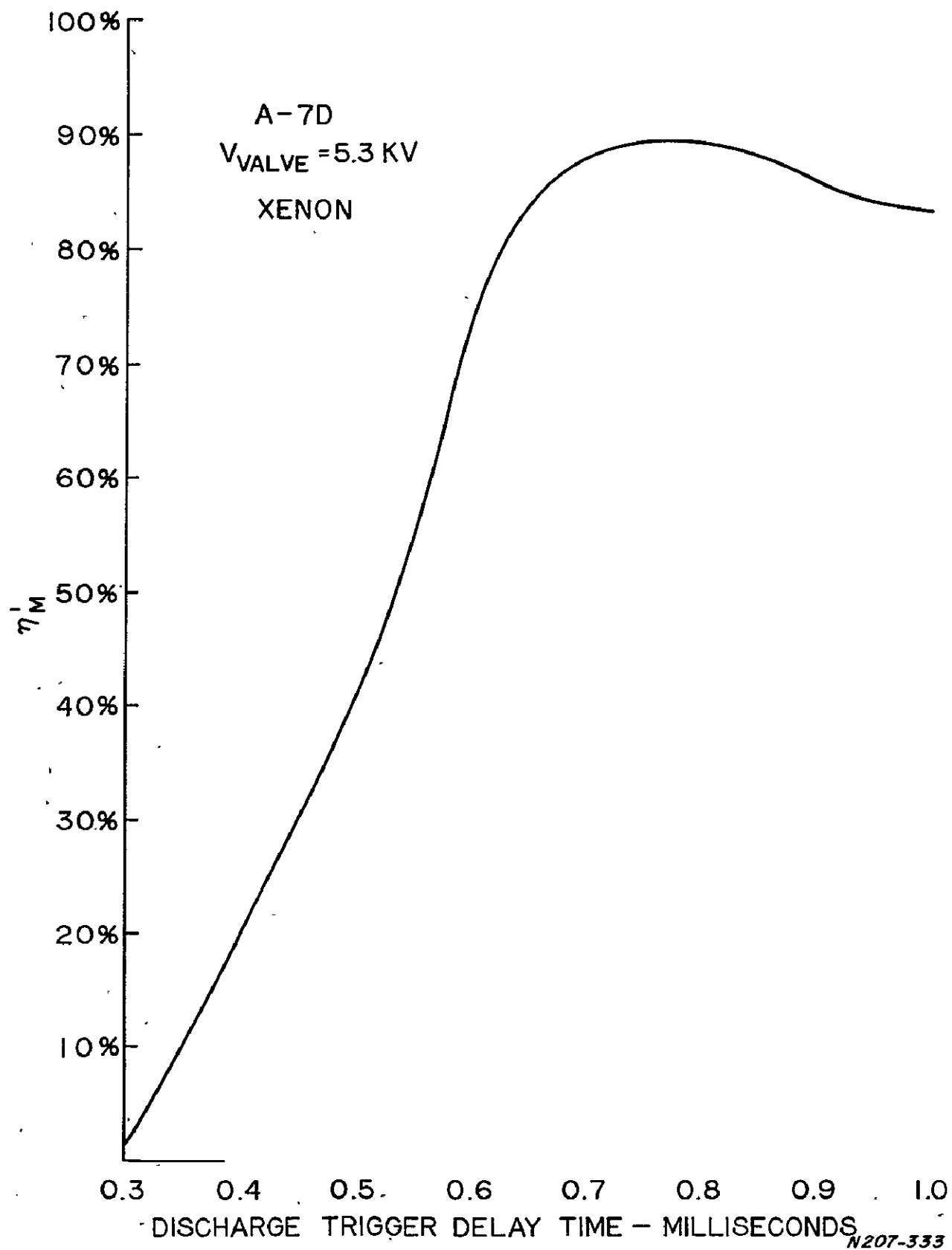


Figure 7. Fraction of Propellant Between the Accelerator Electrodes at Various Discharge Trigger Delay Times

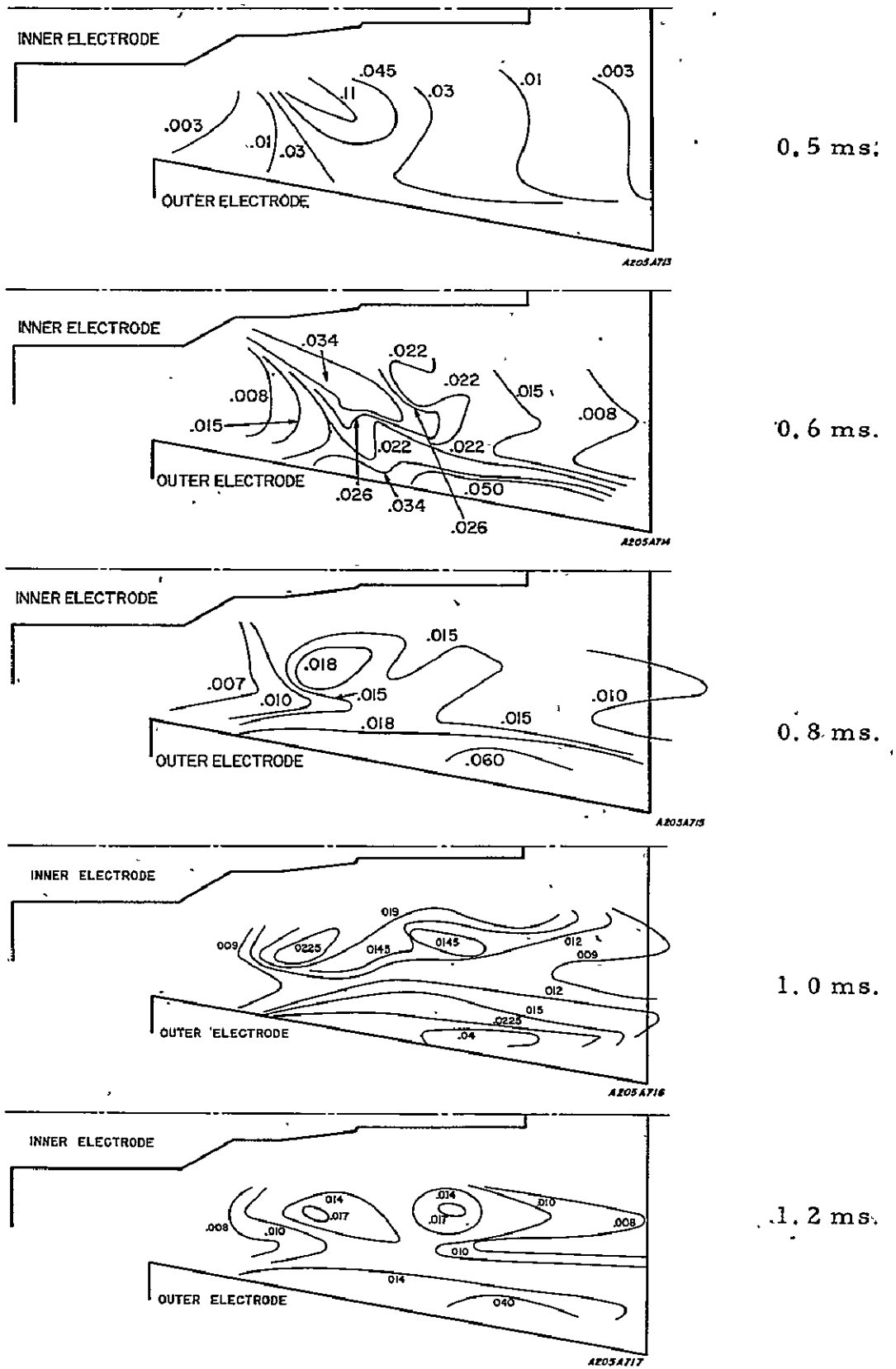
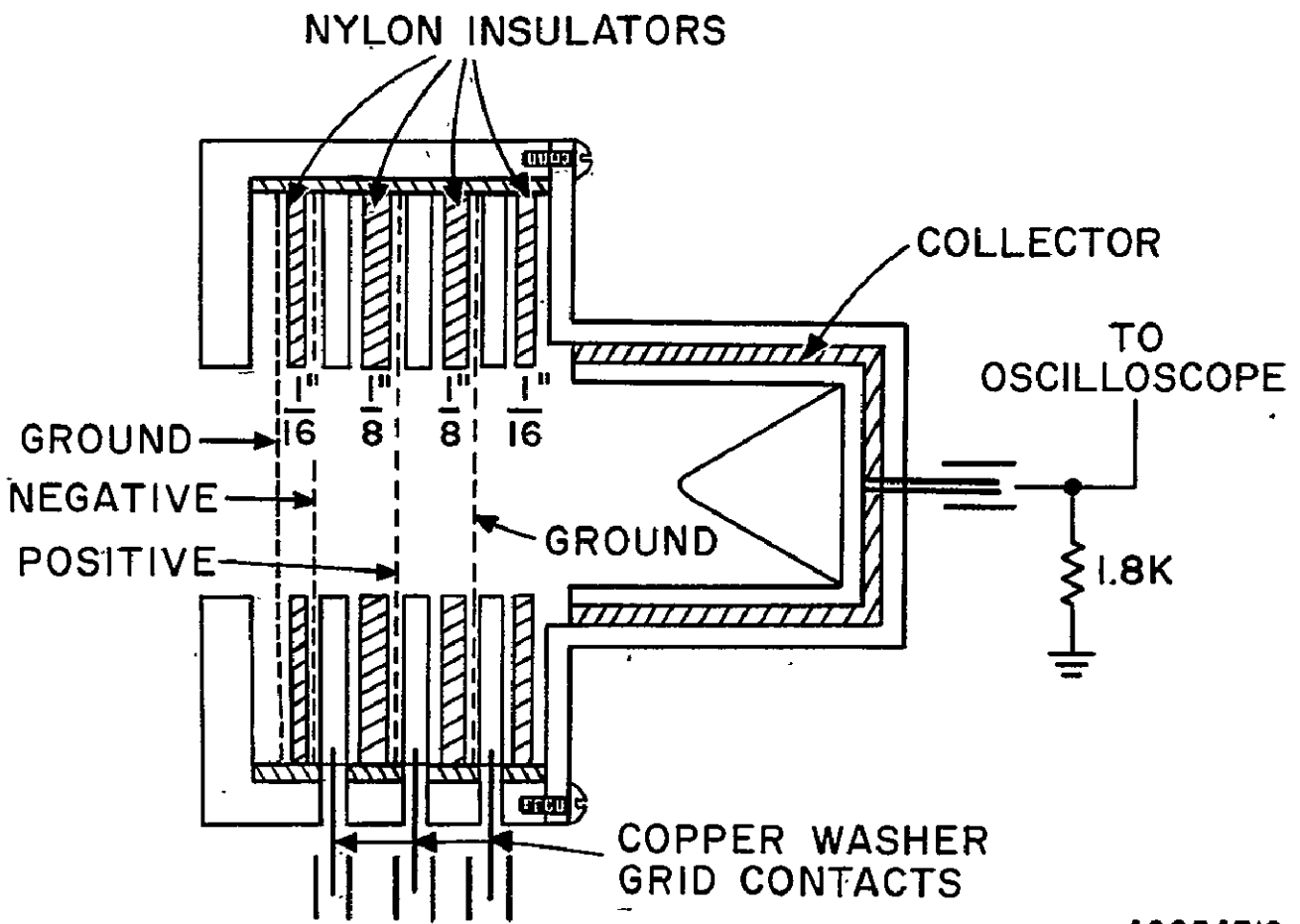


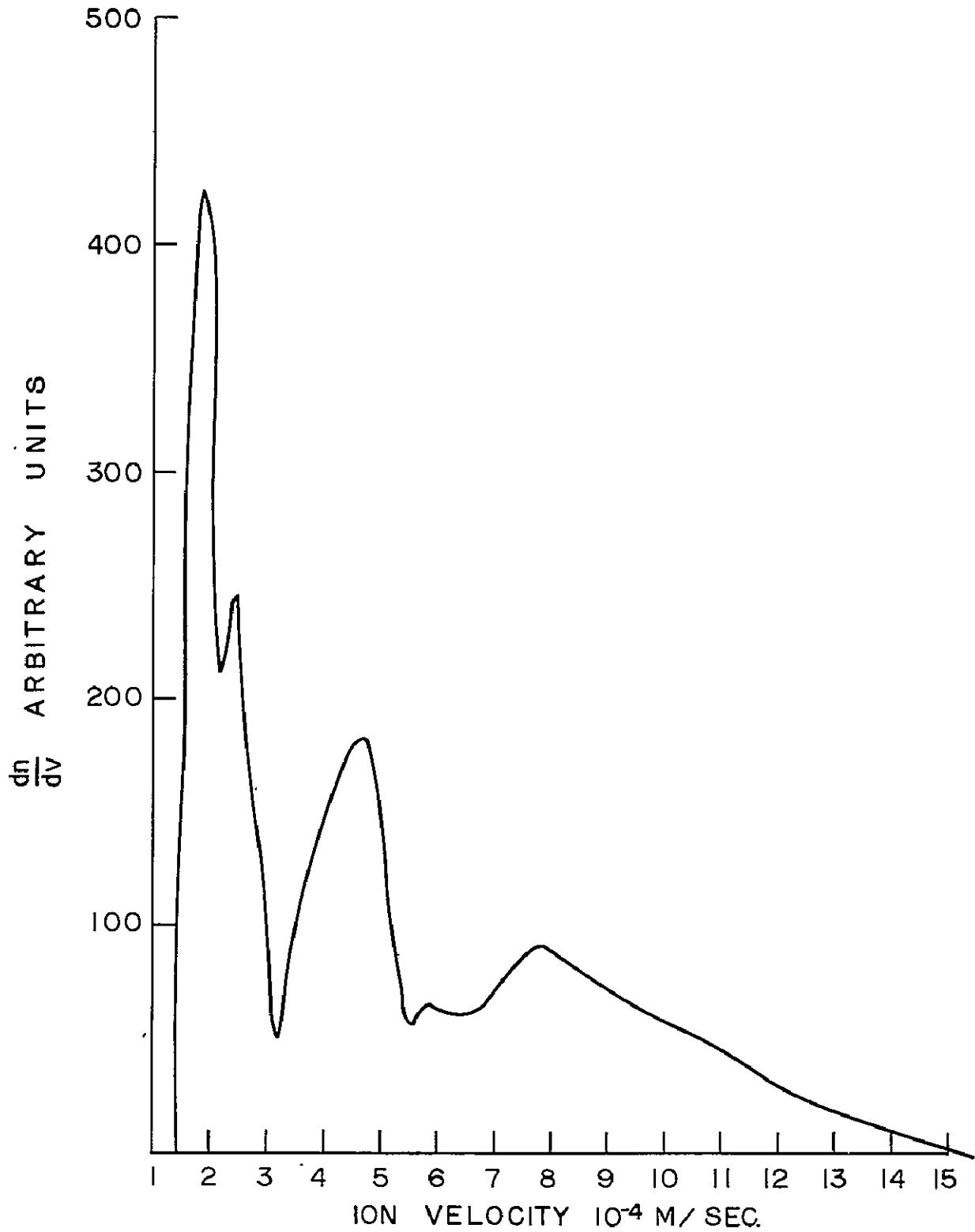
Figure 8. Isobars, Xenon, Valve: 3900 Volts.





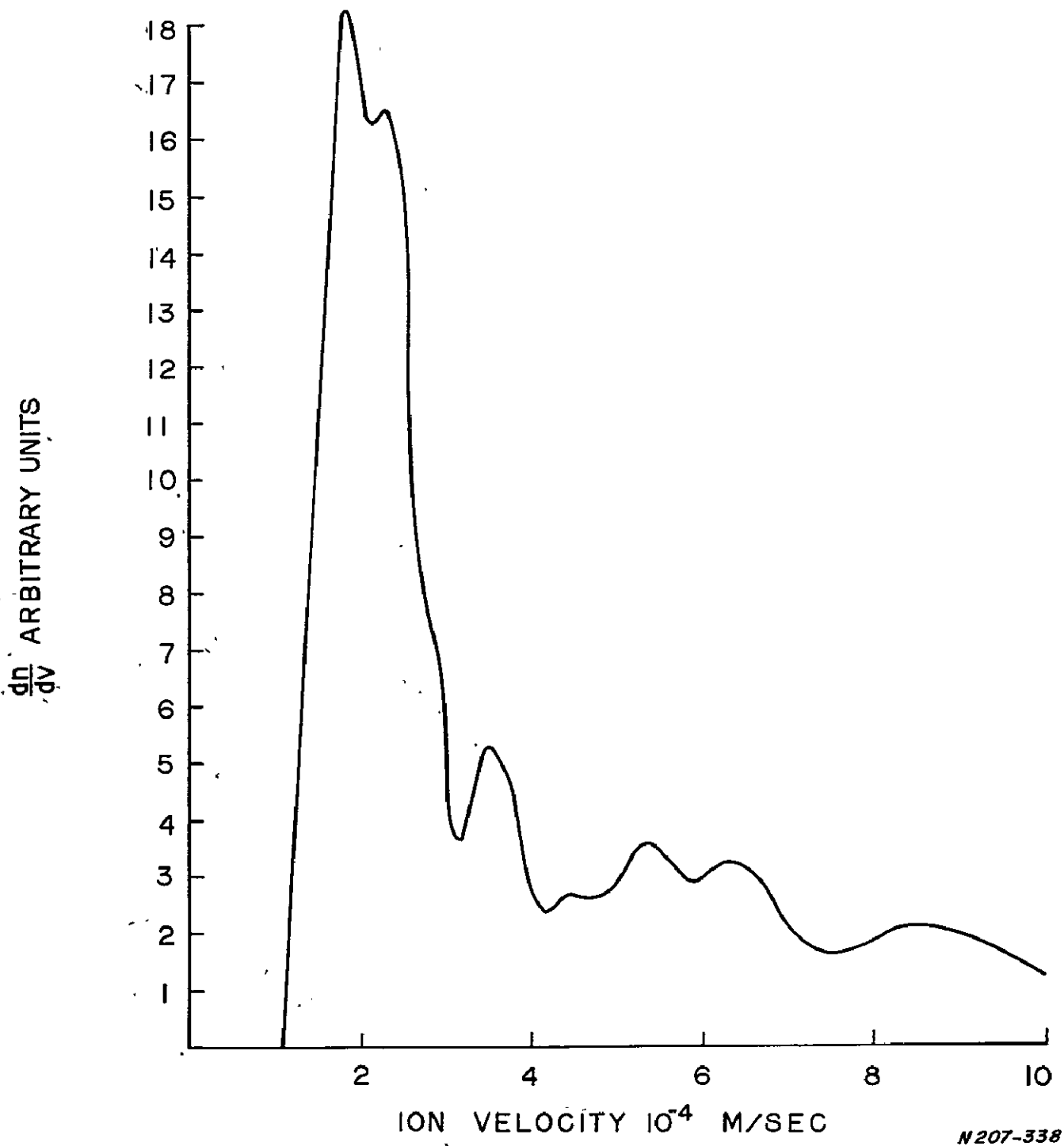
A205A719

Figure 9. Gridded Probe for Measurement of Ion Energies



N107-158

Figure 10. Total Ion Velocity Distribution on Axis, A-7D Gun,  $\eta = 57\%$ ,  
 $I_{sp} = 4800$  sec., 950V, 144.5  $\mu$ fd, .296 mg/sec Xenon



N207-338

Figure 11a. Total Ion Velocity Distribution 45 cm. off Gun Axis, A-7D Gun  
 $\eta = 57\%$ ,  $I_{sp} = 4860$  sec., 950V, 144.5  $\mu$ fd, .296 mg/sec. Xenon

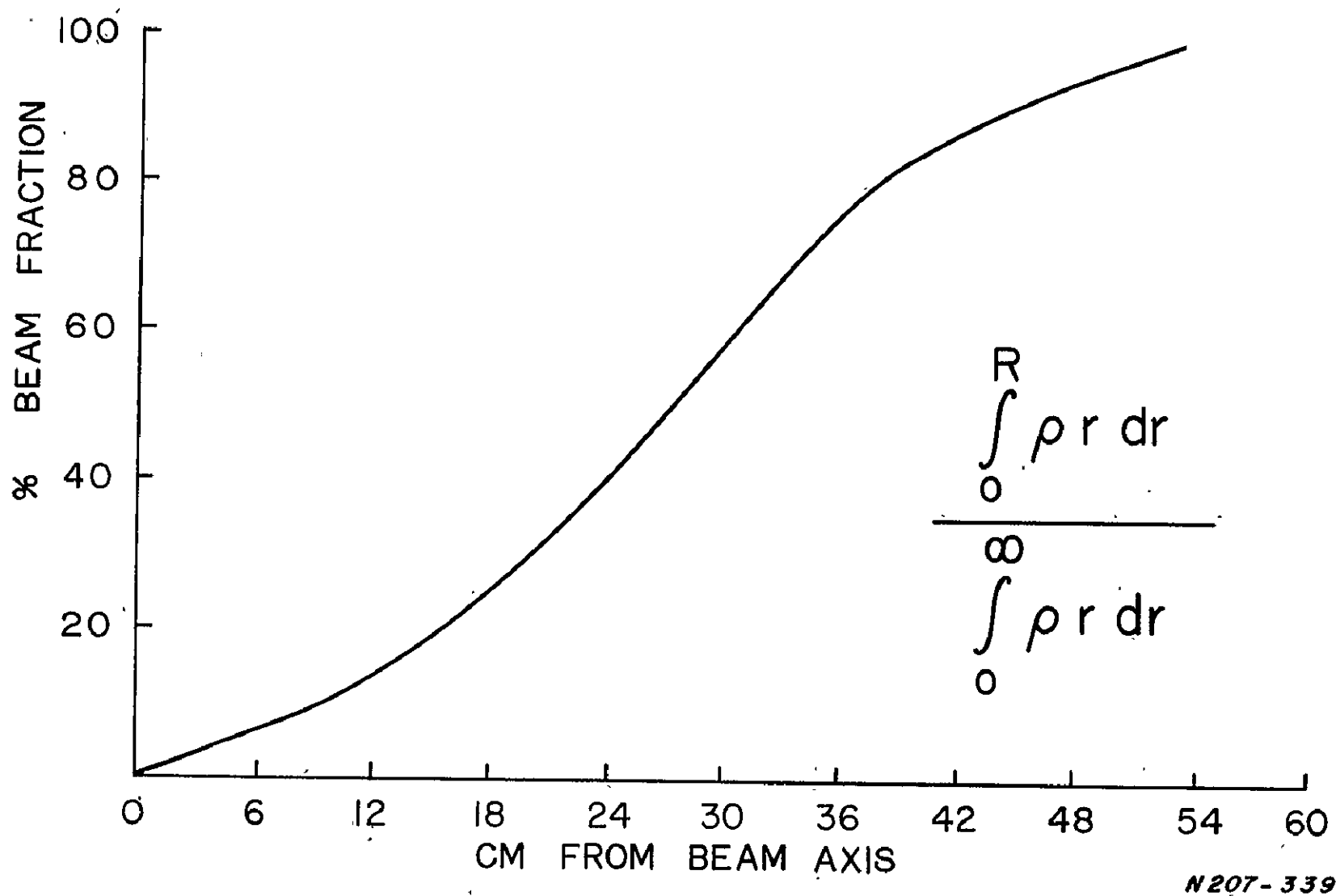
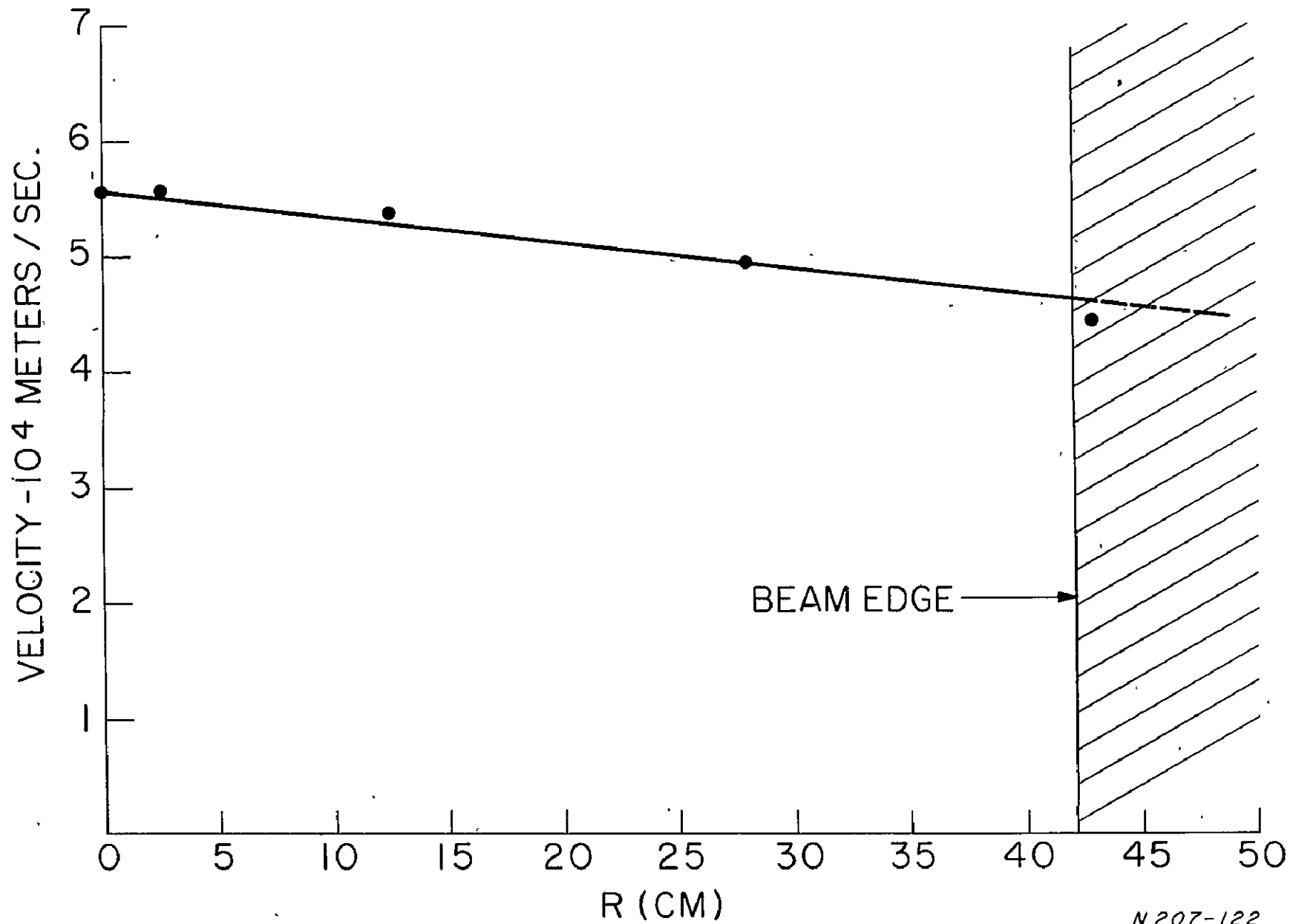


Figure 12. Fraction of Accelerated Propellant within a Beam Radius, 2m Downstream from Accelerator Muzzle. Mod A-7D,  $\eta = 57\%$ ,  $I_{sp} = 4800$  sec., 950V, 144.5  $\mu$ fd, .296 mg/sec Xenon



N 207-122

Figure 13. Average Ion Velocity at Various Radial Positions in a Plane Two Meters Downstream From the Accelerator Muzzle. Mod A-7D,  $\eta = 57\%$ ,  $I_{sp} = 4800$  sec., 950V, 144.5  $\mu$ fd, .296 mg./sec Xenon

## COAXIAL PLASMA GUN

A. V. Larson, L. Liebing, A. R. Miller, and R. Dethlefsen  
Space Science Lab., General Dynamics Convair, San Diego, Calif.

Since 1961, a development program for pulsed plasma guns has been jointly sponsored by NASA-Lewis and General Dynamics Convair. The principal Lewis goal has been to demonstrate competitive thrust efficiencies in such devices. This year the number of industry competitors in this field has been reduced to one, the decision being based on the efficiency of presently existing accelerators. As the Convair program nears completion, it is appropriate at this conference, to summarize the effort and results, and to list the related publications. The accomplishments of the last year are given in abstracts of recent meetings and are reproduced here. Finally, the results will be given of recent experiments which were designed specifically to measure the performance of the pulsed plasma device of Gloersen, Gorowitz, and Karras.

The Convair program began with a strong diagnostic effort to examine the plasma energy transfer processes. Electromagnetic field probes were developed and applied to measuring the phenomena within the discharge. The techniques of Faraday cups, gridded electrostatic analyzers, and other particle analyzers were established for the exhausts of pulsed plasma guns. Scaling laws were verified for the control of  $I_{sp}$  for guns operating with various propellant distributions, e.g., uniform fill and slug fill. The applicability of the snow-plow model was established. Fundamental limitations, due to the physics of the plasma processes in two modes of plasma accelerators were recognized. Important parametric relationships which affect performance were empirically determined. Three technological spin-offs have occurred: an order of magnitude improvement in energy storage capacitors; a high speed, low power, compact gas valve; the founding of the pulsed MPD arc technology.

To illustrate our recent work, we include abstracts of two papers given at the Fifth Electric Propulsion Conference, March 1966.

Paper (66-199), "Experiments with a Pulsed Arc Plasma Thruster."

A series of experiments with an improved version of our pulsed arc plasma thruster will be described. This thruster is similar to the MPD arc jets except that it is pulsed. The propellant feed system and the power supply are built so that the thruster operates in a steady-state mode for 650  $\mu$ sec. The power level ranges between 10 kw and 1.5 Mw. Hall current, radial current, and magnetic field measurements have been made within the thruster discharge. The Hall current density is generally an order of magnitude larger than the radial current density. The  $j_{\theta}B_r$  force is about twice larger than the  $j_rB_{\theta}$  force. It is estimated that  $\omega r$  equals 5 for the electrons. The thruster current, voltage, ion exhaust velocity, and ion density have been measured as functions of the injected mass flow rate with helium, nitrogen, and argon propellants. The thrust is not strongly dependent upon the injected  $\dot{m}$  and, therefore, the apparent efficiency is very high at low  $\dot{m}$ . It has been found that the cathode erosion becomes important at low mass flow rates, but complete erosion studies have not been done

Paper (66-238), "Experiments with a Voltage Switched Pulsed Coaxial Gun."

An experimental program will be described which investigates the behavior of a pulsed coaxial thruster in which slug-model propellant distributions are used.

The propellant is injected radially through ports located near the insulator. The gas valve opens in about 100  $\mu$ sec and a plenum is used to control the amount of propellant injected. A triggered voltage switch is used to delay the time between propellant injection and thruster discharge. Measurements are made of the neutral gas distribution prior to the discharge, the current distribution, the ion velocity and energy in the exhaust, and the calorimetric and thrust efficiency. The variables include the firing delay, mass load, capacitor voltage, and barrel geometry. The thruster operates in an axially-symmetric stable manner over an interval in which the gas distribution changes from the slug-model approximation to a nearly uniform distribution. Peak calorimetric efficiencies of 70% occur for propellant distributions which approximate the slug model. The efficiency increases with capacitor voltage and is rather insensitive to plenum pressure.

Since March, we have concentrated on measuring a duplicate of the G. E. accelerator for which high efficiencies have been reported. Performance has been measured as a function of propellant species, port location, direction of propellant injection, firing delay, and barrel geometry. The important result is that it has not been possible in our installation to achieve the efficiency reported by General Electric, or to exceed efficiencies achieved by the various General Dynamics accelerator designs.

#### Publications for NASA Related Work

"The use of Magnetic Probes in Plasma Diagnostics," R. H. Lovberg, Ann. Phys., 8, 311 (1959).

"Current Sheet in a Coaxial Plasma Gun," L. C. Burkhardt and R. H. Lovberg, Phys. Fluids 5, 341 (1962).

"The Use of a Coaxial Plasma Gun for Space Propulsion," Final Report, Contract NAS 5-1139, GD/Astronautics Report No. AE 62-0678, dated May 1962.

"Use of Ballistic Pendulums with Pulsed Plasma Accelerators," T. J. Gooding, B. Hayworth, and R. H. Lovberg, ARS J., Oct. (1962) p. 1599.

"Impulsive MHD Devices as Space Engines," R. H. Lovberg, Proc. of Third Symp. on Adv. Propulsion Concepts, held at Cincinnati (Oct. 1962), publ. by Gordon and Breach, New York, 1963, p. 95.

"Physical Processes in a Coaxial Plasma Gun," T. J. Gooding, B. R. Hayworth, R. H. Lovberg, AIAA Electrical Propulsion Conference, Paper 63-004, Colorado Springs, March (1962).

"Instabilities in a Coaxial Plasma Gun," T. J. Gooding, B. Hayworth, and R. H. Lovberg, AIAA J. 1, 1289 (1963).

"Development of a Coaxial Plasma Gun for Space Propulsion," Final Report, Contract NAS 3-2501, GD/Astronautics Report No. GDA 63-0454, dated May 1963.

"Inference of Plasma Parameters from Measurement of E and B Fields in a Coaxial Accelerator," R. Lovberg, Phys. Fluids 7, Part 2-Supplement, S57 (1964).

"Development of a Coaxial Plasma Gun for Space Propulsion," Final Report, Contract NAS 3-2594, NASA Report No. CR-54149, GD/Astronautics Report No. GDA DBE 64-051, dated June 1964.

"An Energy Inventory in a Coaxial Plasma Accelerator Driven by a Pulse Line Energy Source," A. V. Larson, et al., AIAA J. 3, 977 (1965).

"Energy Loss in Pulsed Coaxial Plasma Guns," D. E. T. F. Ashby, AIAA J. 3, 1045 (1965).

"Exhaust Measurements on the Plasma from a Pulsed Coaxial Gun," D. E. T. F. Ashby, T. J. Gooding, B. R. Hayworth, and A. V. Larson, AIAA J. 3, 1140 (1965); also AIAA Reprint 64-704 (1964).

"Development of a Coaxial Plasma Gun for Space Propulsion," Final Report, Contract NAS 3-5759, NASA Report No. CR-54245, dated April 1965.

"Energy Storage Capacitors for Pulsed Plasma Thrusters," B. R. Hayworth, A. R. Miller; and C. W. White, AIAA Paper No. 65-337, San Francisco, July 1965.

"Quasi-Steady-State Pulsed Plasma Thrusters," D. E. T. F. Ashby, T. J. Gooding, and A. V. Larson, AIAA Paper No. 65-338, San Francisco, July 1965; to be published (AIAA J.).

"Note on the Use of Mass Analyzers in Plasma Physics," H. Fleischmann, D. E. T. F. Ashby, A. V. Larson, (to be published in Nuclear Fusion); also available as Report GA-6219, General Atomic, San Diego, Calif.

"Generation of Plasma Streams with Pulsed Arc Discharges," T. J. Gooding, D. E. T. F. Ashby, and L. Liebing, General Dynamics Convair Report No. ERR-AN 739, May 1965.

"Experiments with a Pulsed Arc Plasma Thruster," L. Liebing, A. V. Larson, T. J. Gooding, AIAA Paper No. 66-199, Fifth Electric Propulsion Conference, San Diego, March 1966.

"Experiments with a Voltage Switched Pulsed Coaxial Gun," A. V. Larson, L. Liebing, A. R. Miller, AIAA Paper No. 66-238, Fifth Electric Propulsion Conference, San Diego, March 1966.



## DIAGNOSTICS OF ACCELERATING PLASMA

Drs. C. C. Chang, T. N. Lie and A. W. Ali  
The Catholic University of America

ABSTRACT

In pulsed plasma accelerator, the process by which the neutral gas is ionized, heated and acquires momentum is not fully understood. A simple model in which a shock wave, with no losses, is accelerated by magnetic piston is certainly inadequate. In order to understand these processes, the transient plasma state must be known, i.e., electron densities, composition, temperatures are required for comparison with theoretical models.

In our project, it is intended: a) to apply spectroscopic techniques to diagnose the plasma produced in some typical plasma accelerator and compare the results with those obtained by other investigators; b) to compare existing theory for plasma acceleration with the measurement; c) to account for the energy deposited in the plasma in order to give further information on losses.

As a first step of the project, accelerated plasma produced by a coaxial plasma gun which was operated at static ambient pressure (helium) was studied. Electron temperature, electron density, and other particle densities are determined at a location which is 1 cm outside the gun end. Furthermore, the electron temperature and the density were obtained as a function of radius of outer electrode using Abel inversion procedure with a series of measurements.

The same technique has been extended into the gun barrel to diagnose accelerating current layer. The electron densities and temperatures inside the gun were relatively high and were found to be  $T_e \simeq 11$  eV and  $N_e \simeq 7 \times 10^{17}$  cm<sup>-3</sup> at the location which is 7.5 cm from the insulator.

## MPD ARC JET THRUSTOR RESEARCH

Contract NAS 3-2593  
 AVCO Corporation  
 Space Systems Division  
 Wilmington, Massachusetts

Investigators: Principal - Dr. R. R. John and Dr. S. Bennett  
 Associates - Mr. G. Enos and Dr. A. Tuchman

Objective: The overall purpose of the subject research and development program is to establish whether the laboratory MPD arcjet, which appears to be an efficient gas accelerator, can be converted into a reliable low thrust space propulsion engine.

Background: A typical MPD arcjet configuration is shown in figure 1. The basic unit is axially symmetric, consisting of a central cathode surrounded by a co-axial anode, and can be operated both with and without a magnetic field. The working fluid is accelerated both by aerodynamic and magnetoplasmadynamic forces as it passes through and around the discharge. Although there is considerable controversy regarding the exact nature of the gas acceleration process, the basic thrust producing mechanisms characteristic of the MPD arcjet are associated with: (1) Aerodynamic pressure forces (thermal acceleration); (2) Self-induced magnetic field forces; and (3) External magnetic field forces.

Progress and Results: Five basic thrust producing mechanisms have been proposed as being characteristic of plasma generators of the type shown in figure 1. These are: (1) Aerodynamic pressure forces; (2) Magnetic pumping; (3) Magnetic blowing; (4) Aerodynamic swirl introduced by electromagnet forces; and (5) Hall current acceleration. Aerodynamic pressure forces are associated with thermal expansion of a gas within confining solid walls; magnetic pumping results from the interaction of the axial discharge current density,  $j_z$ , with the self-induced azimuthal magnetic field,  $B_\theta$ , i.e.  $T_{\text{pump}} = 1/2 I^2$ ; magnetic blowing results from the interaction of the radial component of the current density,  $j_r$ , with the self-induced azimuthal magnetic field,  $B_\theta$ , i.e.  $T_{\text{blow}} = I^2 (1/4 + \ln r_a/r_c)$ , where  $r_a$  and  $r_c$  are respectively the radial extent of the current distribution at the anode and cathode. These three thrust mechanisms have been clearly identified and their existence is not dependent on the presence of a magnetic field<sup>1</sup>. The remaining mechanisms are associated with an external field. The magnetic swirl is associated with the bulk rotation of the gas and results from the interaction of  $j_r$  with  $B_z$ . Finally, the Hall current term is associated with the interaction of  $j_\theta$  with  $B_r$ . No simple analytical expressions have been derived for the external field terms except empirically it has been established that  $T_{\text{total}} = T_{\text{aero}} + T_{\text{self}} + T_{\text{external}} = f(I, B)$ .

As was originally pointed out by Fahleson for the case of a plasma rotating in a magnetic field<sup>2</sup>, and by Cann for the MPD arcjet<sup>3</sup>, the available gas flow,  $\dot{m}$ , and the gas flow,  $\dot{m}_d$ , accelerated and ionized by the discharge are not, a priori, equal. The concept of a characteristic discharge mass flow has been strikingly verified experimentally at this laboratory by the observation that the engine will operate and produce thrust with no mass flow passing through

the propellant feed line<sup>4</sup>. By analogy with conventional arcs Cann<sup>3</sup> proposed that the MPD discharge would operate at a power level such that the input power is minimized; Fahleson<sup>2</sup>, on the other hand, following a suggestion of Alfven, postulated the discharge would operate at a mass flow such that the kinetic and ionization energies of the particles in the discharge mass flow are equal. Assuming that the input power is primarily absorbed in kinetic and ionization energy the two postulates are identical. From energy considerations the flow velocity at minimum input power is given by  $U_{crit} = \sqrt{2eV_i/m_a}$ ; the critical mass flow becomes  $\dot{m}_{d,min} = T/\sqrt{2eV_i/m_a}$ ; and the minimum power is  $IV)_{min} = T\sqrt{2eV_i/m_a}$ . The empirically observed linearity between  $V$  and  $B$  and  $T$  and  $IB$ , shown in figures 2 and 3, is compatible with these minimum energy considerations.

The preceding discussion has been based on a macroscopic description of accelerator performance. It has been proposed that the external magnetic field forms a magnetic nozzle in which azimuthal kinetic energy resulting from the interaction of  $B_z$  and  $j_r$  is "spun out" into axially directed kinetic energy; however, the exact nature of acceleration and confinement process is not at all clear. Local current measurements in the MPD arcjet discharge obtained with Hall effect sensors, suggest that the basic acceleration process occurs within two or three diameters of the engine face. The local cathode tip pressure is observed to decrease with increase in magnetic field suggesting magnetic confinement effects; and, finally, local velocity measurements with a Faraday probe indicate strong radial velocity dependence. The local diagnostic measurements have, however, not yet been carried out in sufficient detail to distinguish between different possible acceleration mechanisms.

Plans: The future direction of the research program will be to continue to attempt to clarify the nature of the acceleration process by means of local diagnostic measurements. The Doppler shift technique will be used to establish both axial and azimuthal ion velocities within the discharge region. Detection of significant azimuthal kinetic energy would imply that the principle thrust production mechanism is indeed due to  $j_r B_z$  interaction. From the engine development viewpoint effort will be directed to the design and construction of a radiation-cooled MPD arcjet engine for the power range 5 to 50 kilowatts.

#### References

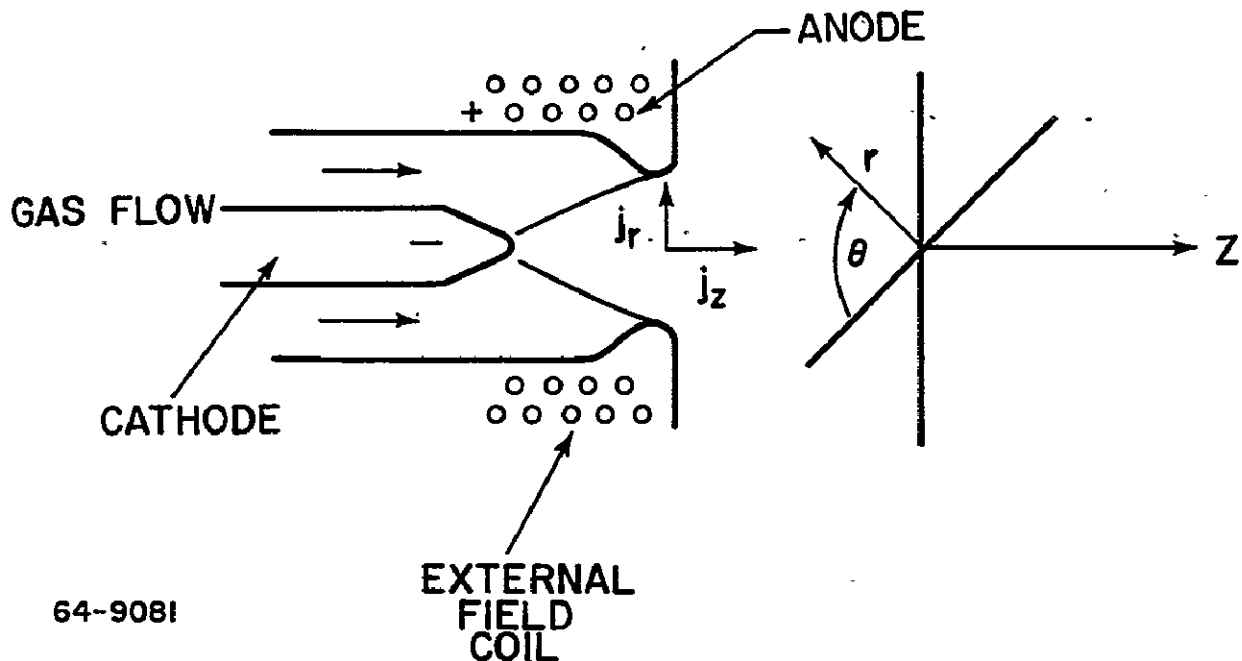
1. John, R. R., Bennett, S., and Connors, J. F., "Experimental Performance of a High Specific Impulse Arcjet Engine", *Astronautica Acta* 11, 97 (1965).
2. Fahleson, U. V., "Experiments with Plasma Moving Through Neutral Gas", *The Physics of Fluids*, Vol. 4, No. 1, pg 123-127 (1961).
3. Cann, G. L. et al, "High Specific Impulse Thermal Arcjet Thrustor Technology", AFAPL-TR-65-48 Part I, AF Aero Propulsion Laboratory (1965).
4. John, R. R., and Bennett, S., "Recent Advances in Electrothermal and Hybrid Electrothermal-Electromagnetic Propulsion, AFOSR Fourth Symposium on Advanced Propulsion Concepts, Palo Alto, Calif., (1965).

#### Additional Papers

Powers, W. E., "Measurements of the Current Density Distribution in the Exhaust of an MPD Arcjet", AIAA 3rd Aerospace Sciences Meeting, AIAA Paper No. 66-116, January, 1966.

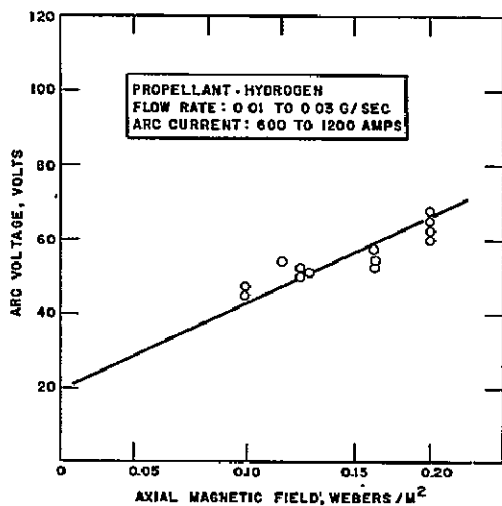
Bennett, S., Enos, G., John, R. R., and Tuchman, A., "Cesium Fueled MPD Arcjet Engine Performance", 2nd Annual AIAA Meeting, AIAA Paper No. 65-296, July 1965.

Bennett, S., John, R. R., Enos, G., and Tuchman, A., "Experimental Investigation of the MPD Arcjet", AIAA Fifth Electric Propulsion Conference, AIAA Paper No. 66-239, March 1966.



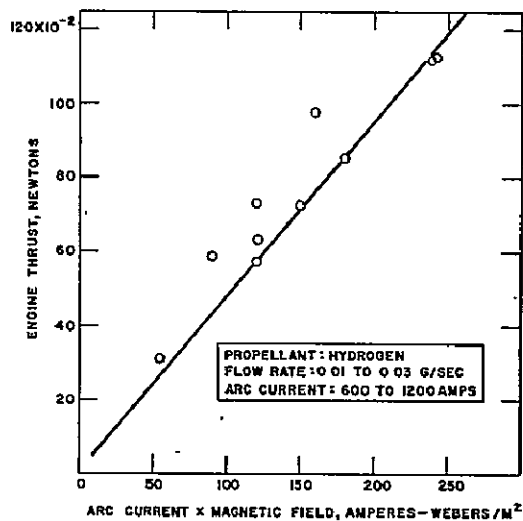
64-9081

Figure 1 SCHEMATIC DIAGRAM OF THE HYBRID (ELECTROTHERMAL-ELECTROMAGNETIC) ARC JET



28-0732

FIGURE 2 ARC VOLTAGE VERSUS APPLIED AXIAL MAGNETIC FIELD FOR AN HYDROGEN-FUELED MPD ARCJET



28-0735

FIGURE 3 ENGINE THRUST VERSUS PRODUCT OF ARC CURRENT AND APPLIED AXIAL MAGNETIC FIELD FOR A HYDROGEN-FUELED MPD ARCJET

5th NASA Intercenter and Contractors' Conference on Plasma Physics

Washington, D. C. , May 24-27, 1966

PERMANENT MAGNETS FOR MPD ARC THRUSTERS

(Contract NAS 3-7923)

A. C. Eckert and D. B. Miller

General Electric Space Sciences Laboratory

King of Prussia, Pennsylvania

ABSTRACT

A cylindrical Alnico 8 permanent magnet assembly is being tested in order to evaluate the magnet requirements to satisfy MPD thruster field needs. A multisectional design has been employed so that the effect of magnet length and area on gap field can be evaluated. Gap field strengths of over 2000 gauss have been generated. The measured dependence of gap field on magnet geometry will be discussed.

5th NASA Intercenter and Contractors' Conference on Plasma Physics

Washington, D. C., May 24-27, 1966

ELECTRON CYCLOTRON RESONANCE  
PLASMA THRUSTER DEVELOPMENT

(Contract NAS 3-8903)

D. B. Miller, A. C. Eckert and C. S. Cook

General Electric Space Sciences Laboratory

King of Prussia, Pennsylvania

ABSTRACT

The short version of the X-band ECR accelerator has been operated on a thrust stand at c-w r-f power levels up to 2000 watts. Although thrust efficiencies  $(T^2/2\dot{m}P)$  of over .30 have been measured, a good deal of randomness has yet to be understood. A retarding potential ion energy analyser has been employed simultaneously with the thrust stand to obtain an independent measure of specific impulses and velocity distribution. Ion probe specific impulses are significantly lower than the corresponding thrust-based  $I_{sp}$ , possibly as a result of the relatively important charge exchange process occurring with these experiments. Measured velocity distribution efficiencies  $(\overline{v^2}/\overline{v}^2)$  are generally greater than .80.

## HALL CURRENT ACCELERATOR

G. L. Cann, P. F. Jacobs  
Electro-Optical Systems, Inc.,  
A Subsidiary of Xerox Corporation

## ABSTRACT

A program to investigate experimentally and analytically axisymmetric Hall current accelerators has been completed. The results are reported in Ref. 1. The purpose of the investigations was to determine the performance potential of such a device as an electric space propulsion engine. Parametric studies of the accelerator were made with several propellants, emphasis being placed upon the tests using hydrogen and sodium. The accelerators used in these tests are shown schematically in Figs. 1a and 1b. The overall performance measured in these devices is presented in Figs. 2a and 2b. Some diagnostic measurements on the engine and exhaust beam were made and are reported, the most important being a determination of the current path in the exhaust beam of the hydrogen accelerator. The results of one such measurement is shown in Fig. 3. Mechanisms to explain thrust production and other engine characteristics are postulated and discussed in detail. The concept of an "effective" mass flow rate, which is determined by a minimum potential hypothesis, is developed to the point where a complete analysis of a simplified model of the accelerator can be made. Such an analysis is completed and the results are compared, where possible, with experimental results.

Adequate detailed knowledge of accelerator mechanisms to use in an engine optimization program was not generated by the above program nor is it available elsewhere. A detailed diagnostic program, coupled with an analytic investigation, has been undertaken to fulfill this need in our present contract work with NASA.

The fundamental goals of this study are to investigate the operation of an alkali metal accelerator with background pressures less than  $10^{-4}$  torr, input power 5 → 50 kw over the specific impulse range of 1000-6000 sec. A parametric investigation of overall performance (thrust, thrust efficiency and thermal efficiency) with variations in input power, mass flow rate and magnetic field is to be carried out. The following diagnostic measurements are to be made:

- 1) Axial Ion Velocity
- 2) Rotational Ion Velocity
- 3) Thrust
- 4) Torque
- 5) Magnetic Field Distribution
- 6) Current Density Distribution
- 7) Total Beam Power
- 8) Local Mass Flux
- 9) Local Energy Flux

The axial ion velocity is being measured by both Doppler spectroscopy and tracer techniques. The ion rotational velocity is being determined solely by spectroscopy. The accelerator thrust is measured with a reaction balance, and the angular momentum in the beam will be measured with a torque target. The spatial distribution of the three components of the magnetic field will be measured with a Hall-effect magnetic probe composed of three mutually orthogonal sensing elements. The distribution of current density within the plasma is determined from these measurements through graphical differentiation and the use of Maxwell's equations. The total beam power will be measured with a calorimeter composed of 16 separate, water cooled, concentric, ring elements. The use of separate elements is important not only from the standpoint of a more detailed distribution throughout the plasma, but also to avoid shorting the radial electric fields which are probably present. The local energy and mass flux distributions will be measured with two new probes. The former consists of an open ended, water cooled, calorimeter and the latter depends upon the time varying resistance of a deposited layer of alkali-metal (viz. lithium) between two collecting elements on an insulating substrate. The time rate of change of the current is then related to the instantaneous local value of the alkali metal mass flux.

Preliminary results indicate rotational ion velocities of about 4000 meters/second at a radial position 1 cm from the jet centerline. A number of spectral lines associated with transitions between the upper excited states of the lithium ion have definitely been observed. Since these states have energies in excess of 50 electron-volts, relative to the atomic ground state, this indicates reasonably high plasma electron temperatures. The preliminary tests with the mass deposition probe indicate the utility of this device as a plasma diagnostic tool. Further calibration and elimination of effects related to variations in the local plasma potential are still necessary.

#### Reference:

1. G. L. Cann, et al., "Hall Current Accelerator" NASA Report CR-54705, 4 February 1966 (Contract NAS 3-5909, NASA-LRC)



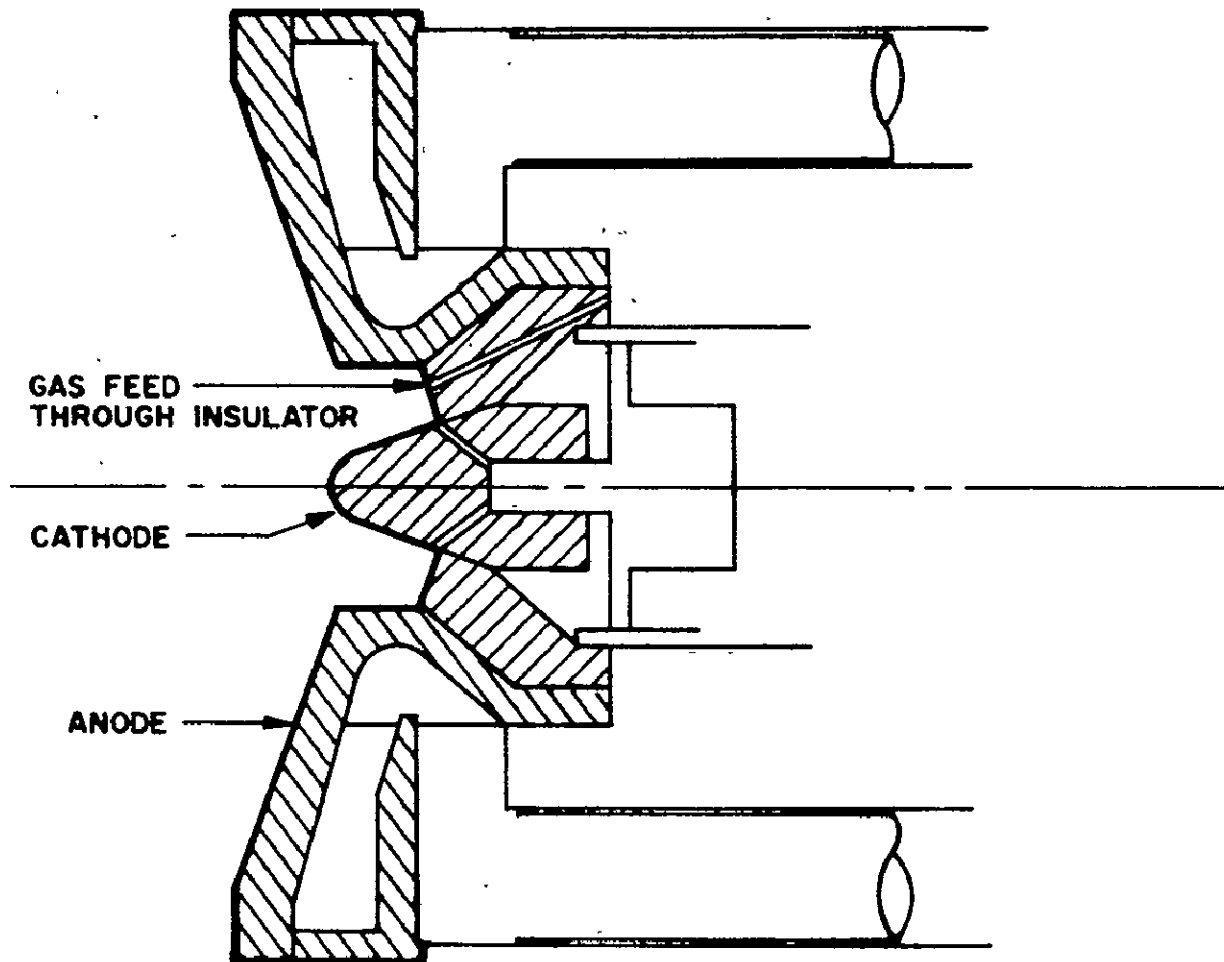


FIG. 1a HALL CURRENT ACCELERATOR WITHOUT TUNGSTEN ANODE INSERT  
( $H_2-I$ )

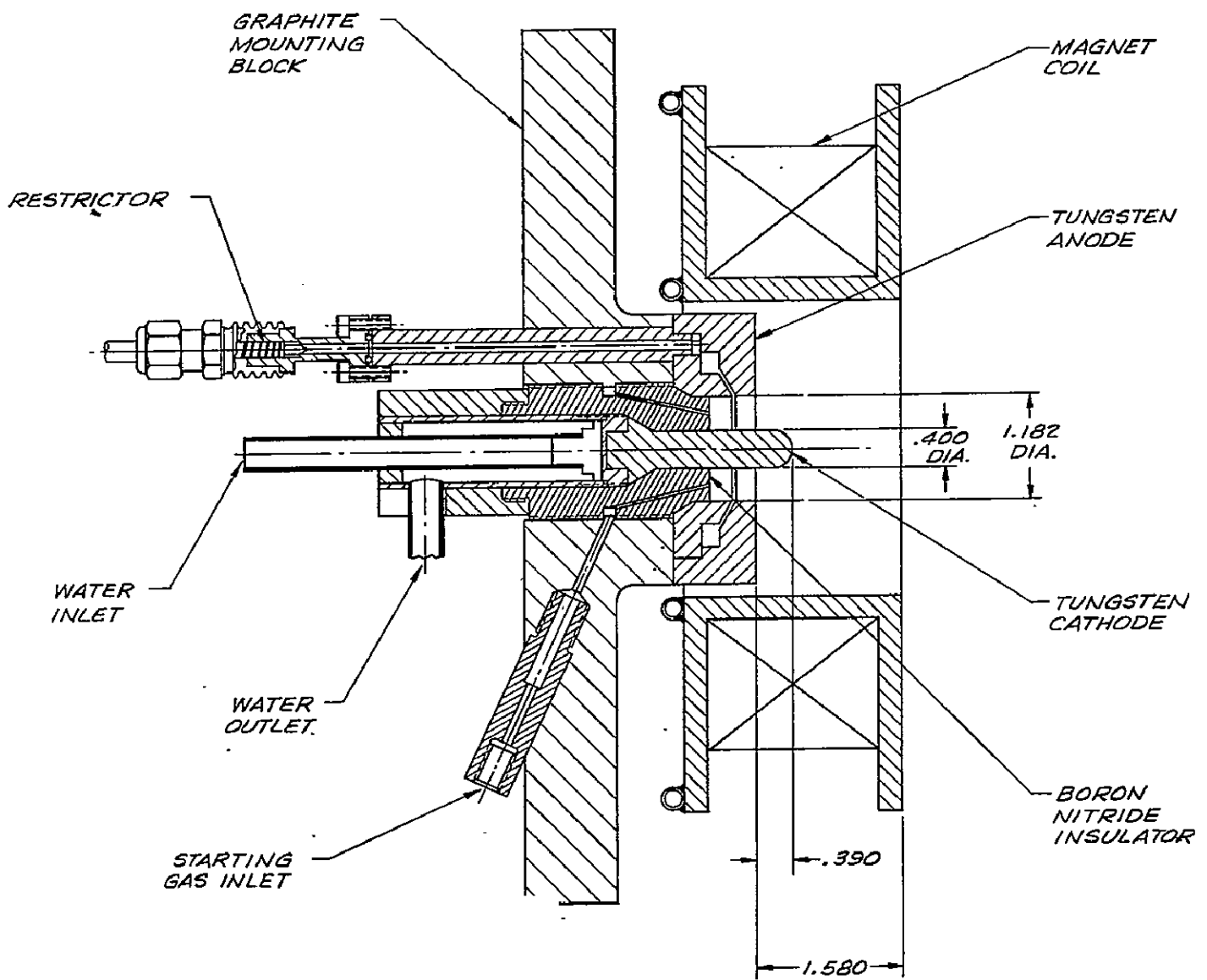


FIG. 1b. ENGINE CONFIGURATION USED IN SODIUM TESTS

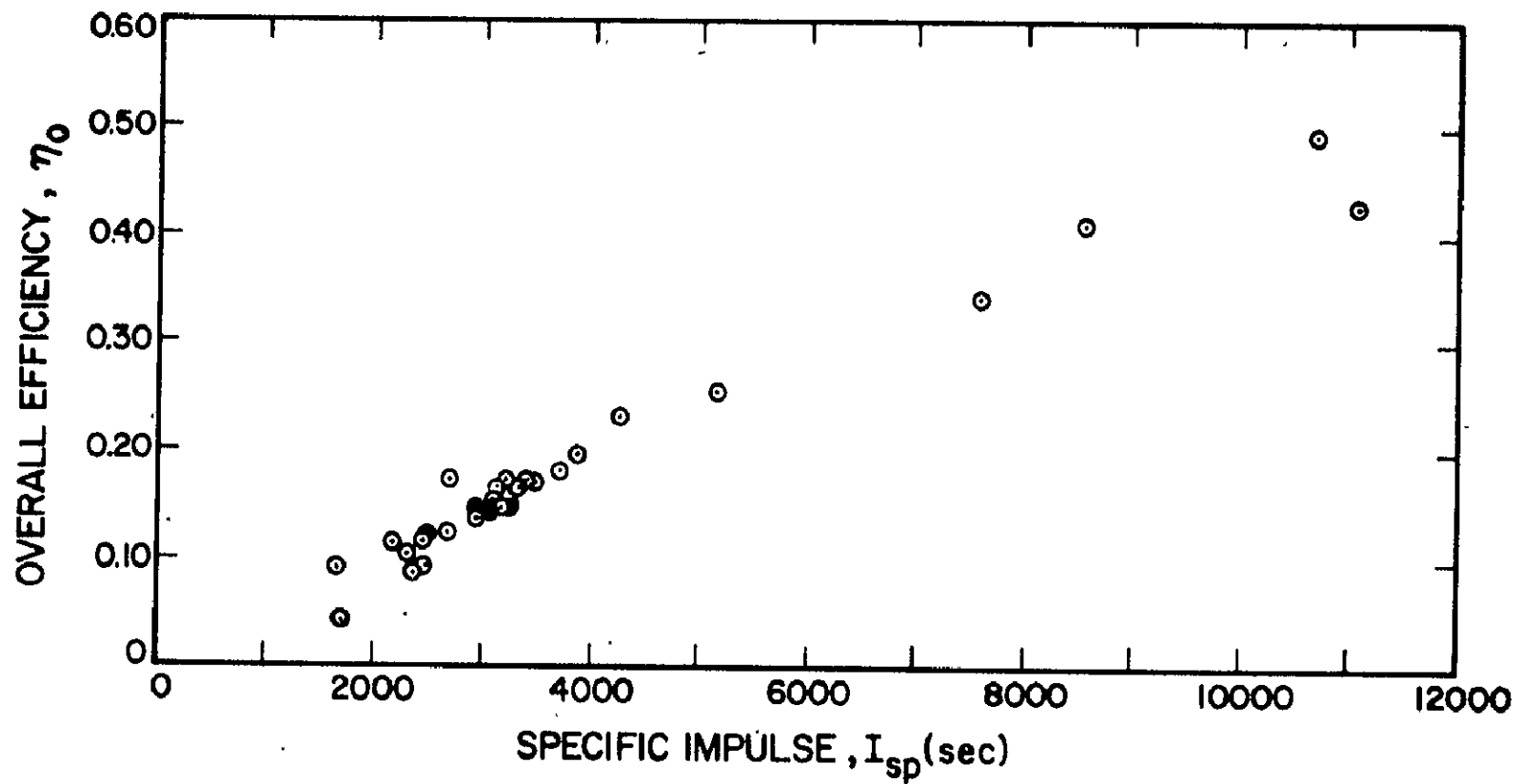


FIG. 2a OVERALL EFFICIENCY VS. SPECIFIC IMPULSE FOR H<sub>2</sub>-I HALL CURRENT ACCELERATOR

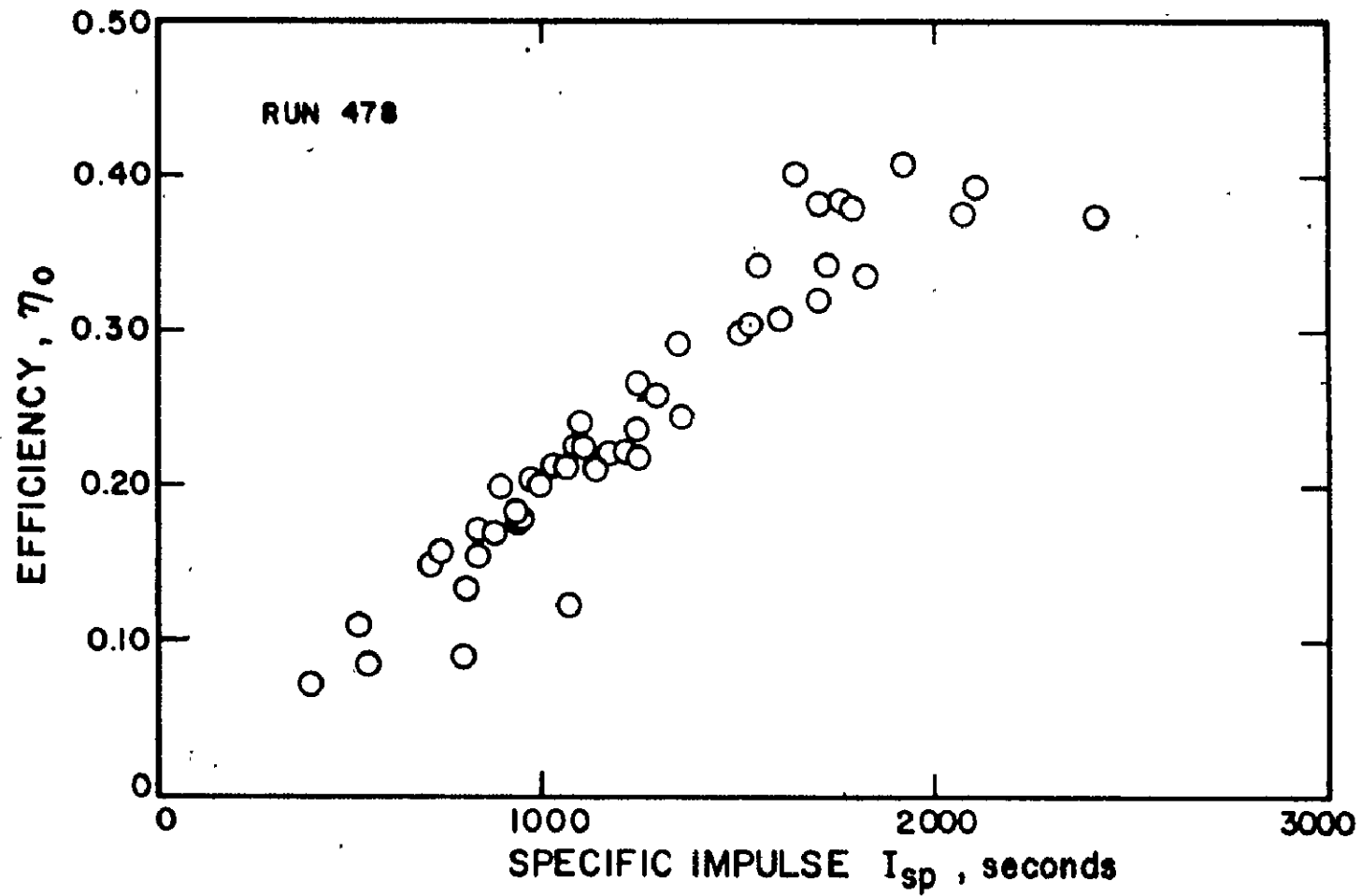


FIG. 2b EFFICIENCY AS A FUNCTION OF SPECIFIC IMPULSE (SODIUM PROPELLANT)

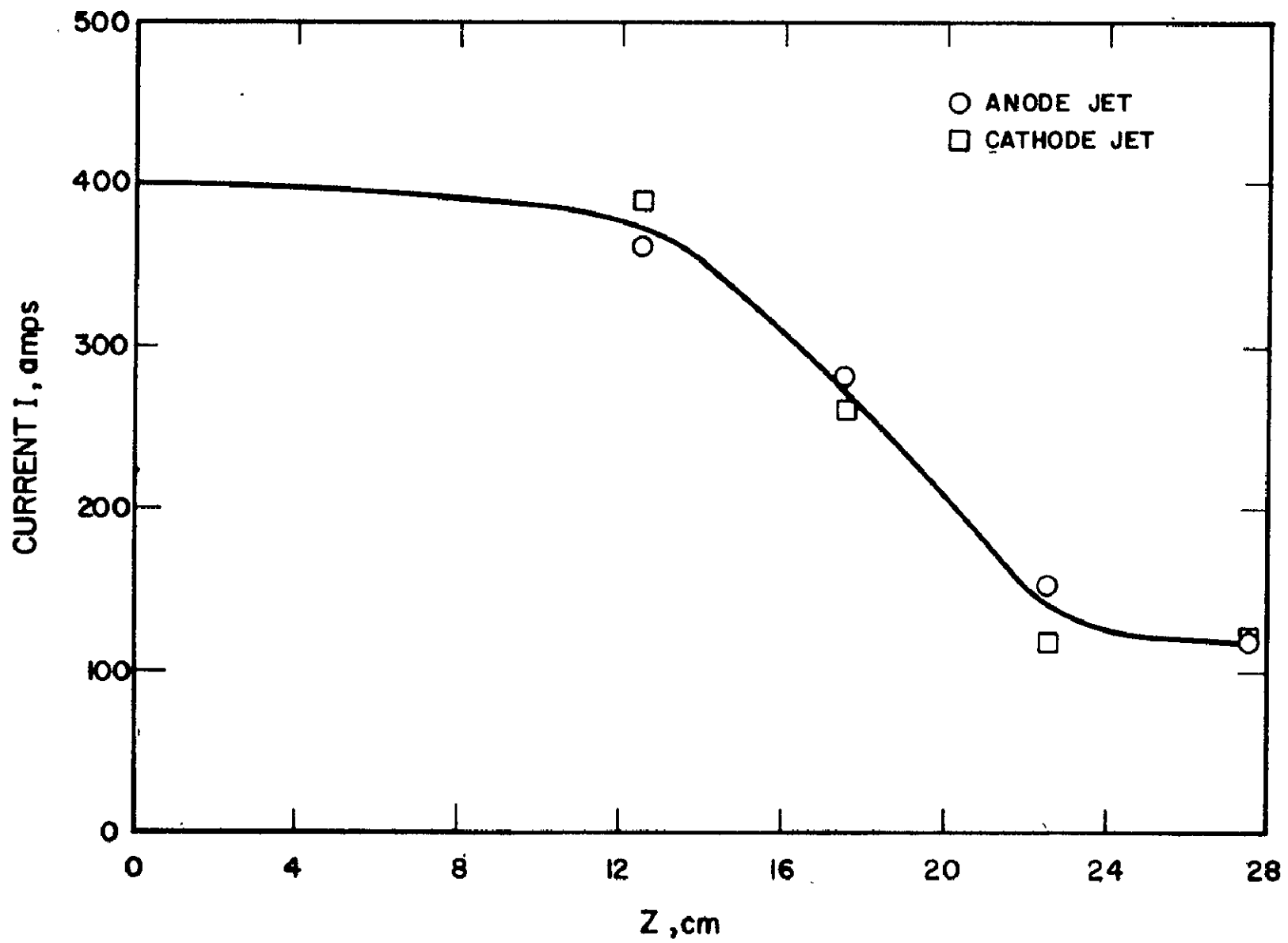


FIG. 3 CURRENT CARRIED IN ANODE AND CATHODE JETS AS A FUNCTION OF AXIAL POSITION

PLASMA ASPECTS OF SPACE PHYSICS

A. G. Opp/Physics and Astronomy Programs  
Office of Space Science and Applications, NASA

One of the objectives of the Physics and Astronomy Programs is to understand the physical processes occurring in space. Space is one of the most nearly perfect low density collisionless plasma laboratories available. Thus, many of the phenomena which are of interest to space physicists are also of great interest to plasma physicists, and vice versa.

Space plasmas exist from the lower boundary of the ionosphere to the outer limit of the Universe. Before the advent of satellites the terrestrial ionosphere was probably the best understood space plasma. None the less, ionospheric satellites enabled observations to be made above the range of ground based ionosondes and increased immeasurably the knowledge of the topside of the ionosphere. They also presented plasma physicists with observations of a new phenomenon, the so-called Alouette resonances.

Beyond the ionosphere one finds the trapped radiation belts. The mechanisms of trapping, particle acceleration and containment in the earth's magnetic field are still poorly understood, as is the magnetospheric tail and its relation to the radiation belts and auroral zones.

The earth's magnetic field and the radiation belts are terminated at approximately 10 earth radii in the subsolar direction by the solar wind. The transfer of energy from the solar wind to the magnetosphere is one of the most challenging problems of contemporary space plasmas. Extensive satellite and theoretical investigations of the interaction of the solar wind with the earth's field are being conducted in an attempt to understand the physical processes associated with the energy transfer.

The nature and origin of the solar wind is also being actively investigated. The existence of the solar wind has been firmly established. It remains, however, to define its detailed spectral characteristics and temporal variations, particularly as these can be related to events on the sun or in near interplanetary space.

The sun has been studied for centuries. Yet there still exist no fully satisfactory theories for many solar phenomena. Undoubtedly, the ultimate

explanations will have their foundations in plasma physics, and conversely, solar physicists will undoubtedly present plasma physicists with new phenomena for explanation.

The radial extent of the solar wind is a matter of speculation. Estimates range from 2 or 3 to over 100 astronomical units. The interaction of the solar wind with the galactic cosmic ray gas and galactic magnetic field are matters of considerable interest to cosmologists as well as the origin and propagation of the cosmic ray gas in the Galaxy

EXPERIMENTAL AND THEORETICAL INVESTIGATION ON  
SELECTED ASPECTS OF PLASMA TURBULENCE

I. B. Bernstein, Yale University, New Haven, Conn.

The theoretical work accomplished thus far has included studies of the quasi-linear theory of plasma waves appropriate for an understanding of plasma turbulence, and an analysis of the stability of the Chapman-Ferraro model of the magnetopause against gusting in the solar wind. These latter studies are being extended using an ideal magnetohydrodynamic model which includes the bow shock. Also under way are studies of the interaction of electromagnetic waves and the proper oscillations of the plasma in systems exhibiting sheaths.

Experimental studies already well under way are in the areas of (a) light scattering from plasma fluctuations, (b) study of cyclotron resonance plasma echoes, and (c) study of finite geometry plasma resonances. In (a) both plasma production and laser stabilization are essentially solved; in (b) collisionless echoes due to relativistic mass shift have been observed; in (c) resonance spectra both with and without streaming are undergoing study and analysis.



## INVESTIGATION OF PLASMA RESONANCE PHENOMENA

S. J. Tetenbaum

Lockheed Research Laboratories, Palo Alto, California

This investigation was undertaken to obtain an understanding of electron resonance phenomena in laboratory and ionospheric plasmas and to evaluate the applicability of such phenomena to the measurement of charged particle densities, temperatures and magnetic field strengths in planetary atmospheres and interplanetary space. Experiments were performed on RF-excited, electrodeless, pulsed and steady state, low-pressure Helium discharges of relatively simple geometry which simulate a plasma slab in a uniform magnetic field. The wave frequency,  $\omega$ , the magnetic field intensity,  $B_0 = m\omega_c/e$ , the gas pressure,  $p$ , the electron density, electron temperature and the geometry were chosen to provide an approximate correspondence between the laboratory plasma and the plasma environment of the Alouette satellite. The major resonances studied were the electron cyclotron harmonic resonances which occur near  $\omega = N\omega_c$  where  $N$  is a positive integer. A schematic of the experimental arrangement is shown in Figure 1. The plasma was created by a 22 MHz pulsed or CW transmitter capacitively coupled to a rectangular Pyrex vessel having a 16.5 x 16.5 cm cross-section and an inside thickness  $d$  of 9.7 cm in the direction of propagation. Its walls were ground to a thickness of a half-wavelength at 9.15 GHz, the frequency of the incident wave  $P_{in}$ . The vessel was located in a DC magnetic field which was uniform to better than 0.5% over the plasma volume. The measured magnetic field positions of the resonances are estimated to be accurate to 0.1%. A 36.0 GHz interferometer measured the average electron density over a 2 cm diameter cylindrical region through the plasma coaxial with the interferometer horns. Measurements were taken of  $P_e$ , the incoherent noise emission, of  $(P_\omega)_T$  and  $(P_\omega)_R$ , the coherent transmitted and reflected fundamental waves and of  $(P_{2\omega})_T$  and  $(P_{2\omega})_R$ , the corresponding second harmonic waves. The CW microwaves propagated in free space on either side of the plasma container in a direction perpendicular to the static magnetic field. The waves were launched and/or detected by microwave horns located a few wavelengths from the plasma. The horns could be rotated to propagate or receive either the extraordinary wave ( $\vec{E}_{9.15} \perp \vec{B}_0$ ) or the ordinary wave ( $\vec{E}_{9.15} \parallel \vec{B}_0$ ). The intensity of a given wave at a fixed frequency of 9.15 GHz or 18.3 GHz was recorded as the magnetic field was slowly swept in intensity and precise measurements were made of the positions, amplitudes and line shapes of the resonances under varying conditions of the plasma parameters. Figure 2 shows the resonance amplitudes of some of the waves as a function of harmonic number  $N$ , where smooth curves have been drawn through the measured points. The incoherent wave resonances reach maximum amplitude near  $N = 4$  or 5 and thereafter gradually decrease with increasing  $N$ , the ordinary wave resonances being 1 or 2 dB less than the extraordinary wave resonances. The latter were observed up to  $N = 46$ . The coherent wave resonances were only observed when the incident microwave electric field was perpendicular to the magnetic field. Fundamental wave resonances were observed up to  $N = 7$ , their amplitudes decreasing with increasing  $N$ . They exhibited an increase in power relative to the background power in transmission, and a decrease in power relative to the

background power in reflection. Second harmonic wave resonances were observed up to  $N = 7$ . They exhibited an increase in power relative to the background power in both transmission and reflection. The amplitudes of the  $(P_{2\omega})_T$  resonances were about 3 dB greater than those of  $(P_{2\omega})_R$ , and in some cases were 16 dB above the second harmonic wave background. The rapid decrease in resonance amplitude with increasing  $N$  may be related to the rapid decrease in the generated second harmonic in this magnetic field region. Resonances were also observed in the sum frequency wave,  $P_S$ , due to two incident waves of frequency  $\omega_1/2\pi = 8.8$  GHz and  $\omega_2/2\pi = 9.2$  GHz. These resonances occurred close to  $\omega_1 = N\omega_c$  and  $\omega_2 = N\omega_c$ ,  $N = 2, 3, 4$  and  $5$ . Attempts to observe resonances in  $P_{2\omega}$  near  $2\omega = N\omega_c$ ,  $N = 3, 5, 7, \dots$  and in  $P_S$  near  $\omega_1 + \omega_2 = N\omega_c$ ,  $N = 3, 4, 5, \dots$  were unsuccessful. The coherent wave and incoherent wave resonances exhibit different behaviour not only in their amplitude dependence but also in their positions. Figure 3 shows how the emission resonance positions vary with  $N$ . The positions remained constant for all harmonic numbers, for pressures from 0.02 to 0.3 Torr and for values of  $\omega_p/\omega$  at the center of the discharge from 0.8 to 2.6, where  $\omega_p$  is the electron plasma frequency. The resonance positions of the two waves differed by 0.3%, those of the extraordinary wave occurring at a higher magnetic field than those of the ordinary wave. In contrast, the coherent wave resonances were complicated functions of  $N$ ,  $p$  and  $\omega_p/\omega$ . Their positions varied as much as 4% with variations in these parameters, but always occurred on the low frequency side of the exact harmonic. The coherent and incoherent wave resonance amplitudes also differ in their pressure dependence. The former show definite collisional damping effects, the amplitudes decreasing with increasing pressure, while the latter exhibit a maximum amplitude at a pressure whose value depends upon  $\omega_p/\omega$ , the amplitude decreasing for higher and lower pressures. The incoherent wave resonances had symmetrical but non-Lorentzian line shapes. The  $Q$ 's of the extraordinary wave resonances were about 40 and were about one third larger than the  $Q$ 's of the ordinary wave resonances. The coherent wave resonances had asymmetrical line shapes, their asymmetry decreasing with increasing  $N$ , and  $Q$ 's of about 30. The coherent wave resonance lines were broader on their high magnetic field side and occasionally, for  $N = 2$  and  $N = 3$ , showed the presence of additional small resonances. Experiments in which the center of the plasma was moved relative to the center of the magnetic field have shown that the cyclotron harmonic emission is a volume effect rather than a sheath effect and that the radiated ordinary and extraordinary wave resonances originated in different regions of the plasma.

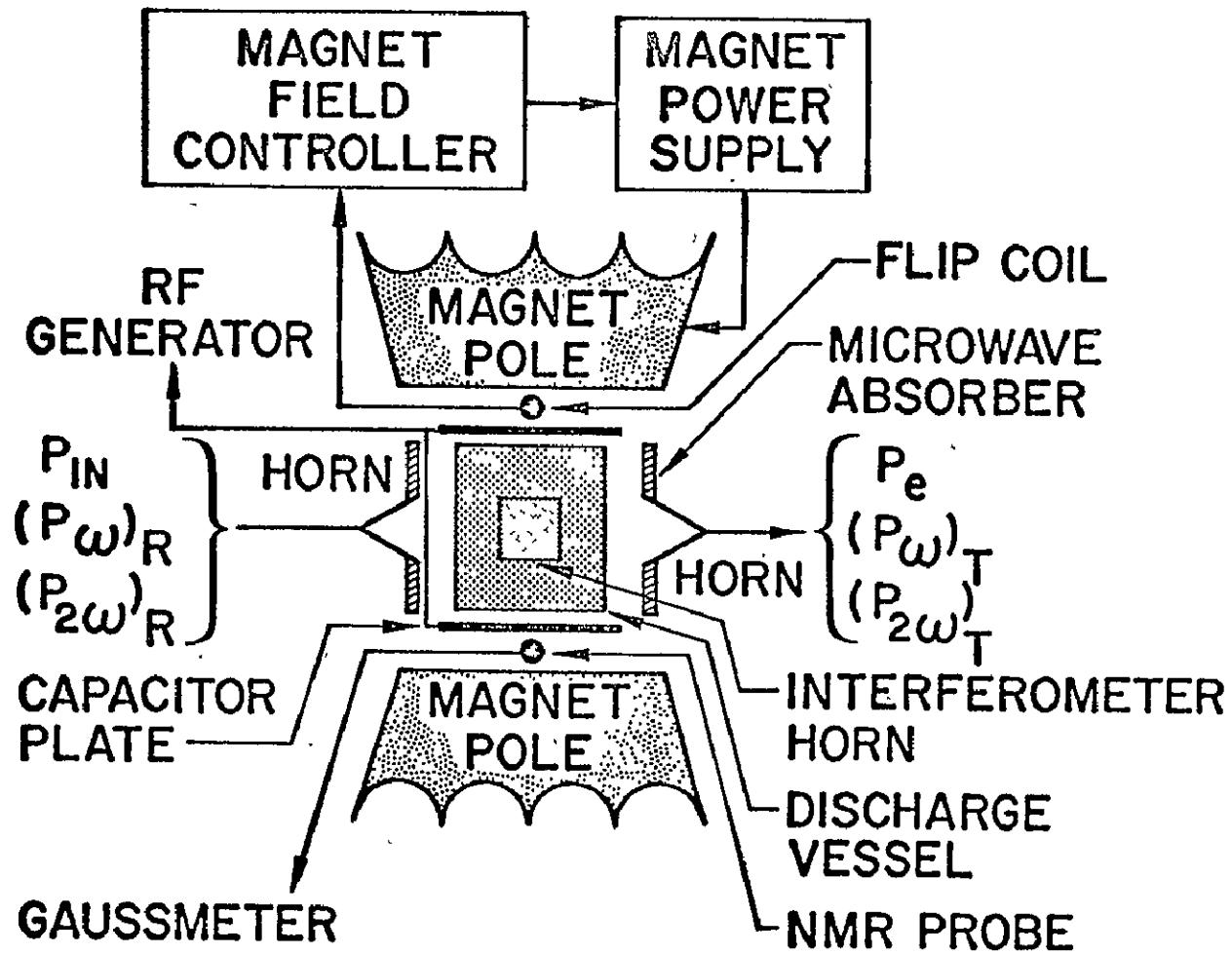


FIGURE 1

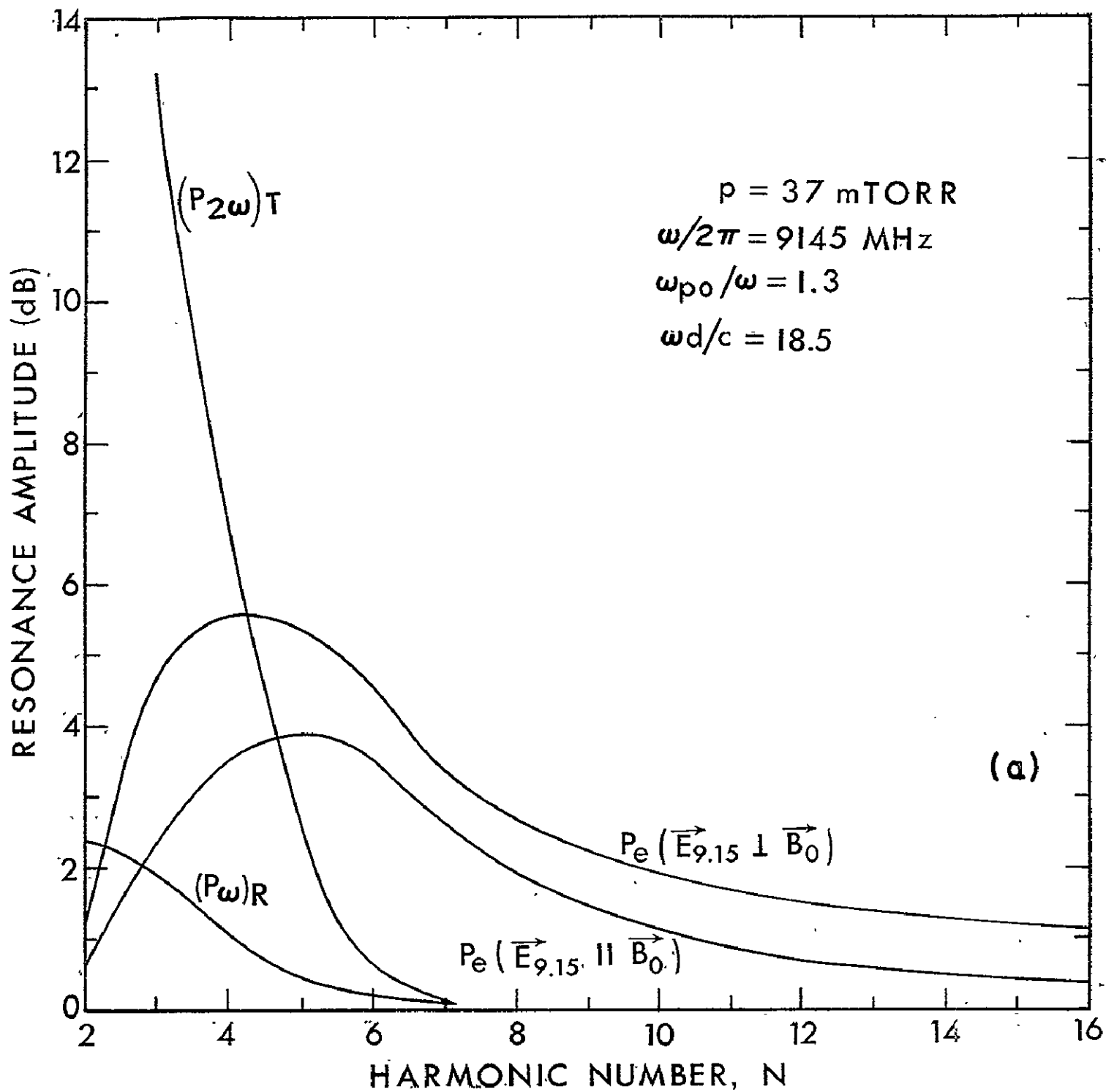


FIGURE 2

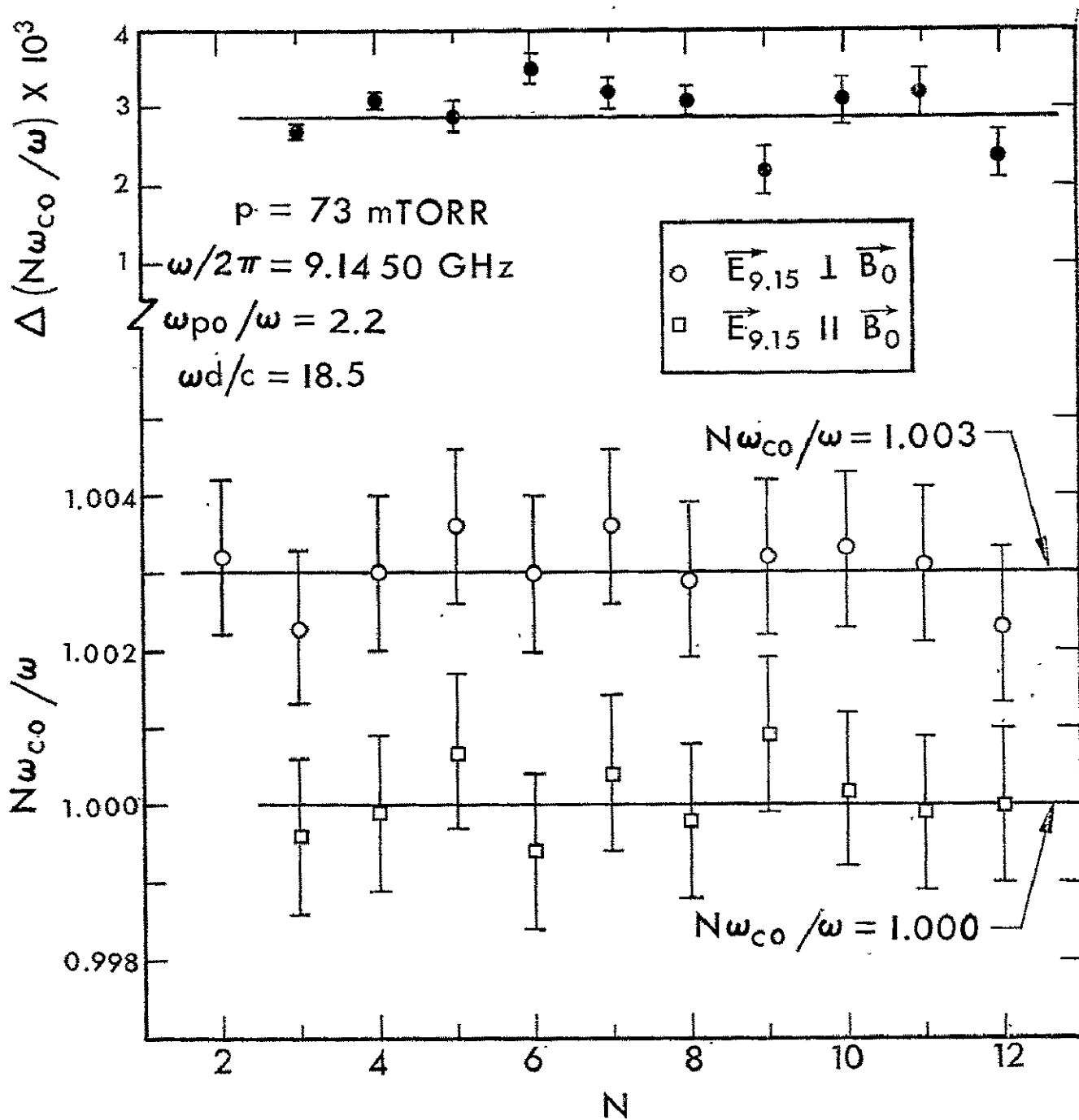


FIGURE 3

## A-C TRAVELLING WAVE-PLASMA STREAM INTERACTIONS

Martin Lessen

The University of Rochester  
Rochester, New York

NsG-350-63

The motivation of this problem was to investigate the interaction of a travelling magnetic wave with a plasma. The configuration selected for this research was a pair of coaxial cylinders with an inner and outer shell of low reluctance magnetic material. The configuration was chosen to provide an electrodeless machine with a nearly radial magnetic field. The concept of this machine was first presented in reference (1) in which a single fluid model was used for analysis. Subsequently, this type of configuration was discussed by Carter and Laubenstein (2) and more recently by Penfold et al (3) and Schwirian (4).

The approach was initially in two directions. The first was the analysis of a three fluid one dimensional model of the device in which the principal mechanism for plasma neutral interaction was assumed to be charge exchange. The second was experimental which involved construction of the coaxial cylindrical device including the windings low reluctance, magnetic material shells, gas metering system and some diagnostic elements. This latter area indicated that a great deal had to be done before significant physical results could be obtained as to the internal interaction mechanisms.

Initially several sets of windings were made and tuned in an attempt to obtain the strongest radial field with as little axial component as possible. The final design consisted of four 9 turn coils each approximately 9 inches long. For this configuration the radial field strength varied from about 100 gauss to 160 gauss along the tube - having maximums between the coils. At the same time, the axial component was about 20 to 25 gauss representing an angularity of the field midway in the annulus of some significance. The phase angle of the field fluctuated over a  $12.5^\circ$  range along the tube from an assumed linear  $360^\circ$  total phase shift. Due to the field angularity the reaction with the plasma would drive many of the particles to the walls before the exit were reached, however, there should be some measurable reaction. The most direct measurement was of the pressure distribution along the tube for a given flow rate. By having the field accelerate the plasma,

a pressure drop from  $300\mu\text{Hg}$  to  $110\mu\text{Hg}$  was recorded over  $3/4$  of the tube length; connecting the field in reverse necessitated an inlet pressure of approximately  $800\mu\text{Hg}$  to realize the  $100\mu\text{Hg}$  at the same point. Considerable changes in the electrical power input were noted during these interactions. Some estimate of the power transferred to the plasma was desired and coils wound in the annulus and connected to non-inductive resistances were used for this purpose. Induced power in the coils amounted to approximately 6 KW. At this time the power to the coils totaled 10.2 KW. In the discharge mode the power dropped to 5 KW to the coils due to considerably more detuning.

Work is continuing with the construction of a new machine with conical geometry which should alleviate some of the problems of field angularity and the small annulus. Also more room will exist for diagnostics than could be affected in the current machine. It is anticipated that the question of the magnitude of elastic scattering of particles and radial electric field effects can be looked at as well as the continued investigation of overall interaction.

#### REFERENCES

- 1 K. H. Fishbeck, "On the Theory of AC Induction Plasma Motors and Generators," Ph.D. Dissertation--Graduate School of the University of Pennsylvania, June 1961.
- 2 R. L. Carter and R. A. Laubenstein, "A Non-Equilibrium Alternating Current Magnetogasdynamic Linear Induction Generator," 3rd Symposium, Engineering Aspects of Magnetohydrodynamics, N. W. Mather and G. W. Sutton Ed. Gordon & Breach, N. Y., 1964.
- 3 J. M. Rocard, J. A. Thornton, A. S. Penfold, G. Fonda-Bonardi, R. M. Rosen, and M. Alperin, "Development of Alternating Current Plasma Accelerator for Application as an Ultra-High-Velocity Tunnel" Technical Report No. AFFDL-TR-64-157 Air Force Flight Dynamics Laboratory, November 1964.
- 4 Richard E. Schwirian, "Analysis of Linear-Induction or Traveling-Wave Electromagnetic Pump of Annular Design", NASA Technical Note NASA TN D-2816, May 1965.